

8-2014

Construction of 3D Biomimetic Tissue Niches for Directing Pancreatic Lineage Differentiation of Human Embryonic Stem Cells

Weiwei Wang

University of Arkansas, Fayetteville

Follow this and additional works at: <http://scholarworks.uark.edu/etd>

 Part of the [Cell Biology Commons](#), [Genetics Commons](#), and the [Molecular, Cellular, and Tissue Engineering Commons](#)

Recommended Citation

Wang, Weiwei, "Construction of 3D Biomimetic Tissue Niches for Directing Pancreatic Lineage Differentiation of Human Embryonic Stem Cells" (2014). *Theses and Dissertations*. 2154.

<http://scholarworks.uark.edu/etd/2154>

This Dissertation is brought to you for free and open access by ScholarWorks@UARK. It has been accepted for inclusion in Theses and Dissertations by an authorized administrator of ScholarWorks@UARK. For more information, please contact scholar@uark.edu, ccmiddle@uark.edu.

Construction of 3D Biomimetic Tissue Niches for Directing Pancreatic Lineage Differentiation
of Human Embryonic Stem Cells

Construction of 3D Biomimetic Tissue Niches for Directing Pancreatic Lineage Differentiation
of Human Embryonic Stem Cells

A dissertation submitted in partial fulfillment
of the requirements for the degree of
Doctor of Philosophy in Cell and Molecular Biology

by

Weiwei Wang
Chongqing Medical University
Bachelor of Medicine in Clinical Medicine, 2006
University of Chinese Academy of Sciences
Master of Science in Biochemistry and Molecular Biology, 2009

August 2014
University of Arkansas

This dissertation is approved for recommendation to the Graduate Council.

Dr. Kaiming Ye
Dissertation Director

Dr. Sha Jin
Co-Dissertation Director

Dr. Douglas Duane Rhoads
Committee Member

Dr. Uchechukwu C. Wejinya
Committee Member

Dr. Christa Hestekin
Committee Member

ABSTRACT

The potential of human embryonic stem cells (hESCs) to differentiate into insulin producing β cells offers great hope for cell-based therapy for diabetes treatment. However, *in vitro* pancreatic differentiation of hESCs remains challenging. In the past decade, most protocols for differentiating pancreatic cells have been focused on the use of signaling molecule cocktails on 2D substrates. Studies on embryonic development biology strongly suggest that extracellular matrix (ECM) plays a critical role on hESCs behavior. In this work, we first established a 3D collagen scaffold culture system for hESCs differentiating into definitive endoderm (DE), which is the first and most important step for coaxing hESCs into transplantable β cells. Collagen scaffold have shown to promote the attachment, proliferation and DE differentiation of hESCs in 3D microenvironment. Furthermore, we optimized the 3D scaffold compositions by integrating various ECM proteins into collagen scaffold. Our data showed that compared to collagen with single ECM protein, collagen combined with fibronectin, laminin, and vitronectin can greatly enhance DE differentiation generating up to 93% SOX17 positive DE population. Finally, we demonstrated that mature insulin-producing cells can be achieved by differentiating hESCs in 3D biomimic scaffold made of collagen and Matrigel, combined with a modified step-wise protocol. More mature insulin-producing cells were generated with our 3D scaffold compared to traditional 2D culture. The 3D differentiated pancreatic endocrine cells were assembled into tissue-like structure and displayed greater similarities in phenotype and gene expression profile to adult human islets. These hESC-induced pancreatic cells comprised 20% insulin positive cells in 3D culture and can response to high glucose and release four-fold insulin as compared to 2D culture. Insulin-secreting granules were also observed, which confirmed the generation of insulin-producing cells in 3D scaffold.

©2014 by Weiwei Wang
All Rights Reserved

ACKNOWLEDGEMENTS

First, I would like to express my sincere appreciation and gratitude to my major advisor Dr. Kaiming Ye for his continuous support, encouragement, guidance, and advice throughout my journey in achieving the PhD degree. I am very thankful and grateful to him for giving me this opportunity and for his support both in my academic and personal life. I would also like to thank him for the time he spent on reading and editing the draft of this dissertation.

I would like to convey my gratitude to my co-advisor Dr. Sha Jin for mentoring me throughout the project that culminated into this defense. I would not be able to get come this far without her guiding hand and I truly appreciate her continues support. I would also like to take this opportunity to thank Dr. Douglas D. Rhoads for all the support he has provided through these transformative years of my life especially through the last 12 months. His support both as my committee member and the head of CEMB program has made it possible for me to complete my dissertation.

I would like to thank my committee members Dr. Uchechukwu C. Wejinya and Dr. Christa Hestekin for their valuable advice and technical input throughout my PhD program. I would also like to thank them for their time and agreeing to serve on my doctoral dissertation committee. I would also like to thank Dr. Mourad Benamara and Dr. Betty Martin for their all the technical help they have provided with electron microscopy.

It would not have been possible for me to earn my degree without the unfailing support of my family, my mother Qiong Liu and my father Changqing Wang. I would like to offer my most sincere appreciation to both of them, who have dealt with many hardships to provide better education for their child. I would like to thank my fiancé and dearest friend Dr. Bhanu prasanth Koppolu, for the care and support he provided from day one of my Ph.D program. He has been

my rock throughout these tumultuous times. I would also like to thank all my colleagues at Stem cell and Tissue Engineering lab who shared my burdens without expectations.

TABLE OF CONTENTS

1. BACKGROUND	1
1.1. Stem cells	1
1.1.1. Embryonic stem cells	1
1.1.2. Adult stem cells	2
1.1.3. Induced pluripotent stem cells (iPSCs)	3
1.2. Current and future therapies for diabetes mellitus	5
1.2.1. Diabetes mellitus	5
1.2.2. Islet transplantation	7
1.2.3. <i>In vivo</i> regeneration of pancreatic β -cells	8
1.2.4. <i>In vitro</i> expansion of pancreatic β -cells	10
1.3. Directed differentiation of hESCs towards pancreatic β cells	12
1.3.1. Pancreas and β -cell development	12
1.3.2. ESCs-derived insulin-producing β cells	14
1.4. Extracellular matrix (ECM) and stem cell	16
1.4.1. The role of ECM in stem cell niches	16
1.4.2. ECM-stem cell interaction	18
1.4.3. ECM and growth factors presentation	19
1.4.4. ECM biomechanical properties and stem cell fate determination	21
1.4.5. Engineering three-dimensional (3D) scaffold for stem cell differentiation	22
1.5. Objectives and Hypothesis	26
2. Differentiation of Human Embryonic Stem Cells into Definitive Endoderm in 3D Type I Collagen Scaffold	27

TABLE OF CONTENTS

2.1. Abstract	27
2.2. Introduction	27
2.3. Materials and Methods	30
2.3.1. hESCs culture	30
2.3.2. 3D hESCs definitive endoderm differentiation	31
2.3.3. Scanning electron microscopy (SEM)	32
2.3.4. Cell viability assay within 3D collagen scaffolds	32
2.3.5. AlamarBlue cell proliferation assay	33
2.3.6. RNA extraction and quantitative RT-PCR (qRT-PCR)	33
2.3.7. Statistical analysis	34
2.4. Results	34
2.4.1. hESCs maintenance on two culture system	34
2.4.2. Collagen I scaffold characterization	35
2.4.3. Morphological and viability analysis of DE differentiated hESCs within collagen scaffolds	35
2.4.4. Proliferation rate of DE differentiated hESCs within collagen scaffolds	36
2.4.5. hESCs DE differentiation in 2D and 3D	36
2.5. Discussion	37
3. Combinatorial Effect of ECM Proteins on 3D Human Embryonic Stem Cells	
Definitive Endoderm Differentiation	40
3.1. Abstract	40

TABLE OF CONTENTS

3.2. Introduction	40
3.3. Materials and Methods	42
3.3.1. 3D hESCs culture	42
3.3.2. hESCs DE differentiation	44
3.3.3. Cell viability	44
3.3.4. Scanning electron microscopy	45
3.3.5. RNA extraction and RT-PCR analysis	46
3.3.6. Flow cytometry	46
3.3.7. Immunohistochemical and immunocytochemical staining	47
3.3.8. Statistical Analysis	48
3.4. Results	48
3.4.1. PI3K inhibitor enhanced DE differentiation from hESCs	48
3.4.2. Proliferation and morphological changes of hESCs-differentiated DE cells within scaffolds	49
3.4.3. Morphological analyses of DE differentiated cells in 3D collagen-ECM scaffolds	50
3.4.4. Enhancement of DE differentiation in 3D collagen-ECM scaffolds	51
3.4.5. 3D scaffolds improve the secretion of ECMs by DE-differentiated cells	52
3.5. Discussion	53
4. Enhanced Pancreatic β cells Differentiation from Embryonic Stem Cells in 3D Collagen I-Matrigel Scaffolds	56

TABLE OF CONTENTS

4.1. Abstract	56
4.2. Introduction	57
4.3. Materials and Mehtods	59
4.3.1. hESCs culture	59
4.3.2. Collagen/Matrigel scaffolds preparation	59
4.3.3. hESCs Pancreatic differentiation of on Matrigel and in Collagen/Matrigel scaffolds	60
4.3.4. Scanning electron microscopy	61
4.3.5. Quantitative real-time polymerase chain reaction	61
4.3.6. live/dead cell staining in 3D collagen/Matrigel scaffolds	62
4.3.7. Immunofluorescence staining	62
4.3.8. Flow cytometry	63
4.3.9. Glucose stimulated insulin secretion assay	64
4.3.10. Transmission electron microscopy (TEM)	64
4.3.11. Statistical analysis	65
4.4. Results	65
4.4.1. Scaffold morphology	65
4.4.2. Effect of Matrigel on the hESCs definitive endoderm differentiation	66
4.4.3. The morphological and viability analysis of hESCs pancreatic differentiation in collagen/Matrigel scaffolds	66
4.4.4. ILV treatment promoted the generation of pancreatic progenitor cells	67

TABLE OF CONTENTS

4.4.5. Immunohistochemical characterization of hESCs-derived insulin-producing cells in collagen/Matrigel scaffold	68
4.4.6. Gene expression profile of hESCs-derived insulin-producing cells in 2D and 3D	69
4.4.7. Insulin secretion in 2D and 3D culture	70
4.4.8. Ultrastructural characteristics of hESC-derived pancreatic cells	70
4.5. Discussion	71
5. Conclusions and future directions	75
6. REFERENCES	101

LIST OF TABLES

Table. 1. List of PCR primers

Page 77

Table. 2. List of Antibodies used in immunocytochemistry and immunohistochemistry.

Page 78

LIST OF FIGURES

Figure. 1. Morphological changes and expression of pluripotent markers of hESCs before differentiation. (A-F) Phase-contrast microscopy images of hESCs cultured on MEF feeder layers (A-C) or Matrigel™ (D-F). hESCs proliferated from day 2 (A, D), day 3 (B, E) and day 4 (C, F). (G-I) Immunocytochemical analysis of pluripotency in H9 hES cells. Cells were stained with antibodies against pluripotency marker proteins SOX2 (G), SSEA4 (H), and TRA-1-60 (I) after five passages. Cells were also labeled with diaminophenylindole (DAPI) in order to localize the nucleus. Stained cells were observed under a fluorescence microscope (Olympus IX 71) equipped with a CCD camera. Scar bar (A-C, G-I) 50 µm, (D-F) 300 µm. **Page 79**

Figure. 2. Scanning electron microscopy (SEM) images of the collagen I scaffold. (A) Micrographic structure of 1.5 mg/ml collagen I scaffold. (B) hESCs integrated in collagen scaffold. Scale bar: 2µm. **Page 80**

Figure. 3. Morphological and viability analysis of hESCs-derived definitive endoderm in 3D collagen cultures. hESCs were seeded into a 3D collagen scaffold (1.5mg/ml) as single cells (A, B, E, F) or cell clusters (C, D, G, H) in a 24-well plate (2.5×10^6 cells/ml). Bright field images of hESCs on day 2 (A, C) and day 4 (B, D) of DE differentiation in 3D cultures. hESCs proliferated and maintained a high viability on day 2 (E, G) and day 4 (F, H) as determined by live/dead cell staining. Scale bar: 30 µm. **Page 81**

Figure. 4. hESCs proliferation in 3D collagen scaffold. hESCs were seeded in collagen scaffold as single cells or cell clusters and time course of cell proliferation was performed by Alamarblue assay from day 0 to day 5. Fluorescence intensity was detected at excitation wavelength of 570 nm and fluorescence emission at 590 nm. Data were the measurements in triplicate experiments at indicated time intervals. **Page 82**

Figure. 5. Quantitative PCR analysis of DE marker genes and other germ layer marker genes of hESCs-induced DE cells after 4 day of differentiation by using single cells inoculation method or cell clusters inoculation method. Undifferentiated hESCs were served as control and the mRNA levels were normalized to β-actin. **Page 83**

Figure. 6. Comparison of DE differentiation efficiency by culture hESCs in DE differentiation medium A (Activin A and Wnt3a) or medium B (Activin A and wortmannin). (A) Quantitative PCR analysis of DE and three germ layers marker genes expression of hESCs-induced cells on day 1, day2 and day4 of DE differentiation. Expression levels were normalized to β actin. (B) Flow cytometric analysis of SOX17 positive cells in hESCs-induced cells on day 4. (C) Immunofluorescence staining of SOX17 (red), FOXA2 (green) in hESCs-induced cells on day 4. **Page 84**

LIST OF FIGURES

Figure. 7. Bright field microscopy images of hESCs-induced cells in 2D and 3D ECM scaffolds. hESCs were induced into DE in 2D (A and B), type I collagen scaffolds (Col I, C and D), and collagen along with laminin (LAM, E and F), fibronectin (FN, G and H), vitronectin (VN, I and J) or mixture of ECM proteins (Mix, K and L). Morphologies were observed on day 2 (left panel) and day 4 (right panel) of DE differentiation. Scale bar (A-B) 200 μm , (C-L) 100 μm . **Page 85**

Figure. 8. The viability of hESCs-induced DE cells in 3D ECM scaffolds. hESCs were cultured into type I collagen scaffolds (Col I, A and B), and collagen I along with laminin (LAM, C and D), fibronectin (FN, E and F), vitronectin (VN, G and H) or mixture of ECM proteins (Mix, I and J) in DE differentiation medium for 4 days. Live/dead staining were performed on day 2 (left panel) and day 4 (right panel) of DE differentiation. Images were taken using an inverted fluorescence microscopy Olympus IX-71. Scale bar = 200 μm . **Page 86**

Figure. 9. Scanning electron microscopy of collagen scaffolds along with various ECM proteins without (left panel) or with hESCs (right panel). The following scaffolds were presented: Col I (A, B), Col I + LAM (C, D), Col I + FN (E, F), Col I + VN (G, H), Col I + Mix (I, J). Scale bar = 2 μm . **Page 87**

Figure. 10. Enhancement of DE differentiation in 3D collagen-based ECM scaffolds. (A) Quantitative PCR analysis of hESCs-induced DE cells after 4 days of culture in 2D and 3D collagen gel along with ECM proteins LM, FN, and VN. Relative gene expression levels in DE cells cultured in 3D were normalized to DE cells in 2D culture and beta-actin was used as calibration gene. (B) Flow cytometric analysis of Sox17 in definitive endoderm derived from human embryonic stem (ES) cells. DE cells were stained with either PE Mouse IgG1, κ isotype control (filled histogram) or PE Mouse Anti-human Sox17 antibody (open histogram) at matched concentrations. **Page 88**

Figure. 11. Immunohistochemical staining of definitive endoderm markers, Sox17 and Foxa2 in hESCs-induced cells culture in 2D and 3D scaffolds made of collagen I along with laminin, fibronectin, and vitronectin. The definitive endoderm cells were examined after 4 days of differentiation. The nuclei were counterstained with DAPI. Scale bar = 50 μm . **Page 89**

Figure. 12. Quantitative PCR analysis of ECM gene expression of hESCs-induced DE cells in 2D and 3D culture. hESCs were induced into DE cells for 4 days in 2D or 3D collagen gel along with various ECM proteins such as LM, FN, and VN. Relative gene expression levels in DE cells cultured in 3D scaffolds were normalized to DE cells in 2D and beta-actin was used as calibration gene. **Page 90**

LIST OF FIGURES

Figure.13. Immunohistochemical staining of collagen IV secretion by DE differentiated cells in 3D scaffolds made of various ECM proteins. After 4 days of DE differentiation, cells in 2D and 3D culture were stained with rabbit anti-collagen IV primary antibody and TRITC conjugated donkey anti rabbit secondary antibody. Nucleus was counterstained with DAPI. Scale bar=50 μm .. **Page 91**

Figure. 14. A modified step-wise protocol for differentiating human ES cells into insulin-producing cells. Stage I: human ES cells were induced into definitive endoderm in the presence of activin A and wortmannin. Stage II: the differentiated endoderm cells were treated with RA, KGF, Noggin and ILV to induce pancreatic progenitor formation. Stage III: cells were exposed to EGF to endorse pancreatic endoderm lineage specific differentiation. Stage IV: a cocktail of factors including nicotinamide, extendin-4, BMP4 and bFGF as utilized to promote the maturation of pancreatic β cells (this protocol is similar to Zhang, D. *et al.*'s approach but with some modification). **Page 92**

Figure. 15. Scanning electron micrographs of collagen I network incorporated with various concentration of Matrigel: (A, D) 10% Matrigel, (B, E), 35% Matrigel, (C, F) 50% Matrigel. Scale bars: A-C, 50 μm , D-F, 10 μm . **Page 93**

Figure. 16. Effect of Matrigel concentration in 3D collagen-I based scaffold on hESCs differentiation into definitive endoderm. (A) Quantitative PCR analysis of definitive endoderm markers of hESCs-derived DE cells after 4 days of differentiation in 2D and 3D collagen gel along with 10%, 35%, 50% Matrigel. Expression level were normalized to β -actin. For each sample, relative expression levels were normalized to corresponding levels in cells under 2D culture. (B) Intracellular flow cytometric analysis of Sox17 at day 4 of DE differentiation in 2D and 3D collagen gel along with 10%, 35%, 50% Matrigel. DE cells were stained with either PE Mouse IgG1, κ isotype control (filled histogram) or PE Mouse Anti-human Sox17 antibody (open histogram) at matched concentrations. **Page 94**

Figure. 17. The morphology and viability of hESCs during pancreatic differentiation process in 3D collagen/Matrigel scaffolds. (A-D) Phase contrast microscopy images of hESCs pancreatic differentiation at day 4 (A, C) and day 10 (B, D) in 2D (A, B) and collagen/Matrigel scaffold (C, D). (E-F) Live/dead staining of hESCs-differentiating cells in collagen/Matrigel scaffold on day 4 (E) and day 10 (F). **Page 95**

LIST OF FIGURES

Figure. 18. The effect of (-)-indolactam V (ILV) on the differentiation of pancreatic progenitor from DE. (A) Immunofluorescence analysis of coexpression of PDX1 and HNF6 in hESCs-induced pancreatic progenitor cells treated with or without ILV in 2D and 3D collagen/Matrigel. (B) Quantitative PCR analysis of pancreatic progenitor marker genes in hESCs-induced cells treated without or with ILV on day 5 and day 8. Expression level were normalized to β -actin. All values are normalized to cells cultured on day 5 without ILV treatment. **Page 96**

Figure. 19. Double immunofluorescence analysis of pancreatic cells differentiated from hESCs. (A-C) PDX1 (A); NKX6.1 (B); merged images of PDX1, NKX6.1 and DAPI (C). (D-F) PDX1 (D); NGN3 (E); merged images of PDX1, NGN3 and DAPI (F). (G-I) Insulin (G); C-peptide (H); merged images of insulin, C-peptide and DAPI. (J-L) Insulin (J); Somatostatin (K); merged images of insulin, somatostatin and DAPI. (M-O) Insulin (M); polypeptide (N); merged images of Insulin, polypeptide and DAPI. (P-R) Insulin (P); glucagon (Q); merged images of insulin, glucagon and DAPI (R). **Page 97**

Figure. 20. Quantitative PCR analysis showed the dynamic expression of several key genes during hESCs-induced pancreatic β cell development. Cell samples were collected at the end of stage I, stage II, stage III, and stage IV. mRNA of hESCs-induced cells at stage I in 2D culture was used as control to normalize gene expression level. β -actin was used as house-keeping gene. **Page 98**

Figure. 21. Insulin secretion in 2D and 3D culture. (A) ELISA of glucose-response insulin release from 2D- and 3D- induced pancreatic cells exposed to 5.5 mM, 15 mM, and 25 mM glucose. (B) Flow cytometric analysis was performed using anti-human insulin antibodies with hESCs-induced pancreatic cells at the end of stage IV in 2D and 3D collagen/Matrigel scaffolds. **Page 99**

Figure. 22. Transmission electron microscopic examination of insulin secretory granules in hESCs-differentiated pancreatic cells seed in 2D (A) and collagen/Matrigel scaffold (B). Scale bar = 2 μ m. **Page 100**

CHAPTER 1

INTRODUCTION

1.1. Stem cells

Stem cells are type of cells that have the capability of self-renewal and differentiation [1]. More explicitly, stem cells can divide and generate daughter cells that are identical to their mother cells (self-renewal), as well as give rise to other daughter cells that produce differentiated descendants with more lineage-restricted potential (differentiation). There are three basic types of stem cells: embryonic stem cells (ESCs), induced pluripotent stem cells (iPSCs), and adult stem cells (ASCs). Tremendous attentions and interests have been directed toward research in the area of stem cells, owing to their unique properties. By understanding stem cells, it will offer insight into the biology of cells as well as a path for cell replacement and transplantation therapy.

1.1.1 Embryonic stem cells

Shortly after fertilization, mammalian embryos undergo a series of divisions to form the morula, a solid ball-like aggregate of totipotent cells which, if isolated, have the ability to develop into a complete organism [2, 3]. Further cell divisions convert morula into a blastocyst, a cystlike structure with an inner cavity surrounded by cells. The cells of outer layer of blastocyst differentiate into the trophoblast that eventually become the placenta and sustains nutrient supply to the embryo. In contrast, the cells of inner layer, called inner cell mass (ICM), which remain pluripotent and are capable of extensive, perhaps unlimited, self-renewal, ultimately develop into the fetus. In 1981, similar work by Martin Evans and Matthew Kaufman as well as Gail Martin showed that mouse embryos can be cultured *in vitro* and ICM cells can be isolated from these

embryos and cultured outside the body without losing their pluripotency [4, 5]. These cultured cells were then named as embryonic stem cells (ESCs). In 1998, Thomson *et al.* developed a technique to isolate and grow human embryonic stem cells (hESCs) *in vitro* [6]. The isolation of stable hESCs from donated, otherwise discarded, human blastocysts, therefore, creates a potentially unlimited source of any human cell types, and thus sets the stage for cell replacement therapy. hESCs hold enormous promising for understanding development of many diseases as well as for treating devastating and currently incurable disorders such as spinal cord injury, neurological disease, blindness and type 1 diabetes.

1.1.2 Adult stem cells

Adult stem cells, also called somatic stem cells, are undifferentiated cells that reside in developed tissues of juvenile as well as adult bodies. Adult stem cells have the ability of indefinite self-renewal, so they can divide regularly to replenish dying cells and to regenerate damaged tissues. Unlike ES cells, the differentiation ability of adult stem cells are more lineage-restricted, i.e. they can only generate progeny of several distinct cell types, which related to their tissue origin (multipotency), as opposed to the pluripotency of ES cells. Adult stem cells have been found in blood, brain, muscle, skin, bone etc.

Adult stem cells have been successfully used for disease treatment for many years. Bone marrow transplantation has been approved for patients with inherited blood disorder, blood cancers such as lymphoma and leukemia, or who are undergoing chemotherapy or radiotherapy. Autologous hematopoietic stem cells (HSCs) have been successfully applied to treat spinal cord injury [7], liver cirrhosis [8] and peripheral vascular ischemia [9]. Mesenchymal stem cells

(MSCs) have been used in the treatment of patients with osteogenesis imperfect, infarcted myocardium, or joint disease [10-12]. Neural stem cells (NSCs) can differentiate to neurons, astrocytes and oligodendrocytes and have been used in a number of clinical trials for neurometabolic and neurodegenerative diseases like Parkinson's disease [13, 14]. Although the use of adult stem cells in research and therapy is not considered to be controversial, these cells may not be as versatile and durable as ESCs. First, adult stem cells are rare in adult tissues and are difficult to isolate and maintain *in vitro*. Also, their proliferation potential is not comparable to ESCs, so harvesting and culturing them up to scale for clinic purpose remains challenge. Second, adult stem cells are not able to produce all cell types, limiting their use in disease treatment. Furthermore, they are more likely to contain abnormalities due to environmental hazards, such as toxins, or from cell replication error.

1.1.3 Induced pluripotent stem cells (iPSCs)

In 2006, Dr. Yamanaka made a breakthrough discovery that through retroviral transfection of a defined set of transcription factors (Oct3/4, Sox2, c-Myc, and Klf4), adult somatic cells can be genetically reprogrammed into cells which have pluripotent capability and behave equivalent to ESCs, termed as induced pluripotent stem cells (iPSCs) [15]. This discovery has made Yamanaka won the Noble Prize in Physiology or Medicine in 2012. To date, iPSCs have been successfully generated from multiple types of human somatic cells, including fibroblasts [16-18], blood cells [19], neural progenitors [20], and terminally differentiated mature B lymphocytes [21]. Also, as alternatives to potentially harmful retroviruses strategy, multiple approaches have been proposed to generate iPSCs, including virus-free transposonsystem [22], mimicking transcription factors with small-molecule compounds [23-25], drug-inducible systems

[26, 27], recombinant proteins [28, 29] and microRNAs [30, 31]. The high degree of similarity between iPSCs and ESCs has been confirmed on many levels, such as the expression of certain stem cell genes and proteins, *in vitro* differentiation analysis, teratoma formation [15, 16, 18], epigenetic studies [32], and tetraploid complementation [33, 34]. The development of iPSCs allows researchers to obtain patient-specific iPSCs that are theoretically tolerant to immune rejection. Thus, the development of iPSC technology has provided a powerful tool for biomedical research and widened the era of hope for patient-specific cell therapy, drug discovery, and disease modeling.

However, the potential clinical application of iPSCs remains some limitations. First, the use of viruses for inducing iPSCs could potentially introduce cancers, which is considered a major obstacle to stem cell based regenerative medicine. Furthermore, although many similarities between ESCs and iPSCs, several studies have shown that these two pluripotent cell types display significant differences. A study of gene expression profile of mouse and human ESCs and iPSCs revealed that a recurrent gene expression signature appeared in iPSCs regardless of their origin or the method by which they were generated [35]. Also, reprogrammed iPSCs retained an epigenetic memory from their parental cells of origin, which directed iPSCs favor their differentiation along lineages related to the donor cells, while restricting alternative cell fates [36]. Meissen, J. K. *et al.* demonstrated that iPSCs showed metabolomic differences to ESCs, specifically for amino acids metabolism [37]. Also, a recent study reported that teratomas formed by iPSCs were mostly immune-rejected by recipients, which challenged the assumption of immunogenicity of iPSCs [38]. In addition, some studies showed iPSCs possess some somatic coding mutations of currently unknown functions [39-41].

1. 2. Current and future therapies for diabetes mellitus

Insulin-secreting pancreatic β -cells are important for regulating mammalian metabolism. The deficiency of β -cell functions leads to diabetes, making patients suffer from hyperglycemia and mainly dependent on exogenously supply of insulin. Generating new functional β -cells would provide unprecedented opportunities for diabetes treatment. Based on the progressed understanding on β -cell development and the discovery of pluripotent stem cells, tremendous progress has been made to generate new pancreatic β -cells, including discovering and improving conditions that promote β -cell replication *in vivo* and *in vitro*, differentiating pluripotent stem cells into insulin-secreting β -cells, or converting terminally differentiated cell types into β -cells. Here, we summarized existing technologies that have been developed for generating physiological functioning β -cells that might be potentially used for cell transplantation for diabetes treatment.

1.2.1. Diabetes mellitus

Diabetes mellitus is a leading metabolic disease characterized by hyperglycemia. Glucose level in blood is basically balanced by two types of cells, pancreatic β -cells and α -cells, which reside in pancreatic islets of Langerhans. Explicitly, increased glucose level stimulates insulin secretion by pancreatic β -cells. Tissues such as liver and muscle will sense the signal of insulin and take up glucose from the blood. In contrast, when glucose level drops, α -cells secrete glucagon and trigger the liver and muscles to produce glucose from stored glycogen. According to the statistics of the 2011 National Diabetes Fact Sheet from American Diabetes Association (ADA) (<http://www.diabetes.org>), 25.8 million children and adults have diabetes in the United

States alone, which is 8.3% of the population. Also, the total cost of diagnosed diabetes was \$245 billion in the United States in 2012. Worldwide, the prevalence of all diabetes types is increasing, and the total number of diabetes patients is estimated up to 366 million by 2030 [42]. Therefore, diabetes has become a growing global health problem with a striking impact on health, society and economy.

Diabetes is clinically classified into two major types: Type I or insulin-dependent diabetes (T1DM), which results from destruction of insulin-secreting β cells in the pancreatic islets of Langerhans by T cell-mediated autoimmune [43], and Type II diabetes (T2DM) or non-insulin-dependent diabetes, which develops when the body does not produce enough insulin or is not able to use it effectively, called insulin resistance, which is often associated with obesity, age and genetic component [44]. Insulin resistant in peripheral tissues such as fat and muscle causes high demand on β -cells and leads to β -cell malfunction, de-differentiation and death [44]. A decrease in β cell mass of up to 60% has been reported in T2DM [45].

Since the successful isolation of biologically active insulin in the early 1920s, exogenous insulin injection combined with blood glucose monitoring and lifestyle adaption has remained the main treatment for diabetes. Although exogenous supply of insulin have greatly improved the lives of diabetic patients, the method is inaccurate and was not fully capable of mimicking the tight control of endogenously produced insulin release from pancreatic β -cells, thus cannot completely control the minutes-to-minutes fluctuations in systemic blood glucose. Poorly managed diabetes can lead to secondary complications including infections, cardiovascular disease, renal disease, autonomic and peripheral neuropathy, as well as visual impairment which can progress to blindness [46]. Therefore, in order to prevent these complications and improve patients' life quality, more precise glycemic control is necessary. The ultimate goal of diabetes

therapy is to restore patients' physiological insulin-secretion capability through β -cell transplantation or regeneration.

1.2.2. Islet transplantation

Replenishing the functional β -cell mass is a commonly accepted strategy for diabetes treatment. The Edmonton Protocol first described an effective cell replacement therapy for T1DM [47]. Cadaveric donor islets were isolated and infused into the liver of diabetic patients *via* the portal vein, in conjunction with immunosuppressive regimen. The clinical outcomes of islet transplantation were very encouraging. The five year follow-up report from Shapiro and his colleagues reported that about 10% of the 65 patients enrolled in the Edmonton Center study remained insulin independence for 5 years after islet transplantation [48, 49]. The remaining patients, although not free from insulin replacement therapy, were protected from severe hypoglycemic episodes and diabetes-related complications. In recent data of 2010 annual report, the Collaborative Islet Transplantation Registry (<http://www.citregistry.org>) reported that about 25% of the 481 patients who received islet transplantation from 1999-2009 achieved insulin independence for 3 years.

The Edmonton protocol presents great potential as a treatment and cure for diabetes; however, its use has been limited by the scarcity of organs from cadaveric donors. Keymeulen *et al.* showed that the initial beta cell mass transplanted should be at least 2×10^6 cells/kg body weight in order to achieve a functioning graft and to achieve a reproducible metabolic control [50]; thus, the treating of one diabetic patient with this approach requires more than one donor for cell transplantation. Additionally, as islets are currently derived from cadavers, the host-graft

immune rejection is a significant limitation to transplantation therapy. Therefore, strategies to promote either the expansion of existing β -cells within the body or the supply of novel sources of clinically relevant β cell alternatives, which are reliable and reproducible, are currently debated as future treatment options.

1.2.3. *In vivo* regeneration of pancreatic β -cells

Inadequate β -cell mass is common to both type 1 and type 2 diabetes (T1DM, T2DM). Recent studies using genetic lineage tracing or other cell labeling methods have shown that the growth and regeneration of adult β -cells do not involve specialized progenitors or non- β -cells [51-53]. In contrast, the postnatal β -cell mass are predominantly maintained *via* self-replication of pre-excising β -cells rather than stem cell differentiation. In Dor *et al.*'s study, they labeled pancreatic β -cells with human alkaline phosphatase by Cre-loxP-based conditional recombination in adult pancreas, and chased the fate of pre-existing β -cells. The results showed that the labeling frequency of the β -cells remained unchanged, indicating that the new β -cells were generated primarily from pre-existing β -cells, rather than pluripotent stem cells, during adult life and after pancreatectomy in mice [51].

Normally, pancreatic size appears to be limited by the size of initial progenitor cell pool that is set aside in the developing pancreatic bud during embryogenesis [54]. Human adult pancreatic β -cells are known that they are highly specialized and have a low turnover rate due to tight cell cycle [55-57]. However, β -cell mass is dynamic and it undergoes significant changes under certain circumstances, including neonate, pregnancy and obesity. The pancreatic fractional area was increased by 1.4-fold to match dynamic physiological demands [58]. There is evidence

that circulating maternal hormones in the blood stream such as prolactin, placental lactogen can directly regulate β -cell proliferation in pregnancy through the intracellular factor menin [59-61]. Conversely, the turnover rate of β -cells slows down with aging [62]. Kassem *et al.* found that the rate of β -cell replication progressively decreased from 3% among fetal β -cells to less than 0.5% by 6 months of age [55]. The mechanism of these changes are unknown. At molecular level, there is evidence that cyclin-dependent kinase 4 (cdk4)-cyclin D complex is required for β -cell replication during neonatal and adult growth [63, 64]. In cyclin D^{-/-} mice, pancreatic islets were dramatically smaller and β -cell mass was reduced 4-fold in comparison to wild-type mice. Thus, cyclin D plays a key role in β -cell replication, which might be the primary mechanism underlying the maintenance of postnatal β -cell mass. Furthermore, a recent study showed that EGF-receptor signaling is essential in β -cell mass expansion in mice during high-fat diet and pregnancy [65]. These discoveries may provide a target for development of therapeutic strategies to induce the expansion of β -cells.

Most diabetic patients, even those with long-standing T1D, have a small number of β -cells that continually replicate and undergo destruction, thus giving a hope that diabetes may be cured by preventing autoreactive β -cell destruction, and/or by supporting replication of the surviving β -cells [66]. Therefore, screening for factors that increase β -cell replication *in vivo* may have direct therapeutic benefits to diabetic patients. *In vitro* studies have shown that nicotinamide, an inhibitor of poly (adenosine diphosphate-ribose) synthetase/ polymerase, has the ability to induce proliferation and differentiation of pancreatic endocrine cells [67, 68]. Betacellulin, a growth factor of epidermal growth factor (EGF) family, has shown to promote neogenesis of β -cells and ameliorate glucose tolerance in mice [69] and promote proliferation of β -cells in 90% pancreatectomized rats [70]. Exendin-4, an analog of GLP-1, has shown to

stimulate both β -cell proliferation and neogenesis in rat with 90% pancreatectomy, resulting in increased β -cell mass and improved glucose tolerance [71]. Also, the replication-inducing effects of exendin-4 have also been observed in human islets [72, 73]. Additional small-molecules acting as β -cell replication regulators, including phorbol esters, thiophene-pyrimidines, dihydropyridine derivatives and adenosine kinase inhibitors, have been identified through high-throughput screening of small molecular libraries for β -cell proliferation inducers in immortalized β -cell lines or primary rodent islets [74, 75]. More recently, Schultz *et al.* identified a novel small molecule, WS6, increased both rat and human β -cell replication *in vitro* by six-fold in dispersed islets and by more than ten-fold in intact islets [76].

Promoting endogenous β -cell replication by biological signals or small molecules is a promising treatment, but this method has not been applied for clinical application yet. A particular risk of such a strategy is the inadvertent promotion of tumorigenesis [77]. For success, putative molecules would have to show β -cell specificity. Also, targeted molecules would have to be tested with regard to their effect on other cell type within the body in order to exclude unwanted neoplastic effects. If we can find a way to harness endogenous β -cell replication without affecting other cell types, then we might develop a new therapy for diabetic patients.

1.2.4. *In vitro* expansion of pancreatic β -cells

In vitro expansion of pancreatic β -cells represents an attractive strategy for obtaining a substantial quantity of β -cells for transplantation. Studies have demonstrated that human β -cells have the capacity of *in vitro* proliferation; however, it was generally agreed that human β -cells are difficult to be expanded in culture due to their low turnover rate and loss of function easily.

Noguchi and colleagues showed that even after culture of 48-72 hours, human islets lost half the islet cells, as well as dramatically decreased glucose-stimulated insulin secretion (GSIS) *in vitro* and a reduced ability to restore normoglycemia after transplantation into diabetic mice [78]. These studies suggested that studies that are focused on identifying *in vitro* conditions for increasing the proliferative potential of adult human β -cells while maintaining their glucose-responsive insulin secretion is critical to realizing this treatment.

A line of evidence divulges that different growth factors and hormones, including glucagon-like peptide-1 (GLP-1), parathyroid hormone-related protein (PTHrP), lactogens, hepatocyte growth factor (HGF), insulin, and insulin-like growth factors (IGFs) are important to β -cell survival and maintenance of their function *in vitro* [79]. Additionally, several studies have been focused on exploring pathways that drive β -cell proliferation while maintaining their function. By using *in vitro* and *in vivo* models, the delivery of transcription factors associated with cell cycle, such as cyclin D1 [80, 81], cyclin-dependent kinases 2 (cdk2) [82], cyclin E [82], cdk6 [81, 83], c-Myc [84], and hepatocyte nuclear factor-4 α [85], has been shown promising for enhancing the replication of adult human β -cells and their functions *in vitro*. More recent study showed Wnt/GSK-3/ β -catenin and mTOR signaling pathways are necessary to stimulate growth and proliferation of human β -cells [86, 87]. Despite the development of various strategies that promote the replication of β cells by using growth factors or molecules, the risk of cancer after transplantation would be particularly important to consider.

With more insights gained into the pancreas structure in the last decades, researchers realized that another reason for the loss of β -cell functions in *in vitro* culture is the change of cellular environment. Most β -cell expansion cultures are carried out based on monolayer culture, which neglects one of the important tissue niches, i.e. extracellular microenvironment essential

for maintaining cell functions. *In vivo*, β -cells reside in a three-dimensional (3D) islet structure and interact directly with basement membranes in fetal and adult tissues [88]. Thus, re-establishment of the islet-matrix relationship to mimic *in vivo* environment may present a natural stimuli for *in vitro* β -cell expansion. A line of studies has showed that extracellular matrix protects pancreatic β -cells against apoptosis and improves their insulin-secreting function [89, 90]. However, the underlying mechanism for these improvements remains elusive.

Some reports suggested that β -cells cultured *in vitro* can dedifferentiate through epidermal-mesenchymal transition (EMT), a biological process in the development stage that allows a polarized epithelial cell to go through multiple biochemical changes and assure a mesenchymal cell phenotype and finally be directed redifferentiating into insulin-secreting β -cells [91, 92]. However, the β -cell phenotype was not fully recovered, such as the new β -cells expressed only a fraction of their original insulin levels. Moreover, the origin of these new β -cells derived in this way is not clear due to a possible contamination by other pancreatic cells which are mitotic active, e.g. duct, acinar, stromal, and endothelial cells, suggesting that these cells do not represent a useful source for the generation of physiological competent β -cells for diabetes treatments [93].

1.3. Directed differentiation of hESCs towards pancreatic β cells

1.3.1. Pancreas and β -cell development

In embryogenesis, three germ layers are formed during gastrulation: ectoderm, mesoderm, and endoderm. A thin cup-shaped sheet of definitive endoderm (DE) is formed between embryonic day E5 and E6 in mice. DE develops into the primitive gut tube that can be divided

into several region with distinct development potential and gives rise to different endodermal organs such as liver, lung, thymus, stomach, pancreas [94]. The first specification of pancreas occurs around embryonic day 8.5 (E8.5) in mice and 3 weeks in human, with the independent budding of the dorsal and ventral buds in the posterior region of foregut [95]. The formation of pancreatic bud is marked by the expression of the pancreatic and duodenal homeobox 1 (Pdx1). Lineage tracing studies demonstrated that Pdx1 is expressed from E8.5 until adults and Pdx1⁺ multipotent progenitors give rise to all pancreatic cells [96]. Soon later, these two buds grow into the surrounding mesenchymal, branch in a tree-like structure and eventually fuse after rotation of the gut to form definitive pancreatic endoderm around E12.5 [95]. The formation of endocrine progenitors is marked by the expression of transcriptional factor neurogenin 3 (Ngn3). Genetic lineage tracing studies showed that Ngn3⁺ cell exclusively give rise to pancreatic endocrine cells [66]. Loss of functional phenotype of Ngn3⁺ cells leads to the specific and complete loss of all pancreatic endocrine cells, while exocrine and duct compartment remain unaffected. The expression level of Ngn3⁺ reaches maximum around E15.5 and declines towards birth. Subsequently, the predifferentiated epithelium grows significantly in size and with distinct endocrine and exocrine differentiation. Endocrine cells migrate into mesenchymal and aggregate into islets of Langerhans. Although in the endocrine compartment, glucagon-expressing cells, and dual glucagon- and insulin-expression cells appear as early as E9.5, these cells do not contribute to mature islets of adult animals. The fully differentiated β -cells and other true hormone-secreting cells become evident around E13.5. At E14.5, dramatic changes in pancreatic development, termed as secondary transition, lead to the generation of numerous endocrine and exocrine cells. During the final stages of islet formation and maturation, vascularization and nerve innervations are frequently observed [97].

Pancreas contains two types of functional compartment: endocrine and exocrine.

Exocrine compartment occupies more than 90% of the pancreatic mass. Residing in the exocrine compartment, there are acinar cells that secrete digestive enzymes such as lipases, carbohydrates, and amylases, as well as ductal cells that transport these enzymes into the duodenum [98].

Although hormone-secreting endocrine cells make up only 1-2% of the pancreatic cell population, they play an essential role in regulating glucose concentration in the body. Endocrine compartment harbors five different endocrine cell types residing in islets of Langerhans: insulin-producing, glucagon (GCG)-secreting α cells, somatostatin (SST)-secreting δ cells, pancreatic polypeptide (PP)-secreting PP cells, and a newly found ghrelin (GHRL)-secreting ϵ cells. β cells are the most abundant cell population in the islet. In rodents, β cells make up 60-80% of the islet and are located in the center of islets, surrounded by other endocrine cells [99]. Human endocrine islets are composed of 40-60% β -cells and 30% α -cells. The β -cells are mixed with other endocrine cells and are distributed evenly throughout the islet structure.

Many of the studies took years to work on embryonic development in order to deepen our understanding for directed differentiation of ES cells into therapeutic β cells. Despite significant progress achieved in understanding pancreatic development, many aspects of pancreatic organogenesis are still a mystery. Therefore, studies addressing progressive lineage commitment mechanisms and cell fate in organogenesis are of great value and significance for understanding cell fate in pancreas development and directed differentiation.

1.3.2. ESC-derived insulin-producing β cells

After the isolation of mammalian ESCs and the establishment of *in vitro* culture conditions for maintaining their pluripotency, numerous approaches have been developed to generate insulin-producing β cells from ESCs. The first report of the *in vitro* generation of β -like cells was based on the selection of nestin-positive progenitor cells derived from mouse ESCs in 2001 [100]. This approach was proposed based on the idea that adult pancreas and central nervous system (CNS) have similar developmental mechanisms and induced production of neural cells from ES cells could be adapted for endocrine pancreatic cells. However, cells generated by using this protocol showed low insulin production and poor insulin secretory response. Also, later studies showed that nestin-positive progenitor cells give rise to insulin-producing cells as a result of uptake of exogenous insulin [101, 102].

In 2001, Assady et al. first reported that insulin-producing β cells can be generated from hESCs by spontaneous differentiation [103]. It was the first proof-of-principle study showing that hESCs was a potential candidate for generating β cells *in vitro* for cell therapy, even though the number of insulin-positive cells was low. As of today, many groups have claimed the generation of β cells from hESCs *in vitro* with modulated progress. The real breakthrough of hESCs differentiation into β cells was transformed by D'Amour and colleagues in 2006 [104], who first developed the stepwise approach by mimicking pancreatic organogenesis using signals that regulate embryonic endoderm and pancreas formation.

The first and most crucial step in differentiating hESCs towards pancreatic lineage is the specification of DE. Efficient DE differentiation is a prerequisite for generating therapeutic insulin-producing β cells. Studies have shown that both TGF- β and Wnt signals are critical for DE formation during gastrulation. Activin A, a TGF- β family member, has been used together with Wnt3a to effectively induce DE specification [104-106]. Recent studies showed that the

removal of a serum during the initial differentiation step was critical because serum components contain activators of the phosphatidylinositol 3-kinase (PI3K) pathway that antagonizes the ability of hESCs to differentiate in response to Activin A and Nodal [107]. Further studies revealed that the inhibition of PI3K signaling using inhibitors such as LY294002 and wortmannin can efficiently promote the differentiation of hESCs into DE [108, 109]. Approximately 70%~80% hESCs can be differentiated into DE cells under the treatment with PI3K pathway inhibitors, which is higher than that achieved by activin A or Nodal treatment alone [107]. The efficiency of DE formation can be confirmed by quantitative PCR and immunohistochemical staining patterns of endodermal markers including SOX17, Foxa2, and CXCR4. Expression of mesendoderm markers like Brachyury, spikes rapidly upon activin treatment and then quickly decreases when cells assume endodermal properties.

1.4. Extracellular matrix (ECM) and stem cell

1.4.1. The role of ECM in stem cell niches

Stem cells reside in a dynamic, specific microenvironment termed as ‘niche’, which provides extrinsic signals to control stem cell behaviors, in particular the balance between self-renewal and differentiation. It helps sustain a stem cell pool within each tissue/organ. Since the concept of niche was first proposed by Scholfield in 1978 in reference to mammalian hematology [110], the content of the niche has increased in complexity. Generally, niches are composed of stem cells and supportive stromal cells, together with the ECM in which they are located. Also, some other factors, such as growth factors, cytokines, oxygen tension, as well as

physiochemical factors including pH, ionic strength, shear stress and metabolites, within niches are contributed to the regulation of stem cell behaviors [111]. However, the niche factors are highly specialized for each type of stem cells, mainly depending on the defined anatomical localization and function of the tissue[112]. A line of studies suggests that niches are critical for maintaining stem cell function and the deregulation of the stem cell niche is involved in a number of diseases associated with tissue degeneration, aging and tumorigenesis [113]. Thus, the ability to replicate *in vivo* stem cell niches *in vitro* is likely a critical requirement for developing fully functional cell types from stem cells.

ECM, a three-dimensional network of fibrous proteins and polysaccharides, has been recognized as an important component in niches. It plays many essential roles in regulating stem cell fate. The primary components of ECM are fibrous structural proteins, such as collagen, fibronectin and laminin, and proteoglycans such as glycosaminoglycans, heparan sulfate, chondroitin sulfate and non-proteoglycan polysaccharide like hyaluronic acid [114]. In living tissues, cells synthesize these macromolecules and deposit them into the existing matrix *via* exocytosis. However, the composition and assembly pattern of the ECM vary widely among tissues. The intrinsic properties of ECM, such as matrix composition, structure, and elasticity, are extremely spatially- and temporally-controlled, suggesting that they play a morphogenetic role in guiding stem cell differentiation. Studies on the dynamics of the ECM have shown that the interplay between cells and ECM is reciprocal [115]. As a scaffold, ECM provides anchor sites for cells to attach and a structural support for tissues. Cells are not only able to sense and respond to their outside environment, but also to change their environment's chemical and mechanical properties through various signal transduction pathways. These interactions further deliver signals to residing stem cells for guiding cell growth, differentiation, migration, survival and

reorganization of the resident tissue [116]. Evidences have shown that laminin is the first ECM protein produced in the eight-cell stage of embryos and involved in cell adhesion and migration during gastrulation, whereas fibronectin, collagen, and heparan sulfate glycosaminoglycans are produced later and assist further in germ layer differentiation and ultimate organogenesis [117, 118]. Numbers of studies have shown that the mutation or depletion of ECM genes such as collagen, fibronectin, laminin, etc. can either impair tissue remodeling during embryonic development or result in post-natal lethal phenotypes [119-121]. Therefore, the recognition of the importance of ECM encourages the creation of 3D systems for growing and differentiating stem cells.

1.4.2. ECM-stem cell interaction

Stem cells interact with ECM directly *via* cell membrane receptors, known as integrin. Integrins are heterodimeric transmembrane receptors composed of α and β subunits, with extracellular domains that bind to ECM, and cytoplasmic domains that are associated with actin cytoskeleton and affiliated cytoplasmic proteins, such as talin, vinculin, paxillin, and α -actinin [122]. Not only being as an integrated hook that couple the inside of a cell to ECM, integrins also transduce external signals to the cytoskeleton and recruit a number of intracellular proteins to ECM ligand-integrin binding sites, such as focal adhesion kinase (FAK), mitogen-activated protein kinases (MAPKs). The activation of these signal-transduction pathways ultimately leads to specialized patterns of gene expression and enforces a cellular decision on biological functions such as adhesion, migration, proliferation, differentiation and survival [123, 124].

At least eighteen α and eight β subunits have been characterized in mammals and different types of integrins are involved in their ligand-binding specificities. ECM protein Collagen I regulates the self-renewal of mouse embryonic stem cells through $\alpha_2\beta_1$ integrin [125]. The $\alpha_6\beta_1$ integrin, a laminin receptor, is required for the adhesion of neural stem cells (NSCs) to their vascular niche [126]. Moreover, α_6 integrin is identified as the only common element of a variety of "stemness" signatures on ES cells, embryonic NSCs, and hematopoietic stem cells [127]. An increasing body of data suggests that β_1 integrin maintains stem cell niche, preserving a stable stem cell population by controlling the balance between symmetric and asymmetric division, and strictly regulating stem cell self-renewal and differentiation by modulating Notch activity [125, 128-130]. Therefore, it is possible to engineer integrin-dependent cellular interactions with ECM to control stem cell fate.

1.4.3. ECM and growth factors presentation

Beside the ability to interact directly with stem cells, recent studies discovered that ECM also modulates stem cell behaviors by binding and establishing stable gradients of growth factors. ECM proteins like fibronectin, vitronectin, collagens and proteoglycans (PGs) themselves, or in combination with heparin and heparin sulphate, bind avidly to many growth factors, such as fibroblast growth factors (FGFs), hepatocyte growth factor (HGF), vascular endothelial growth factors (VEGFs), BMPs and TGF-beta through conserved structure modules [131]. Moreover, in some cases, the interaction between growth factors and ECM is required for the binding of growth factors to their receptors on the surface of cells. The interaction of FGF and heparan sulfate chain is necessary for its binding to the receptor (FGFR) [132], and transforming growth factor- β (TGF- β) first bind to integral-membrane PGs during signaling [133]. Alternatively, the

intrinsic domains within ECM proteins may act as ligands for canonical growth factor receptors [116]. For example, EGF-like domain from laminin [134] or tenascin [135] can bind to EGF receptors (EGFR) as solid-phase ligands and trigger signal as those induced by soluble ligands. ECM proteins degradation by proteolytic enzymes metalloproteinases can induce local release of intrinsic growth factor-like fragments of ECM proteins or matrix-bound growth factors from their insoluble anchorage. Thus, ECM acts as a sink or reservoir of growth factors (bound or intrinsic), which can be released to modulate the biological activities of stem cells.

Interaction between growth factors and ECM matrix can influence the biological activities of growth factors. The binding of growth factors to ECM proteins protects them from proteolytic degradation and increases their stability. Studies showed that heparin potentiates the activity of growth factor FGF by prolonging its biological half-life from 7 to 39 hours [136]. Also, the interaction with ECM affects the diffusion of growth factors. Basic FGF diffuses further in the presence of heparin because bFGF-glycosaminoglycan complex partitions into a soluble phase rather than binding to insoluble glycosaminoglycans in ECM [137]. It is suggested that the complex of bFGF and glycosaminoglycan may represent one of the active forms of bFGF *in vivo*. Also, ECM functions as a physiological buffer that can trap growth factors at a high concentration and release it slowly for binding to its receptor [138]. This may explain why growth factors released over a short period of time can stimulate a long-term process like angiogenesis. In turn, the interaction of growth factors and ECM may provide signals to stem cells to modulate the expression of ECM molecules or cell surface receptors [139, 140]. It has been proven that TFG- β stimulates the expression of major ECM proteins such as fibronectin and collagen and their incorporation into the matrix [141]. Also, growth factors exert a selective

effect on ECM deposition by regulating the expression of matrix degrading enzymes such as collagenase and metalloproteinase inhibitors [140].

1.4.4. ECM biomechanical properties and stem cell fate determination

In the stem cell niche, not only biochemical properties of ECM compositions regulate a balance between self-renewal and differentiation of cells, but physical and mechanical forces in the local stem cell microenvironment, including the elasticity or stiffness of the ECM and the compression forces exerted by neighboring cells, also contribute to the signaling pathways that are critical for cell development and differentiation. The mechanical properties of ECM are determined by a network of collagen, fibronectin, etc. [142]. The stiffness of a substrate leads to an increasing level of intracellular tension by the contraction of cytoskeletal proteins and triggers "pulling" forces against the matrix. Reciprocally, the forces generated inside of a cell transmit through adhesion proteins to their surrounding structures, and induces the adaption of their mechanical properties to the microenvironment. The interplay between cells and their microenvironment generates an isometric tension within the cytoskeleton. Together with signals from growth factors and morphogens, mechanotransduction pathways that involve Ras/MAPK, PI3K/Akt, Rho/ROCK, Wnt/ β -catenin etc. finely tune the gene expression that allows the maintenance of cell shape and the regulation of cell behaviors [142-144].

It has been discovered that matrix elasticity (or stiffness) can direct stem cell lineage specification. The mechanical deregulation in ECM is also found to be associated with aging, disease, and injury. Diseased tissues often overexpress ECM components, making the tissue more rigid and inhibit the cells' contractility and differentiation. For instance, the grafting of

MSCs after myocardial infarction fails in regenerating contracting cardiomyocytes due to scar-like rigidity in the muscle [145], and instead it induces the trans-differentiation of these cells into bone-like structure in the infarcted myocardium [146]. The elasticity of cell niches varies among tissues, from brain tissues (0.1 kPa) to bone tissues (>30 kPa). Such natural variations in mechanics also occur during embryonic development, e.g. $E_{ESC} < E_{Endoderm} < E_{Ectoderm}$. Thus, the temporal and spatial changes in ECM may guide hESCs as they mature and assemble into tissues. However, most studies on cell biology have been performed on a plastic dish or glass, whose elastic modulus is several orders of magnitude higher than nature tissues, which is one of the possible reasons leading to de-differentiation or loss of function in these cells in some cases. Thus, the development of *in vitro* technologies to mimic tissue elasticity would help stem cells mature and assemble into functional tissues. A body of studies has demonstrated that stem cell commitment changes in correspond to a 3D microenvironment. When human mesenchymal stem cells are cultured on ECM characterized by stiffness values that mimic the elastic moduli of brain, muscle or bone, they undergo tissue-specific cell fate into neurons, myoblasts and osteoblasts, respectively [147]. Also, the increasing of substrate stiffness from 0.041 MPa to 2.7 MPa has found to be able to promote mesendodermal gene expression and terminal osteogenic differentiation in ESCs [148]. Moreover, the inhibition of myosin II blocks all elasticity-directed lineage specification, implying the physical effects of the microenvironment on stem cell differentiation [147, 149]. Therefore, the mechanical environment should be taken into consideration when engineering scaffolds or producing therapeutic cells *in vitro*.

1.4.5. Engineering three-dimensional (3D) scaffolds for stem cell differentiation

Most of stem cell studies have been performed using two-dimensional (2D) cultures. Even though conventional 2D cultures have provided the benefit of ease, convenience, a high cell viability, and also a simplified approach for understanding basic cellular behaviors. Nevertheless, recent knowledge on 3D microenvironments has revealed a lot of drawbacks of this approach. 2D culture is limited in its ability to present spatial and temporal cues to cells. Furthermore, the metabolism and gene expression patterns of cells are frequently altered during growth in 2D culture [150, 151]. Thus, 2D culture is not sufficient to reveal the real situation in the body.

The recognition of the importance of dimensionality of cellular environment has encouraged the creation of 3D cell culture matrices, also known as scaffolds. These scaffolds are porous substrates that mimic a 3D niche, providing an ideal platform for cell-cell and cell-matrix communications, and serving as biointeractive stages to support cell growth, migration, differentiation and organization. The feasibility of a 3D culture for hESCs differentiating into neural [152], cartilage [153], bone [154], vascular [155] and liver [156] tissue have been reported. Notably, ESCs in 3D cultures have been found to display higher degree of functionality and ability of differentiation than those cultured in a 2D culture system [157]. Moreover, hESCs that are differentiated in 3D matrices tend to form 3D structures similar to *in vivo* architecture. For examples, hESCs differentiated in a 3D scaffold have shown to form 3D intestinal 'organoids' consisting of a polarized, columnar epithelium that is patterned into villus-like structures and crypt-like proliferative zones expressing intestinal stem cell markers, whereas 2D culture did not [158].

A wide range of biomaterials has been developed to for their use in 3D studies. Based on its properties, each biomaterial is classified as either natural or synthetic. Synthetic biomaterials

include polymers, ceramics, and metals. These synthetic materials offer the versatility of creating 3D microenvironments with tunable features, such as controllable mechanical properties, degradation rates, porosities, and defined chemical compositions. Biodegradable poly (lactic-co-glycolic acid) (PLGA)/poly (L-lactic acid) (PLA) polymer scaffolds have shown promoting for hESC proliferation and differentiation into 3D structures such as neurons, cartilage, or liver [159]. Many of these synthetic biomaterials, however, have poor adhesion properties due to lack of sites for stem cell attach and proliferate. Moreover, these materials can trigger an immune response. The biocompatibility of these materials is another concern for their suitability for transplantation *in vivo* [160]. The biological or chemical modification of these synthetic materials is thus necessary but remains challenge.

On the other hand, natural materials are attractive and have been frequently used for developing various scaffolds for stem cell studies. They consist of components either found in ECM, such as collagen, fibrinogen, hyaluronic acid, glycosaminoglycans (GAGs) or some other polysaccharides derived from plants, insects or animal components, such as cellulose, chitosan, dextran and alginate. Naturally derived biopolymers offer many advantageous properties that are favorable for stem cell studies. First, these materials are usually biocompatible and have cellular binding domains for cell adhesion and phenotype regulation. Second, they are intrinsically bioactive and can regulate stem cell behaviors orchestrated with soluble signaling factors. For example, adhesion to vitronectin and collagen I has shown to promote osteogenic differentiation [161]. In addition, in recent years, many of these natural materials, e.g. chitosan, hyaluronic acid, silk, Matrigel™ have been well characterized and become commercially available, with reproducible and controlled properties. Among ECM, collagen is the most abundant protein in mammals, comprising 25% - 33% of the whole-body protein mass [162]. So far, twenty-eight

types of collagens have been identified, specifically, type I collagen is the most frequently used to form hydrogels for 3D studies. 3D collagen scaffolds have been used to culture a wide variety of stem cells for forming different variety of tissues, such as bone, cartilage, heart, ligament, nerve, and vasculature. However, the use of a collagen gel for hESCs pancreatic differentiation has not been reported yet.

Objectives and Hypothesis

The use of hESCs as unlimited cell sources for generating transplantable β cells has ignited the hope for cell-based diabetes treatment. Current studies have mostly been focused on stepwise hESC differentiation approaches that use cocktails of various soluble signaling molecules for directing hESC pancreatic lineage differentiation. However, cells generated with these protocols have exhibited immature pancreatic endocrine phenotypes and cannot function normally *in vivo* to correct the glucose level after transplantation in diabetic animal models. A major difference between β -cell in the pancreas and the β -cell generated *in vitro* lies in the different environment they reside in. Studies on pancreas organogenesis suggest that the development of β cells highly depend on the interaction with various physicochemical cues in their surrounding microenvironment. Thus, a 3D culture system would be advantageous to imitate *in vivo* stem cell niches favoring cell-cell and cell-matrix interaction. In this work, we explored the feasibility of ECM-based scaffolds for enhanced pancreatic differentiation from hESCs.

We hypothesized that the pancreatic β -cell differentiation can benefit from a collagen I based ECM scaffold. First, we investigated whether the most critical stage in pancreatic differentiation—DE differentiation can be enhanced using a 3D collagen scaffold. Second, we examined the combinatorial effect of ECM proteins on DE differentiation from hESCs, in order to produce a robust protocol for endodermal lineage differentiation. Third, we examined the pancreatic β -cell differentiation from hESCs in collagen-based ECM scaffold. This research will help establish a robust protocol for generating mature β cells that can secrete insulin functionally for cell-based diabetes treatment.

CHAPTER 2

Differentiation of Human Embryonic Stem Cells into Definitive Endoderm in Type I Collagen Gel

2.1. Abstract

The production of pancreatic insulin-producing cells from human embryonic stem cells (hESCs) has emerged as one of the most attractive cell therapy strategies for insulin deficient diabetes treatment. Here, we established a three dimensional (3D) model to culture and differentiate hESCs that are embedded in type I collagen gel. Both single cell and cell cluster seeding approaches were tested. We discovered that cell clusters were formed within 3D collagen scaffolds no matter what seeding format was used. However, cell cluster seeding yielded better cell proliferation. By comparing the DE marker gene expression in cells differentiated within 3D collagen scaffolds and traditional 2D cell culture plates, we found that 3D niches significantly enhanced the DE marker gene expression. The expression of Sox17, Foxa2, and CXCR4, three DE marker genes, in 3D cultures increased 4.5 fold, 5 fold and 4.2 fold compared to 2D differentiation. Furthermore, our experimental results suggest that DE differentiation benefits from single cell seeding when forming 3D cell differentiation scaffolds.

2.2. Introduction

Embryonic stem cells (ESCs) can differentiate into any type of cells in the body. The generation of insulin producing cells from hESCs emerged as the most attractive alternative for diabetes treatment. Current knowledge revealed that the ultimate success of an *in vitro* approach to program ESCs into functional insulin-producing β -cells largely depend on the ability to

sequentially reproduce the individual steps that characterizes normal β -cell ontogenesis during fetal pancreatic development [163]. During this process, the first and the most critical step is the generation of definitive endoderm (DE) population, which can be further induced to adopt a pancreatic endocrine progenitor fate and finally differentiate into β -cells [105, 163, 164]. Unfortunately, many studies overlooked this principle tenet of development and thus limited the progress of generating physiological functioning mature cells in the end. Therefore, it is highly desirable to develop an efficient and reproducible protocol on initial commitment of hESCs towards definitive endoderm.

In the past decades, strategies for inducing DE cells from hESCs has been focused on the use of cocktails of various soluble signaling molecules such as Activin A/nodal, WNT, and FGF, which mimic the key biochemical signaling received by cells during ingress at the primitive peak *in vivo* [165, 166]. Although considerable progress has been made towards DE differentiation *in vitro*, a number of questions and problems remain. For example, although signaling pathways are conserved among many species, their particular functions (repressive or inductive) may vary significantly among other species and activity change with timing, explaining in part the contrasting findings between hESCs and mESCs or different hESC cell lines. Also, these methods produce heterogeneous cell population and furthermore, express pluripotent genes which pose a significant risk of teratoma formation and hind the further application for clinical use [167]. In addition, mature functional β -cells have yet to be convincingly produced *in vitro* [104, 168]. These findings indicate that the use of signaling molecules alone is insufficient to resemble an *in vivo* environment for embryonic development and there may be important factors are neglected in current differentiation protocols.

In nature tissues, cells interact not only with each other, but also with the three-dimensional (3D) extracellular matrix (ECM). Thus, there is a growing interest in developing 3D scaffolds to mimic the local biochemical and mechanical 3D niche and modulate the behavior of stem cells [159, 169]. A line of studies have demonstrated that hESCs that were cultured on 3D biodegradable scaffolds showed distinct characteristics of their cell cycle and enhanced ability to expand and differentiate as compared to those grown on conventional two-dimensional (2D) culture (monolayer cultures on flat plastic cell culture plates/dishes) [156, 170]. Also, it has been reported that ESCs could be induced to differentiate into neural, epithelial, and endothelial lineages in 3D biodegradable scaffolds and form 3D tissue structures that were not observed in 2D culture [159, 171]. 3D structure could be critical for maintaining ESCs' native function and recapitulate embryonic development *in vitro*. The use of a 3D scaffold for ESC differentiation would help develop mature functional cells for cell therapy.

Collagens are most abundant components in the ECM and are fibrillar structural proteins. Due to its biocompatibility and its biodegradable property, it has been widely used as a biomaterial to construct 3D tissue models for investigating cell behavior and differentiation. It has reported that type I collagen can enhance viability and function of many cell types, including smooth muscle cells, neural progenitor cells and hepatocytes [172-174]. Also, collagen I has been shown to improve the differentiation ability of ESCs towards different specific cell lineage [156, 175]. Especially, collagen I 3D culture promotes the reorganization of pancreatic endocrine cell monolayers into islet-like organoids as well as improves β cell survival and insulin secretion [176, 177]. Wang et al. showed 3D collagen scaffold promote ESCs into pancreatic β -cell lineage specification in a mouse cell model [178]. Thus, it has been widely accepted that both

chemical and physical factors, as well as geometric or topographical features of 3D scaffold, contribute collectively to modulate the differentiation of stem cells into specific lineage.

In this study, we hypothesized that the 3D collagen culture may benefit for hESC proliferation and directed differentiation towards definitive endoderm, thus helpful for establishment of a rigorous, standard protocol of fully functional insulin-producing β cells for islet transplantation.

2.3. Materials and Methods

2.3.1. hESC culture

Undifferentiated hES cell line, H9, was acquired from Wicell Research Institute (Madison, WI). Cells were cultured on mitotically inactivated mouse embryo fibroblasts (MEFs) feeder layers in DMEM/F12 medium (HyClone) supplemented with 20% (v/v) Knockout serum replacement (KOSR, Gibco), 2 mM L-glutamine (Cellgro), 0.1 mM 2-mercaptoethanol (β -ME, A.G. Scientific), 1 mM non-essential amino acids (Invitrogen), and 4 ng/ml basic FGF (bFGF, Peprotech). Cells were passaged at a 1:4~1:6 split ratio every 4~7 days through collagenase IV (1 mg/ml, Sigma) treatment combined with manual dissociation. Before use, cells were transitioned from feeder-dependent culture to feeder-free culture to eliminate MEF feeder cells. Briefly, cells were seeded on Matrigel (BD biosciences)-coated plates in mTeSR1 medium (StemCell Technologies, Vancouver, Canada) and maintained in an undifferentiated state under feeder-free conditions. Cultures were passaged at a ratio of 1: 3~1:5 every 3~5 days cells using 1 mg/ml dispase (StemCell Technologies, Vancouver, Canada). The cultures were incubated at 37°C in the atmosphere supplemented with 5% CO₂. The cell culture media exchanged daily.

2.3.2. 3D hESC definitive endoderm differentiation

3D scaffolds were prepared as follows: a type I rat tail collagen solution (BD Biosciences) was first diluted with sterile water and 10X phosphate-buffered saline (PBS, Cellgro) to achieve a final collagen concentration of 1.67 mg/ml. The pH of the diluted collagen solution was then adjusted to 7.4 using 1 N NaOH. The solution was subsequently chilled on ice to prevent from gelation. At the same time hESCs were treated with Accutase™ (Millipore) or dispase (1 mg/ml) (StemCell technology) in order to obtain single cells or cell clusters suspension. The enzyme treated cells were suspended in 10× DMEM medium (maintaining physiologic osmolarity at 250~300 mOsM) and then added to the ice-chilled collagen solution to achieve a final collagen concentration of 1.5 mg/ml and the cell density of 2.5×10^6 cells/ml. Thereafter, 0.4 ml aliquots of the cell-collagen mixture were transferred into wells of a 24-well tissue culture plate and incubated at 37°C, 5% CO₂ for 30 min to form scaffolds. Once a scaffold has formed, 0.5 ml of the cell culture medium was added to the top of the scaffold. The cell-laden scaffolds were then placed into a CO₂ incubator and allowed cells to grow for 24 hours before initiating DE differentiation.

DE differentiation was carried out by following a protocol developed by D'Amour *et al.* [104]. In brief, hESCs were washed briefly with PBS^{+/+} (Cellgro) before initiating the differentiation and then cultured in RPMI 1640 medium (Gibico) supplemented with recombinant growth factors 100 ng/ml Activin A (PeproTech Inc.) and 25 ng/ml Wnt3a (PeproTech Inc.) for 1 day. After 24 hours, the medium was replaced with a fresh RPMI 1640 medium supplemented with 0.2% defined FBS and 100 ng/ml Activin A. The differentiation continued for another 72 hours.

2.3.3. Scanning electron microscopy (SEM)

Cell-collagen scaffolds were fixed with 2.5% (v/v) glutaraldehyde (EM Sciences, Fort Washington, PA) at pH 7.4 for 2 h. After washing with PBS each for 10 min three times, the scaffolds were post-fixed in 2% osmium tetroxide (EM Sciences) for 2 h and dehydrated with 25%, 50%, 75%, 85%, 95%, and 100% (v/v) of ethanol before lyophilization. The lyophilized scaffolds were mounted on aluminum stubs with a double-stick carbon tape and sputter coated with gold before SEM, using a Jeol Field Emission scanning electron microscope (JSM-6335F; JEOL USA, Peabody, MA) at an accelerating voltage of 10 kV.

2.3.4. Cell viability assay within 3D collagen scaffolds

The cell viability within a collagen scaffold was determined using calcein-AM/propidium iodide (PI) staining kit (Falcon) by following the manufacture's instruction. The kit contains two fluorescent probes that measure cell viability. Live cells are stained with green fluorescence due to the enzymatic conversion of the nonfluorescent, cell-permeate dye calcein-AM to the intensely fluorescent calcein (excitation: 495 nm, emission: 515 nm). Dead cells are identified by staining with PI, which enters cells with damaged membranes, and, upon binding to nucleic acids, produces a bright red fluorescence (excitation: 495 nm, emission: 635 nm). PI is excluded by the intact plasma membrane of live cells. Live/dead staining was prepared with 2 mM calcein AM and 4 mM PI in PBS. Form assessment of immobilized cells, 0.2 ml of the dye solution was added to 0.4 ml scaffold samples. The samples were incubated with the dyes (calcein AM and PI) for 10 min. The dye solution was removed and 0.5 ml of PBS was added and incubated for another 30 min. The PBS buffer was subsequently removed in order to

stabilize the cell containing scaffold before taking microscopy images with an Olympus upright fluorescence microscope (IX71, Tokyo, Japan) equipped with a supersensitive CCD camera (mode number ROLERA-XR, Surrey, BC, Canada) controlled by an imaging analysis software Slidebook (Intelligent Imaging Innovations, Inc., Denver, CO).

2.3.5. AlamarBlue cell proliferation assay

The proliferation of hESCs and their derived cells during DE differentiation within 3D scaffolds was determined using an oxidation–reduction indicator alamarBlue (Alamar BioSciences, Sacramento, CA) agent that reacts to viable cells, generating fluorescence to detection. To evaluate cell proliferation within the collagen scaffolds during DE differentiation, we inoculated the scaffolds with 2.5×10^6 cells/ml hESCs. hESCs were differentiated into DE cells, as described above. At specified time intervals, 400 μ l of differentiated medium containing 10% alamarBlue was added to each well after washing the scaffolds once with PBS buffer and the plate was incubated at 37°C for 4 hrs. The fluorescence of the cell culture broth was measured by fluorescence spectrophotometer using a fluorescence excitation wavelength of 540–570 nm (peak excitation is 570 nm). Read fluorescence emission at 580–610 nm (peak emission is 585 nm). All measurements were performed at room temperature. Finally, results were analyzed by plotting fluorescence intensity versus a duration time.

2.3.6. RNA extraction and quantitative RT-PCR (qRT-PCR)

Total RNA was extracted from cultured cells using the RNeasy Plus Mini kit (Qiagen, Valencia, CA). RNA samples were digested with DNase I (1 unit per μ g RNA, Promega Corporation, Madison, WI) prior to reverse transcription (RT) to remove any contaminated

genomic DNAs. A portion of 1 µg of RNA was used to prepare cDNA. The reverse transcription was performed using ProtoScript® First Strand cDNA Synthesis Kit (New England Biolabs). Quantitative PCR was carried out using Realplex Real-Time PCR machine (Eppendorf). The PCR reaction solution consisted of 10 µl of SYBR Green PCR master mix (Roche), 0.15 µl of 10 mM forward and reverse primers that are specific to the target marker genes, 7.7 µl of nuclease-free water, and 2 µl of diluted template cDNA in a total volume of 20 µl. Initial enzyme activation was performed at 95°C for 15 min, followed by 40 cycles of denaturation at 95°C for 15 s, and primer annealing/ extension at 60°C for 1 min. Melting curve analysis was performed at 95°C for 1 min, 60°C for 30 s and 95°C for 30 s. The relative expression level of each gene was normalized against a house-keeping gene, β -actin. RNA samples collected from undifferentiated hESCs served as control. Primer sequences were summarized in Table 1. Each experiment was carried out in triplicate.

2.3.7. Statistical analysis

All experiments were carried out at least in triplicate. Unless otherwise indicated in the text, all analytical measurements were repeated three times. All data were expressed as means \pm standard deviations. Statistical analysis was performed with Student's t-test, with $p < 0.05$ considered as statistically significant.

2.4. Results

2.4.1. hESC maintenance on two culture system

As shown in Figure 1, undifferentiated hESCs grown on MEF feeder layer (A-C) and Matrigel (D-F) showed as compact, multicellular colonies. Also, they exhibited a high nuclear-to-cytoplasm ratio and prominent nucleoli, which is a characteristic feature of hESCs. After 5 passages of culture, the expressed of SOX2, SSEA4, and TRA-1-60 were stained positively (Figure 1. G-I), indicating the pluripotency of the hESCs.

2.4.2. Collagen I scaffold characterization

Unseeded and hESC seeded collagen I scaffolds were characterized morphologically by SEM micrographs (Figure 2). The microscopic structure of a collagen scaffold showed a homogeneous fibrillar and porous 3-D network, indicating spacious areas for cell growth and differentiation. The diameter of the collagen nanofibers was 230 nm on average and pore size was about $0.65 \mu\text{m}^3$ estimated using NIH Image J software. SEM micrographs of seeded scaffolds showed that the hESCs were tightly attached to the scaffolds and secreted ECM-like proteins (Figure 2B), suggesting the suitability of the collagen type I scaffold for hESC growth.

2.4.3. Morphological and viability analysis of DE differentiated hESCs within collagen scaffolds

The study aimed to compare the viability and proliferation between two different cell seeding methods, i.e. single cell vs. cell cluster seeding. Cell morphology and viability were monitored. It was found that cells remained single on day 2 of seeding within collagen scaffolds when the single cell seeding approach was applied (Figure 3A). The formation of cell clusters was observed with the progression of differentiation (Figure 3B). In contrast, cells started forming aggregates on day 2 when the cell cluster seeding approach was used (Figure 3C), and

the size of cell clusters increased significantly on day 4 post differentiation (Figure 3D). The cell viability within 3D collagen scaffolds was approximately 98% during the time period of differentiation (Figure 3E-3H). These results suggest that both single and cluster hESCs can survive and proliferate within the 3D collagen scaffolds.

2.4.4. Proliferation rate of DE differentiated hESCs within collagen scaffolds

To examine cell growth during differentiation, the cell-laden scaffolds were incubated with the AlamarBlue substrates for 4 h and the fluorescence of solution was measured, which indicated the cell proliferation rate. As revealed in Figure 4, cell proliferation rate was 3-fold higher within a collagen scaffold when the cluster seeding approach was used as compared to single cell seeding approach.

2.4.5. hESC DE differentiation in 2D and 3D

We then investigated the directed differentiation of hESCs to DE within collagen scaffolds. For inducement of the DE differentiation, hESCs were seeded into collagen scaffolds as either single cells or cell clusters, and grown in a DE differentiation medium for 4 days. The expression of DE markers: *Sox17*, *Foxa2* and *CXCR4* in the induced cells on day 2 and day 4 were detected to ascertain whether the hESCs were differentiated into DE concomitantly with their proliferation within collagen scaffolds. Undifferentiated hESCs served as a control for the assay. As shown in Figure 5, analysis of gene expression showed that the treated samples, which were differentiated for 4 days under treatment of 100 ng/ml activin A and 25 ng/ml Wnt3a, expressed DE markers *SOX17*, *FOXA2*, *CXCR4* in both 2D and 3D culture, which confirmed the

generation of definitive endoderm from hESCs. Especially, 3D culture by using both cell seeding methods significantly increased the expression level of DE markers as compared to 2D culture, however, the single cell seeding approach resulted in higher expression level of DE markers (*SOX17*>250-fold, *FOXA2* >500-fold, and *CXCR4* >1000-fold on day4 as compared to undifferentiated hESCs) than cell cluster seeding approach (*SOX17*>100-fold, *FOXA2* >300-fold, and *CXCR4* >500-fold on day4 as compared to undifferentiated hESCs). Meanwhile, significant decreases of *OCT4* on day4 after induced differentiation in both 2D and 3D cultures indicated the loss of pluripotency of hESCs. In addition, the cells in 3D scaffold showed a decreased level of ectoderm marker *PAX6* and mesoderm marker *Brachyury*, indicating the DE differentiation was dominant in the cultures.

2.5. Discussion

DE differentiation is critical for hESC pancreatic lineage differentiation. In our previous study, we demonstrated that more mature insulin-producing β cells could be generated from mouse ESCs (mESCs) when differentiating them within a collagen scaffold [179]. In this work, we investigated the feasibility of differentiating hESCs into matured β cells. As the DE differentiation is critical to the hESC pancreatic lineage specification, we investigated its differentiation within a 3D collagen scaffold. We found that the cell proliferation rate and DE differentiation efficiency are significantly affected by the seeding approach. The experimental results suggested that cells proliferated much faster when they were seeded in clusters, as compared to those seeded in single cell suspension. Also, DE differentiation was greatly enhanced in 3D culture, especially when single cell approach was applied. To the best of our

knowledge, this study was the first to explore the feasibility of differentiating hESCs into endoderm lineage in 3D collagen scaffold.

3D culture provides a means to study hESCs growth and differentiation in a physiologically relevant manner *in vitro*. The ideal scaffold for tissue engineering would have a structural component to provide mechanical support and a network structure consisting of large pores to allow cell expansion and the diffusional transport of nutrient and waste molecules [179]. Collagen scaffold is an ideal candidate for hESCs encapsulation and differentiation because it has relatively large pores (Figure 2A), support cell attachment, its gel formation is simple [180]. From SEM images (Figure 2B), collagen has shown to support cells attachment via cell-extracellular matrix interaction. Also, hESCs grown in 3D environment showed formation of 3D aggregates structure, as revealed in bright field images, which was not observed in conventional 2D culture. We think the pore size, fibrillar density and organization of the collagen fibers favor cell migration and promote the formation of aggregates structures in the process of hESCs differentiation.

It is crucial to maintain hESC viability while perform differentiation process. Therefore, we cultured hESCs in growth medium for 24 hours and initiated hESC DE differentiation using Activin A and Wnt3a on day one of seeding, which will prevent apoptosis of hESCs after cell dissociation. As shown here, collagen scaffold was capable of maintaining hESCs viability in the process of differentiation by using both cell seeding methods.

To determine whether DE can also be efficiently derived from hESCs in 3D collagen gel, single cell and cell cluster preparations of hESCs were induced to differentiate in 2D or 3D cultures following a well-established differentiation protocol. It is important that hESCs seeded within the scaffolds maintain their pluripotency prior to differentiation. The pluripotency related

gene *Oct4* was decreased by the process of definitive endoderm differentiation accompanied by a transient expression of mesendoderm marker, *Brachyury*, 24 hours after activin A and Wnt3A treatment (day 2 after inoculation), which indicated the hESCs proceeded through the mesoderm to endoderm transition. Moreover, the embedded cells in collagen gel expressed much higher definitive endoderm marker genes level compared to 2D culture when they reached their peak on day 4 after differentiation, with *SOX17* increase around 4.5 fold, *FOXA2* around 5 fold and *CXCR4* around 4.2 fold as compared to 2D culture. Interestingly, the expression of DE gene of differentiated cells seeded as clusters did not increased as significantly as those cultured as single hESCs. The enhanced efficiency of hESC differentiation into DE by single cells seeding could be explained by proper infiltration of single cells into the pores of the scaffolds, which would provide relatively uninhibited access of media and growth factors to the cells. Also, we observed some outgrowth of cells when hESCs were seeded as cell clusters in collagen gel, which probably inhibit the grow factor diffusion and slow down the differentiation process. However, the proliferation rate in 3D culture by using single cells seeding was lower than cell clusters seeding. The possible reasons could be differentiation could be easily started from single cells which slow down their proliferation.

In summary, we have established a 3D culture model to differentiate hESCs into definitive endoderm, which is most critical stage for pancreatic differentiation. The seeded hESCs proliferated and maintained high viability in the collagen culture. Upon directed differentiation, the seeded hESCs can be differentiated into DE with a higher efficiency when cells were seeded as single cells. This system may provide an alternative strategy for generating insulin-producing cells for cell-based diabetes treatment

Chapter 3

Combinatorial Effect of ECM Proteins on 3D Human Embryonic Stem Cells Definitive Endoderm Differentiation

3.1. Abstract

hESCs are potential renewable cells sources for cell-based therapies. Here, we reported a novel three-dimensional (3D) model to derive DE cells from hESCs by using collagen I and various ECM proteins such as fibronectin (FN), laminin (LN) and vitronectin (VN). It is found that, single ESCs formed clusters and remained a high viability (>95%) within collagen scaffolds. More importantly, demonstrated by qRT-PCR, immunohistochemical staining, flow cytometry results, mixture of ECM proteins by incorporating of FN, LN and VN together in 3D collagen matrices produced more than 90% of *SOX17*⁺ DE cells with DE markers genes *Sox17*, *Foxa2* and *CXCR4* increased by 79-fold, *Foxa2* 60-fold and *CXCR4* 75-fold respectively Also, the cells in collagen-ECM scaffold secreted more ECM proteins such as fibronectin 1, laminin gamma 1, collagen type IV alpha 1, collagen type III alpha 1, collagen type I alpha 2 as showed by qRT-PCR. Immunohistochemical staining showed that more collagen IV produced in collagen scaffold with addition of ECM protein mixture. The method described here presents a significant step towards the efficient generation of DE cells for use in regenerative medicine and drug discovery, as well as a platform for studying cell fate specification during development.

3.2. Introduction

It has proven to be a challenge that ES cells are directed to differentiate into pure endodermal populations *in vitro* [181, 182], likely because the organ development requires a strict temporal and spatial control at each stage. It is well known that extracellular matrix (ECM)

is a key component in stem cell niches and plays an important role in cell adhesion, migration, proliferation, and differentiation [183]. ECM not only provides a support for cells and tissues, but can also bind to growth factors, cytokines, and other soluble signaling molecules and transduce them to cytoskeleton to trigger signaling transduction pathways and ultimately affect gene expression, thereby changing the fate of cells [123, 184, 185]. Consequently, it is critical to mimic this *in vivo* environment when designing an *in vitro* hESC differentiation system.

In this chapter, we showed that DE differentiation can benefit from the use of collagen scaffolds which offer 3D environments that allows cell-cell and cell-ECM interaction. While collagen is a good biomaterial for fabricating a hydrogel scaffolds, it is interested in determining whether the DE differentiation can be further improved if other ECM proteins are mingled with collagen when fabricating scaffolds. It has been known that non-collagenous ECM proteins such as laminin (LAM), fibronectin (FN), and vitronectin (VN) also play important roles in cell adhesion, migration, proliferation, and differentiation. FN is widely expressed by multiple cell types and is critically important during embryogenesis [186]. George *et al.*'s work demonstrated that the disruption of FN gene in ESC resulted in defects in mesoderm, neural and vascular development [187]. In addition, it has shown that FN was acquired when ESCs differentiated into endoderm [188] as well as many endoderm-derived tissues such as lung and pancreas [189, 190]. LM, a family of glycoproteins, is the major constituent of basement membranes between primitive ectoderm and endoderm. By interacting with cells mediated by integrins, dystroglycan, and other cell surface receptors, LM contributes to cell survival, phenotype maintenance, and differentiation [191]. Specifically, LM is upregulated during endoderm epecification [192]. Also, Lin *et al.* demonstrated that the differentiation of insulin-producing cells (IPCs) from human mesenchymal stem cells could be enhanced when LM and FN are used [193]. Another study also

revealed that collagen 3D scaffolds prepared in combination with adhesive ECM proteins, such as FN and LM, offer better cues for mesenchymal stem cell neuron differentiation, even without the use of chemical differentiation factors [194], suggesting that ECM proteins can provide signals for directing cell differentiation. Vitronectin (VN) is another widely distributed high molecular weight glycoprotein found in most sites of ECMs and is known to promote cell adhesion, migration, differentiation, and cytoskeletal organization. It affects cell morphology as well. VN has been identified in fetal islet tissue emerging from pancreatic ducts during development, suggesting its role in DE specification [195]. It has been proved that the addition of VN in gel condition significantly improves β -cell survival and insulin secretion [177]. Even though a lot of studies have been carried out to investigate the influence of ECM proteins on cell behavior and differentiation, there have been few reports on endoderm-derived cell differentiation.

Here, we choose collagen type I as a major component of the scaffold combined with various ECM proteins such as LAM, FN, and VN to investigate the combinatorial effect of these components on DE differentiation within collagen scaffolds.

3.3. Materials and methods

3.3.1 3D hESC culture

The hESC line H9 was acquired from Wicell Research Institute. Cells were maintained in an undifferentiated state on growth-factor-reduced Matrigel (BD Biosciences, Bedford, MA)-coated cell culture plates in mTeSR1 medium (StemCell Technologies, Vancouver, Canada). Cells were passaged every 3~5 days at a splitting ratio of 1: 4~1:6 through dispase (1 mg/ml)

(StemCell Technologies, Vancouver, Canada) treatment combined with manual dissociation. The cells were incubated at 37°C in the atmosphere supplemented with 5% CO₂. The cell culture media was exchanged daily.

3D scaffolds were prepared as follows: type I rat tail collagen solution (BD Biosciences, Bedford, MA) was diluted with sterile H₂O and 10× phosphated-buffered saline (PBS) (Mediatech Inc., Manassas, VA) to maintain the physiologic osmolality at 250~300 mOsm. The final collagen solution concentration was 1.5 mg/ml. To produce ECM protein mixed collagen scaffolds, collagen gel solution was added with variable amounts of FN (BD Biosciences, Bedford, MA), LM (Trevigen, Gaithersburg, MD), or VN (Trevigen, Gaithersburg, MD) stock solution to final concentration of 25, 25, and 4 µg/ml, respectively. The pHs of these solutions were adjusted to 7.4±0.2 by the addition of 1 N sterile NaOH. These solutions were chilled on ice to prevent from gelation until use.

Before seeding hESCs into scaffolds, the ROCK inhibitor, Y-27632 (Calbiochem, California, USA) was added to the cell cultures at 10 µM for 2 hrs before the cells were dissociated by Accutase™ (EMD Millipore, Billerica, MA) treatment. The single cell suspension was obtained after centrifugation at 300 × g for 5 min and suspended in mTeSR1 medium. The live cell number was determined by trypan blue staining assay using a hemacytometer. The cell suspension was then added to the ice-chilled collagen solution along with different ECM proteins to achieve a final cell density of 2.5×10^6 cells/ml. Thereafter, 0.4 ml aliquots of the cell-collagen with ECM protein mixtures were transferred into wells of 24-well tissue culture plates and incubated at 37°C, 5% CO₂ for 30 min to 1 h to achieve gelation. 0.5 ml of cell culture medium (mTeSR1 with 10 µM Y-27632) was added to the top of the scaffolds once the scaffolds have formed. The cell-laden scaffolds were returned to the incubator and allow cells to grow

within the scaffolds for 24 hrs before initiating differentiation. In two-dimensional (2D) cultures, cells were plated onto Matrigel-coated tissue culture plates at the same density, followed by same differentiation procedure as 3D cultures do.

3.3.2. hESC DE differentiation

The DE differentiation was optimized by differentiating hESCs in two different DE medium: (1) hESCs were fed with RPMI 1640 medium (Invitrogen) supplemented with 100 ng/ml activin A (PeproTech Inc.) and 25 ng/ml Wnt3a (PeproTech Inc.) for 1 day and after 24 hours, medium was replaced with fresh RPMI 1640 medium supplemented with 0.2% defined FBS and 100 ng/ml activin A for another 72 hours (medium A). (2) hESCs were fed with DMEM/F12 medium supplemented with 0.2% BSA (Sigma), 0.5% B27 (Invitrogen), 0.5% N2 (Invitrogen), 100 ng/ml activin A (PeproTech Inc.) and 25 nM wortmannin (EMD Millipore) for 4 days (medium B). The DE differentiated efficiency will be compared and the medium that resulted in higher DE efficiency would be used for DE differentiation in 3D culture experiments.

3.3.3. Cell viability

The cell viability within scaffolds was determined using live/dead cell dual staining kit (Sigma-Aldrich, Saint Louis, MO) by following the manufacture's instruction. The kit contains two staining probes for the simultaneous detection of viable and dead cells. Live cells with intracellular esterase activity can convert the nonfluorescent, highly lipophilic, cell-permeable dye calcein-AM into the fluorescent dye calcein which emits green fluorescence (excitation: 495 nm, emission: 515 nm). Dead cells are identified by a nuclei staining dye PI which passes

through damaged cell membranes, and upon binding to DNA double helix, producing red fluorescence (excitation: 495 nm, emission: 635 nm). PI is excluded by the intact plasma membrane of live cells. After washing with PBS three times, cell-laden scaffolds were incubated with 200 μ l of the live/dead staining solution at 37°C for 15 min. The excess dye solution was removed afterwards and 0.5 ml of PBS was added on the top of the scaffold. Excess buffer was subsequently removed in order to stabilize the cell-laden scaffolds for imaging. Samples were examined under an Olympus upright microscope (IX71, Tokyo, Japan) equipped with a supersensitive CCD camera (mode number ROLERA-XR, Surrey, BC, Canada) controlled by an imaging analysis software Slidebook (Intelligent Imaging Innovations, Inc., Denver, CO).

3.3.4. Scanning electron microscopy (SEM)

3D samples were washed with Dulbecco's phosphate buffered saline (DPBS) buffer for at least 3 times to remove all proteins in the culture medium or other impurities. The scaffolds were then fixed with 2.5% (v/v) glutaraldehyde (EM Sciences, Fort Washington, PA) in PBS buffer at pH 7.4 for 2 h at room temperature. After three 10-min washes in PBS, the samples were post-fixed with 1% osmium tetroxide (EM Sciences) for 1 h at room temperature. Followed by two 10-min washes, the fixed scaffolds were dehydrated in a series of graded ethanol: 30%, 50%, 70%, 90% and two times of 100% v/v for 10 min each. Then, the cell-laden scaffolds were allowed to dry overnight on aluminum foil in fume hood. The dried scaffolds were mounted on SEM sample stages using double-stick carbon tape and sputter coated with gold-palladium before examination. Finally, the specimens were analyzed using a FEI/Philips XL30 FEG ESEM (FEI, Hillsboro, OR) at an accelerating voltage of 10 kV.

3.3.5. Total RNA extraction and quantitative RT-PCR

To detect gene expression in cells grown in 2D or 3D cultures, the total RNA was extracted from cultured cells using a RNeasy Plus Mini kit from Qiagen. Prior to reverse transcription (RT), RNA samples were digested with DNase I to remove contaminated genomic DNA. 1 µg of RNA was used to synthesize cDNA. Reverse transcription was performed using a High Capacity cDNA Reverse Transcription Kit from the Invitrogen followed by the manufacture's instruction. Quantitative real-time PCR (qRT-PCR) was carried out using the Power SYBR Green PCR master mix (Applied Biosystems) and was performed on the Realplex Real-Time PCR system (Eppendorf, Realplex4 model). Initial enzyme activation was performed at 95°C for 15 min, followed by 40 cycles of denaturation at 95°C for 15 s, and primer annealing/extension at 60°C for 1 min. Melting curve analysis was performed at 95°C for 1 min, 60°C for 30 s and 95°C for 30 s. The relative quantification was performed against a standard curve and quantified values were normalized against the house-keeping gene β -actin.

3.3.6. Flow cytometry

For 3D culture, hydrogels were digested by using 2 mg/ml collagenase solution (Life Technologies) for 30 min at 37°C. After centrifugation at 300 \times g for 5 min and aspiration of supernatant, the cells were then treated with 0.25% trypsin with EDTA (sigma) to further digest the cells into single cell suspension. Cells were filtered through 70 µm cell strainer (BD Falcon™) to remove the clumps. For 2D culture, cells were dissociated using Accutase™ cell detachment solution (Millipore) for 5 min followed by removal of trypsin by centrifugation. Cells were fixed with 4% paraformaldehyde and permeabilized with ice-cold methanol. Cells

were labeled with PE mouse anti-human Sox17 (BD Biosciences) at 5 μ l per 1×10^6 cells for 45 min at room temperature in the dark. Cells labeled with PE mouse IgG1 κ was used as an isotype control. Cells were washed three times and resuspended in PBS with 10% inactivated FBS and 0.09% sodium azide. Samples were acquired on a Becton-Dickinson fluorescence activated cell sorter (FACS) Calibur 4-color flow cytometer and data analyzed using Becton-Dickinson CellQuest software. Data were gated using forward and side scatter to eliminate debris and the resulting histograms plotted to reflect the mean fluorescence intensity of Sox17 versus IgG1 κ isotype control.

3.3.7. Immunohistochemical and immunocytochemical staining

The cryosectioning of cell-laden scaffolds was performed as described elsewhere [196]. In brief, the scaffolds were fixed using 10% neutral-buffered formalin solution (NBF) for 3 hrs. After overnight infiltration with a series of 20% sucrose and sucrose/OCT[®] solution, the scaffolds were placed in a peel-away mold (VWR, south Plainfield, NJ) in tissue freezing medium (Tissue-Tek OCT Compound, Sakura-Fintek). All the molds were then placed into the MICROM cryostat (Richard-Allan Scientific) chamber and the samples were allowed to freeze at -20°C for at least 30 min. Routine frozen sectioning was performed by collecting 8- μ m sections onto positively charged slides. The scaffold sections were either collected or air-dried for a minimum of 30 min. Before staining, sections were hydrated in PBS for 10 min and then incubated in a blocking buffer (PBS containing 5% normal goat serum, 0.3% Triton X-100) for 1 h and thereafter in primary antibodies for 12 h at 4°C diluted in the blocking buffer. The primary antibodies used in this study were mouse monoclonal anti-human Sox17 (R&D Systems; 1:50), rabbit monoclonal anti-Foxa2 (Abcam; 1:1000), rabbit anti-Collagen IV (Abcam; 1:200). The

secondary antibodies used were DyLight™ 488 conjugated goat anti-mouse IgG (Thermo Scientific; 1:500) and Rhodamine (TRITC)-conjugated donkey anti-rabbit IgG. To stain 2D culture samples, cells seeded on Matrigel-coated plates were fixed with 4% paraformaldehyde (Sigma). After being treated in the blocking buffer for 45 min at room temperature to inhibit nonspecific binding, cells were labeled with primary and secondary antibodies as described above. DAPI (Research Organics) were used to counterstain cell nucleus. Images were captured using an inverted fluorescence microscope (Olympus, IX71, Japan).

3.3.8. Statistical analysis

All experiments were carried out at least in triplicate. All quantitative values were presented as mean \pm SD. Statistical analyses were performed using student's *t*-test and p-value ≤ 0.05 were considered statistically significant.

3.3. Results

3.4.1. PI3K inhibitor enhanced DE differentiation from hESCs

Generating appropriate DE population is a crucial step in producing derivative lineages and functional cell population. Most protocols use Activin A and Wnt3a described by D'Amour [104] to generate DE cells. Recent studies found out PI3K signaling was evolved in DE differentiation, here we tested whether the addition of wortmannin, a PI3K inhibitor, would improve our DE protocol. The qPCR results showed that the addition of wortmannin was able to augment the expression of DE markers *SOX17* and *FOXA2* by 8-fold and 13-fold, respectively,

as compared to D'Amour's protocol (Figure 6A). Low expression of pluripotency marker (*OCT4*), mesoderm (*Brachyury*) and ectoderm (*PAX6*) lineages marker provided evidence that wortmannin can enhance DE differentiation. Also, the differentiation efficiency was evaluated by flow cytometric analysis of *SOX17*⁺ cells, revealing that the percentage of *SOX17*⁺ cells was 70% when cells were treated with Activin A in combination with PI3K inhibitor as compared to 32% when cells were treated with Activin A in combination of Wnt3a. Consistent with the gene expression and flow cytometric analysis, immunostaining revealed that larger population of cells were stained both *SOX17* and *FOXA2* positive when cells treated with wortmannin in combination with Activin A. Taken together, these finding indicated that the inhibition of PI3K pathway does significantly promote differentiation of hESCs into endocrine lineage.

3.4.2 Proliferation and morphological changes of hESCs-differentiated DE cells within scaffolds

To reveal the potential of ECM-collagen scaffolds for directing hESC pancreatic lineage differentiation, undifferentiated single suspended cells were seeded into collagen along with ECM proteins (for 3D cultures) or onto Matrigel-coated cell culture plates at a cell density of 2.5×10^6 cells/ml (for 2D cultures). Cells grown in either 2D or 3D cultures both proliferated rapidly but differed in their morphology (**Figure. 7**). In 2D culture, cells were predominantly flat, stretched endoderm-like cell morphology throughout the entire differentiation period. In contrast, cells formed clusters after 2 days of differentiation in 3D cultures (**Figure. 7**). The number of cells and the size of clusters increased significantly. The spherical tissue-like structures were formed on day 4 of DE differentiation. Interestingly, within the collagen gel matrix containing VN, cells exhibited a highly elongated branch like junctions without forming significant clusters.

The viability of differentiated DE cells within scaffolds was determined on day 2 and day 4 by calcein-AM/PI live/dead cells dual staining. As shown in the fluorescence images (**Figure. 8**), there appear to be a high percentage of live cells (green) with only fewer dead cells (red), mostly found along the side of the cluster. The average size of the cell clusters was about 150-250 μm . The live/dead staining also permitted the observation of the high percentage of live cell clusters with outgrowth and cluster-cluster connection. These results demonstrated that the dissociated hESCs could be immobilized in collagen along with ECM proteins with a high viability.

3.4.3. Morphological analyses of DE differentiated cells in 3D collagen-ECM scaffolds

To characterize the *in vitro* environment of the 3D scaffolds for hESC differentiation, we examined the structure of collagen-ECM scaffolds and the morphology of DE differentiated cells within these scaffolds by means of SEM. The collagen-ECM scaffolds showed similar microscopic structure of porous fibrillar network consisting of packed and long fibrils with approximately 200-300 nm diameter (**Figure. 9**). However, the addition of ECM components (LAM, FN or VN) changed the structures of the network. For example, Col I matrices alone showed heterogeneous fibrillar network in pore size and fiber size (**Figure. 9A**). The addition of LN (25 $\mu\text{g}/\text{ml}$) increased the matrix heterogeneity with some smaller fibrils twisted together to form larger fibrils, which appear like aggregates and amorphous regions (**Figure. 9C**). The mixing with FN and VN induced a much denser fiber network with smaller pore sizes (**Figure. 9D**). Also, SEM micrographs of seeded scaffolds showed that the cells differentiated in 3D cultures were tightly attached to the scaffolds and secreted ECM-like proteins, suggesting the suitability of the collagen-ECM scaffold for hESC growth and differentiation

3.4.4. Enhancement of DE differentiation in 3D collagen-ECM scaffolds

To examine whether ECM-collagen scaffolds can improve the DE differentiation from hESCs, gene expression profile of DE markers such as *Sox17*, *Foxa2*, and *CXCR4* were analyzed after 4 days of DE differentiation through qRT-PCR assay. As shown in **Figure.10A**, the mixing of LM or FN in Col I matrices increased DE marker *Sox17*, *Foxa2* and *CXCR4* expression by 103 fold, 7 fold, 19 fold or 65 fold, 24 fold, 28 fold, respectively as compared to those detected in 2D DE differentiation. However, the mixing of VN with collagen did not improve the DE differentiation, which showed similar expression level as those in 2D DE differentiation. Interestingly, the mixing of LM, FN and VN with collagen significantly improved the DE differentiation, indicated by the increased gene expression of *Sox17* 79-fold, *Foxa2* 60-fold and *CXCR4* 75-fold as compared to those in 2D hESC DE differentiation, suggesting that FN, LM, VN may need to work synergistically to maximize the enhancement of DE differentiation. We also found the remarkable downregulation of pluripotency markers, Oct4 and Nanog in cells differentiated within scaffolds as compared to those detected in 2D differentiation, indicating the 3D cultures could further decrease the pluripotency of hESCs during DE commitment than 2D cultures. In addition, the cells differentiated within scaffolds expressed a decreased level of ectoderm markers *PAX6*, *Sox3* and mesoderm markers Brachyury and N-CAD, suggesting that more cells were differentiated towards DE lineage when they were differentiated within scaffolds. This observation was confirmed by flow cytometric analysis. As shown in **Figure. 10B**, 10% more *SOX17*⁺ cells were detected in hESCs differentiated within collagen scaffolds as compared to those differentiated in 2D cell culture plates. More than 90% of cells in cell clusters formed within FN-LM-VN-collagen scaffolds were DE cells.

Immunofluorescent staining showed that above 95% cells differentiated within FN-LM-VN-collagen scaffolds expressed *Sox17* and *Foxa2* simultaneously, while only about 70% cells were both positive in cells differentiated in 2D cultures (**Figure. 11**). Moreover, the DE differentiated cells are organized into clusters inside of the scaffolds, resembling the formation 3D structures.

3.4.5. 3D matrices improve the secretion of ECMs by DE-differentiated cells

The gene expression level of ECM components produced by DE differentiated cells in 3D and 2D environments were examined through qRT-PCR assay. **Figure. 12** showed that differentiated DE cells cultured in 3D scaffolds expressed higher gene expression levels of fibronectin 1 (FN), laminin gamma 1 (LM), collagen type IV alpha 1 (Col IV), collagen type III alpha 1 (Col III), collagen type I alpha 2 (Col 1 α 2) than in 2D culture, which imply that the ECM secreted by cells in 3D may further improve the DE differentiation of hESCs. However, Col 1 α 1 gene expression in 3D cultures was lower than that in 2D cultures. The mechanism underlying the increased expression of these ECM proteins in 3D cultures needs to be further investigated.

Furthermore, we test the collagen IV secretion and its organization in either 3D or 2D differentiation through immunohistochemical staining assay (**Figure. 13**). The addition of LN or FN and the mixing of LN, FN, VN to the collagen solution when fabricating the scaffolds led to the depositing of more collagen IV to the ECM within the scaffolds (**Figure. 13**). In addition, a more denser fibrillar structure that was observed in cell clusters formed within scaffolds. In 2D culture, we also observed few col IV expressions around the cells; however, the distribution of collagen IV on 2D culture did not display distinct structure and just deposited on the periphery of

cells membrane. Because matrigel, which was used to coat cell culture plate before seeding cells, contains some collagen IV protein, so the expression of col IV on 2D culture may also probably came from Matrigel, not the DE cells secreted.

Discussion

The use of ES cells in combination of with scaffolds holds invaluable promises for engineering all kinds of 3D tissues or organs for transplantation. Nevertheless, the understanding of knowledge on mechanisms underlying ES cell development and differentiation in a 3D environment is crucial to meeting this challenge. It is widely recognized that ECM plays an important role in regulating stem cell differentiation [197]. Here, we designed a novel *in vitro* culture system by utilizing collagen scaffolds combined with ECM proteins to provide a robust hESC DE differentiation system, which may further improve the differentiation efficiency and maturation of DE lineage cells such as insulin-producing β cells.

Successful derivation of β -cells from hESC largely depends on the efficient generation of DE population. hESCs were able to differentiate into DE by the addition of Activin A but only in the presence of low FBS [105]. The possible reason could be FBS contains in insulin-like growth factor (IGF) which was known to activate PI3K in hESCs. In our experiments, Activin signaling was able to augment DE differentiation when PI3K activity is inhibited. This result was consistent with other's work [107, 109]. Also, there are several critical parameters that influence the effect of wortmannin on DE differentiation. Although wortmannin at concentration between 25 nM and 50 nM works effectively, when wortmannin was used below this level, the efficiency of DE formation diminished, presumably because PI3K is not effectively inhibited. Also, when

wortmannin was used a higher concentration (> 50 nM), we saw a concentration-dependent increase in cell death consistent with the role for PI3K in cell survival. This suggested that different thresholds of PI3K signaling in hESCs are responsible for different cell fate outcomes.

Here, the hESCs were cultured under collagen-ECM scaffolds, particular in combination with adhesive proteins, such as FN, LN and VN. The effect of the ECM proteins on the differentiation of hESCs into DE cells was evaluated through the observation of cellular morphologic and protein and molecular genes assays. As shown in **Figure 1.**, multicellular clusters were formed and expanded in size along with some outgrowth and cluster-cluster connection, but not in cells cultured under two-dimensional conditions. Furthermore, immunostaining, flow cytometric and gene expression assays revealed that the cells retained characteristics of definitive endoderm development.

We speculate that the ECM may have enhanced the efficiency of cell differentiation in several ways. First, there may have some direct signaling from the ECM itself, promoting attachment and migration through porous structure. From the bright field and SEM images, the results showed the cells were proliferated and migrated to form clusters during the culture period. Also, the real time RT-PCR results demonstrated that by adding additional ECM proteins like fibronectin, laminin, and vitronectin together in collagen I scaffolds, the DE differentiation efficiency was further improved. These findings are consistent with our earlier report that a collagen scaffold can be used as an attractive model to differentiating pancreatic β cells.

In addition, the 3D tissue formation during DE differentiation facilitated by the 3D ECM may promote cell-cell signaling that controls the interactions among cells, a clear advantage of 3D over 2D system. A 3D environment, in which each cell is surrounded by similar cells, may reinforce chemical signals that each cell experiences from its neighbors, helping synchronize and

promote differentiation of the entire cell population. More than 90% of cells derived from our 3D cultures were *SOX17* positive. As such, our data indicates that compared to individual ECM proteins, ECM protein mixture better promotes cell to cell and cell to ECM interaction resulting in improved differentiation.

In summary, we herein described a new model to culture and differentiate hESCs in 3D culture conditions. The combination of scaffolds with ECM molecules, in the presence of appropriate soluble signals, results in higher DE differentiation efficiency. This system may provide an alternative strategy for generating insulin-producing cells.

Chapter 4

Enhanced Pancreatic β cells Differentiation from Embryonic Stem Cells in 3-D Collagen I-Matrigel Scaffolds

4.1. Abstract

The success in directed differentiation of human embryonic stem cells (hESCs) into insulin-producing β cells raises new hopes for cell-based diabetes therapy. Here we reported a highly efficient approach to induce hESCs to differentiate into mature insulin-producing cells in a biomimic 3D collagen/Matrigel scaffold. Collagen incorporated with 35% (v/v) Matrigel was showed to be the most optimal composition for enhanced DE differentiation as compared to 10% (v/v) and 50% (v/v) Matrigel and resulted in 95% *SOX17*-positive cells. Also, we showed small molecular (-)-indolactam V (ILV) promoted the generation of *PDX1/HNF6* positive pancreatic progenitors when combined with other growth factors. The 3D differentiated pancreatic endocrine cells were assembled into tissue-like structure that displayed greater similarities in phenotype and gene expression profile to adult human islets. Our results showed that approximately 20% insulin positive cells were generated in collagen/Matrigel scaffold as compared to 5% in 2D culture, which correspondingly increased four-fold insulin release in response to high glucose as compared to 2D hESCs-derived pancreatic cells. Moreover, more mature insulin-secreting granules were observed in hESCs-derived pancreatic endocrine cells in collagen/Matrigel scaffold than cells in 2D culture. This work clearly demonstrated the feasibility of utilizing this novel designed biological 3D scaffold for generating mature clinically relevant insulin-producing β cells for treatment of diabetes.

4.2. Introduction

Diabetes mellitus has become a global epidemic with striking impacts on patients' health, society and economy. Islet transplantation has been suggested to be a promising therapeutic treatment for the treatment of diabetes. Even though some improvement has been made in islet transplantation, this therapy was not widely available due to the shortage of donor islet tissue [47] and cell loss during islet isolation [198]. The development of unlimited number of pancreatic insulin-producing β cells from human embryonic stem cells (hESCs) has emerged as the most attractive alternative.

hESCs could spontaneously differentiate into insulin-producing cells, but only 1-3% insulin-positive cells were generated among differentiated embryonic bodies [103]. In some cases, the insulin expression from differentiated embryonic stem cells is due to artifacts of the insulin uptake from medium [101, 102, 199]. To address these issues, a stepwise combination of different growth factors and small molecules has been developed to generate insulin-producing β cells, which mimicking the critical events *in vivo* pancreatic organogenesis by guiding cells through stages of definitive endoderm formation, pancreatic specification, and maturation [104, 109, 200]. In these reported protocols, cells released insulin and C-peptide, expressed certain islet transcription factors. However, these insulin-positive cells most exhibited immature islet characteristics. For example, the insulin-producing cells generated by D'Amour *et al's* five stage protocol [104] released C-peptide in response to secretagogues, such as potassium chloride (KCl), but they were not glucose-responsive and C-peptide content was about 50% lower than in human islets. Also, in general the differentiation efficiency of insulin-producing cells was quite low and the cells are mostly polyhormonal with a poorly defined phenotype [168, 200]. It has also been reported that the hESCs-derived pancreatic progenitors transplanted into athymic nude

rats failed to produce substantial number of beta-like cells [201]. Collectively, further efforts are needed to not only improve the differentiation efficiency, but also promote maturation of insulin-producing from hESCs *in vitro*.

The common disadvantage of the most current protocols for generating insulin-producing cells from hESCs is using conventional 2D monolayer culture, which lack of support from extracellular matrix (ECM), which plays an important role in cell grow and development. Cell-matrix interactions have been shown to improve β -cell survival [90, 177, 202], proliferation [203, 204] and insulin secretion [177, 205]. Yashpal *et al.* work showed that blocking islet-matrix interaction by using β 1 integrin antibody leads to decrease of insulin gene expression and islet-cell apoptosis [206]. Collagen gel has been used as a model for culturing stem cells in three-dimensional (3D) environment, which provides a condition much more similar to native tissue ECM than two-dimensional culture dishes [207]. Specially, the collagen gel and surrounding medium fluid constitute a soft and flexible fibrous network that supports the rounded morphology of cells and allows cells to freely reach out and migrate and from three-dimensional structures. However, collagen I alone was not sufficient to provide multiple cues and sophisticated geometry and composition that existed in native ECM for synergistically enhancement of stem cells differentiation. We therefore augmented a collagen I matrix with Matrigel™, a commercially available preparation of basement membrane proteins comprising laminin, collagen IV, fibronectin, heparin sulfate proteoglycans and entactin and so on. Oberg-Welsh, C. *et al.* have shown that Matrigel significantly enhanced the insulin secretion of fetal porcine islet-like cell clusters *in vitro* [208]. The combination of collagen and Matrigel could provide not only physical supports for ESCs development and differentiation, but also the

necessary components of ECM. This method has been successfully applied to the tissue engineering of cardiac muscle uterus, and kidney [209, 210].

Our goal in this work was to develop a scaffold to serve as a platform for robust differentiation of insulin-producing cells from hESCs for islet transplantation. We hypothesized that the collagen/Matrigel scaffold would support hESCs grow and enhance the differentiation of hESCs into mature insulin-producing β cells. To test this hypothesis, we investigated the formation of islet-like insulin-producing cells in 3D culture by using a modified step-wise protocol. The maturity of final differentiated cells was evaluated.

4.3. Materials and Methods

4.3.1. hESCs culture

Human embryonic stem cells (hESCs), H9 (WiCell Research Institute, Madison, MI), were cultured on Matrigel (BD Biosciences, Bedford, MA)--coated cell culture plates in mTeSR[®]1 medium (StemCell Technologies Inc., Vancouver, BC, Canada). A solution of 1mg/ml dispase in DMEM/F12 medium was used to passage cells every 3-5 days. The cultures were incubated at 37°C in the atmosphere supplemented with 5% CO₂, with the cell culture medium changed daily.

4.3.2. Collagen/Matrigel scaffolds preparation

Collagen type I gels were prepared at 1.5 mg/ml concentration under sterile condition by diluting the rat tail tendon-derived collagen I solution (BD Biosciences, Bedford, MA) with 10×

phosphate buffered saline (Mediatech, Inc., Manassas, VA), cell culture grade DI water (Thermo Fisher Scientific Inc., Waltham, MA). The pH of the mixture was neutralized immediately to 7.4 using 1 N NaOH. To create combinational collagen/Matrigel scaffolds, growth factor-reduced Matrigel (BD Biosciences, Bedford, MA), a solubilized basement membrane preparation, was incorporated in collagen I solution at 10%, 35% or 50% by volume of collagen solution. The solution were then neutralized to pH 7.4, and added into 48-well plates and incubated at 37 °C for 1 hour to induce gelation. No cross-linking agent was used.

4.3.3. hESCs Pancreatic differentiation of on Matrigel and in Collagen/Matrigel scaffolds

H9 cells were treated with the ROCK inhibitor, Y-27632, in cell culture medium for 2 hours before dissociating. After incubating with Accutase™ (StemCell Technologies Inc.), cell suspension was obtained after pelleted and resuspended in addition of mTeSR®1 medium. For 3D cultures, 10% volume of cells suspension (1.2×10^6 cells) was mixed with each 0.5 ml collagen I solution with or without different concentration of Matrigel. The cell-matrices solution was added to a 24-well plates (BD Biosciences, San Jose, CA), resulting in an initial radius of 8 mm and a thickness of 2.5 mm. The 3D constructs were placed in incubator at 37 °C for 1 hour for gelation. Once the gels had set, 0.5 ml of cell media was added to the top of the gels and the matrix was returned to the incubator. Moreover, two-dimensional culture was prepared for comparison by culture H9 cells directly on the top of Matrigel-coated culture plate. The cells were allowed to grow in scaffold or on Matrigel in mTeSR medium supplemented with 10 μ M Y-27632 for 24 hours for attachment and proliferation. A modified step-wise protocol, which is similar to Zhang et al's approach but with some modifications, was carried out for hESCs pancreatic differentiation (Figure 14).

4.3.4. Scanning electron microscopy

For SEM, 3D matrices were washed with PBS to remove proteins in the culture medium or other impurities and then fixed overnight in 2.5% (v/v) glutaraldehyde (Electron Microscopy Sciences, Hatfield, PA) at room temperature. After fixation, the matrices were thoroughly washed off the fixative with distilled water. Then, samples were snap frozen in liquid nitrogen (-196°C) and broken with cold forceps. A fragment of the frozen gel was transferred into a chamber of freeze dryer for low-temperature (-100°C) high-vacuum dehydration. Dried samples were mounted on SEM sample stages using carbon tape and sputter-coated with gold-plutonium (palladium) alloy (Pd/Au) to a thickness of 6 nm under vacuum using a Palaron SC7620 sputter coater (Watford, UK). Samples were then analyzed by Jeol Field Emission SEM (JSM-6335F, JEOL USA, Peabody, MA) using a low-vacuum mode (0.75 Torr), at 10kV accelerating voltage and 7.7mm working distance.

4.3.5. Quantitative real-time polymerase chain reaction

Cell-scaffold constructs were mechanically homogenized with a Tissue-Tearor (BioSpec Products, Bartlesville, OK) while cells cultured on Matrigel-coated tissue culture plate were harvested with a cell scraper. Total RNA was extracted from cultured cells using an RNeasy Plus Mini kit (Qiagen, Valencia, CA) after Prior to reverse transcription (RT), RNA samples were digested with DNase I to remove contaminating genomic DNA. Reverse transcription was performed with 1 µg of total RNA using High Capacity cDNA Reverse Transcription Kit (Invitrogen) followed by the manufacture's instruction. Real-time quantitative PCR was carried out using the Power SYBR Green PCR master mix (Applied Biosystems) and was performed on

the Realplex Real-Time PCR system (Eppendorf, Realplex4 model). Initial enzyme activation was performed at 95 °C for 15 min, followed by 40 cycles of denaturation at 95 °C for 15 s, and primer annealing/extension at 60 °C for 1 min. Melting curve analysis was performed at 95 °C for 1 min, 60 °C for 30 s and 95 °C for 30 s. Primer's sequences are given in table 1. The expression levels of target genes were normalized against endogenous control β -actin. All samples were analyzed in triplicates.

4.3.6. live/dead cell staining in 3D collagen/Matrigel scaffolds

The cell viability within scaffolds was determined using live/dead cell double staining kit (Sigma-Aldrich, Saint Louis, MO). Cell-scaffold 3D constructs were incubated with 200 μ l live/dead staining solution at 37°C for 15min by following the manufacture's instruction. The excess dye solution was removed and 0.5 ml of PBS was added on the top of the gel. Excess buffer was subsequently removed in order to stabilize the cell containing scaffolds sample for imaging. Samples were examined by using the Olympus upright microscope (IX71, Tokyo, Japan) equipped with a supersensitive CCD camera (mode number ROLERA-XR, Surrey, BC, Canada) controlled by an imaging analysis software Slidebook (Intelligent Imaging Innovations, Inc., Denver, CO).

4.3.7. Immunofluorescence staining

Scaffold-embedded cells were fixed in 4% paraformaldehyde for 15 min and washed 3 times with PBS. Permeabilization was performed with 0.1 Triton X-100 for 5 min.

Cryosectioning of scaffolds was performed as described elsewhere [196]. Briefly, Scaffold-cell

constructs were fixed in 10% neutral-buffered formalin solution (NBF) for 3 hours. After overnight infiltration with a series of 20% sucrose and sucrose/OCT® solution, the scaffolds were placed in a peel-away mold (VWR, south Plainfield, NJ) in tissue freezing medium (Tissue-Tek OCT Compound, Sakura-Fintek). All the molds were then placed into the MICROM cryostat (Richard-Allan Scientific) chamber and the samples were allowed to freeze at -20°C for at least 30min. Routine frozen sectioning was performed by collecting 8-µm sections onto positively charged slides. The scaffold sections were either collected or air dried for a minimum of 30min. Before staining, sections were hydrated in PBS for 10min and then permeabilization was performed with 0.1 Triton X-100 for 5 min. then incubated in blocking buffer (PBS containing 5 % normal goat serum, 0.3 % Triton X-100) for 1 h and thereafter nonspecific antibody binding was blocked by 10% normal serum from the species in which the secondary antibodies were raised. Cells were incubated with primary antibodies overnight at 4 °C followed by secondary antibody incubation for 1 hour at room temperature. To stain 2D cultures, cells seeded on Matrigel-coated plates were fixed with 4 % paraformaldehyde (Sigma). After treated in blocking buffer to inhibit unspecific labeling (45 min at room temperature), cells were labeled with primary and secondary antibodies as described above. DAPI (Research Organics) were used to counterstain the nucleus. Images were captured under an inverted fluorescence microscope (Olympus, IX71, Japan). The primary antibody and secondary antibody are described in Table 1.

4.3.8. Flow cytometry

For 3D culture, hydrogels were digested with 2mg/ml collagenase solution (Life Technologies) for 30min at 37°C. After centrifugation at 300x g for 5min and aspiration of supernatant, the cells were then treated with 0.25% trypsin with EDTA (sigma) to further digest

the cells into single cell suspension. Cells were filtered through 70mm cell strainer (BD Falcon™) to remove the clumps. For 2D culture, cells were dissociated using Accutase™ cell detachment solution (Millipore) for 5 min followed by removal of trypsin by centrifugation. Cells were then fixed with 4% paraformaldehyde and permeabilized with ice-cold methanol. Cells were labeled with PE mouse anti-human Sox17 (BD Biosciences) at 5 µl per 1×10^6 cells or mouse anti-human Insulin (Cell signaling Technology, Inc.) for 45min at room temperature in the dark. Cells labeled with PE mouse IgG1κ was used as isotype control. Cells were washed three times and resuspended in PBS with 10% inactivated FBS and 0.09% sodium azide. Samples were acquired on a BD fluorescence activated cell sorter (FACS) Calibur flow cytometer (Becton-Dickinson Biosciences, Franklin Lakes, NJ) and data analyzed using Becton-Dickinson CellQuest software (BD Biosciences).

4.3.9. Glucose stimulated insulin secretion assay

To determine if cells at the end of differentiation were capable of glucose-stimulated insulin release (GSIR), cells in 2D and 3D culture were washed three times with Krebs-Ringer buffer containing 0.1% BSA and 10mM HEPES and first incubated with Krebs-Ringer buffer free of glucose for 60 min at 37°C. Afterward, every dish was exposed to Krebs-Ringer buffer containing 5.5 mM, 15 mM or 25 mM glucose for 90 min at 37°C. Supernatant were then collected and insulin level were measured by using an Insulin ELISA kit. The amounts of insulin secretion were normalized by measuring total intracellular protein using BCA™ protein assay kit (PIERCE). Each experiment was triplicated performance.

4.3.10. Transmission electron microscopy (TEM)

2D cells and 3D matrices were fixed in 3% glutaraldehyde in 0.1 M cacodylate buffer (pH 7.4) for 2 hours at room temperature. After rinsing in 0.05 M cacodylate buffer, samples were post-fix in 1% osmium tetroxide for 2 hours and rinsed with distilled water. After pre-stain overnight in 0.5% uranyl acetate at 4 °C, samples were dehydrated through a graded ethanol series to 100%, rinsed in propylene oxide and embedded in Spurr's epoxy. 80 nm thick sections were cut on a MT2-B ultramicrotome and stained in 2% uranyl acetate and lead citrate. Samples were examined using a Philips EM 410LS TEM operated at 80 kV.

4.3.11. Statistical analysis

All experiments were carried out at least in triplicate. Unless otherwise indicated in the text, all analytical measurements were repeated three times. All data were expressed as means \pm standard deviations. Statistical analysis was performed with Student's t-test, with $p < 0.05$ considered as statistically significant.

4.4. Results

4.4.1 Scaffold morphology

The incorporation of various concentrations of Matrigel in collagen scaffold affects the microstructural features. SEM images of these collagen/Matrigel scaffolds exhibited well-defined, interconnected pore structures (Figure 15). In these constructs, 10% Matrigel constructs appeared less interconnected and less uniformly distributed. As the percentage of Matrigel

increased to 35% and 50%, the relative homogeneity of these scaffold morphological features can be appreciated, with more tightly packed fibrils and smaller pores. It was evident that the increases of Matrigel concentration gave rise to a substantial decrease of both void and interconnect size.

4.4.2. Effect of Matrigel on the hESCs definitive endoderm differentiation

To examine the effect of Matrigel on the efficiency of hESCs differentiation into pancreatic cells, hES cells were seeded into 1.5 mg/ml collagen gel incorporated with 10%, 35% or 50% (v/v) of Matrigel respectively. DE differentiation was implemented for 4 days and cells were harvested at the end of this stage for analyzing the expression of DE marker genes. As shown in Figure 16A, the incorporation of Matrigel in collagen gel significantly improved the expression level of DE genes such as *Sox17*, *Foxa2* and *CXCR4* compared to hESCs differentiated on 2D Matrigel substance. Among the three different scaffolds, 35% Matrigel showed the best effect on the enhancement of DE differentiation, which improved *Sox17*, *Foxa2*, *CXCR4* expression by 35-fold, 22-fold, 10-fold respectively, which was 2-3 fold increases compared to cells differentiated 10% or 50% (v/v) Matrigel constructs. Corresponding to the qRT-PCR results, flow cytometry was used to analyze the *Sox17* positive population in the differentiating cells on day 4. As showed in Figure 16B, 95% of cells are identified Sox17+ in 35% Matrigel as compared to 73% Sox17+ in 10% Matrigel and 85% Sox17+ in 50% Matrigel. This was in good agreement with the gene expression profile.

4.4.3. The morphological and viability analysis of hESCs pancreatic differentiation in collagen/Matrigel scaffolds

To compare the morphological changes of differentiating cells cultured under two- and three-dimensional conditions, undifferentiating single cells were seeded on Matrigel-coated cell culture plates or in 35% Matrigel/Collagen scaffolds and cell morphology was observed by phase-contrast microscopy at day 4 and day 10. Cells under 2D and 3D culture all proliferated rapidly, however, the morphology of cells differed greatly (Figure 17). In monolayer culture, the cells lost classical hESCs morphology and present a confluent monolayer with uniform morphology of flat, polygonal shape on day 4 of pancreatic differentiation, which showed overt differentiation. Upon the differentiation process, the cell cultures were densely packed and formed some tightly packed aggregates on day 10 of differentiation. In the collagen/Matrigel gel culture system, a number of newly formed cell clusters appeared by cell proliferation, homogeneously distributed as shown by phase contrast microscopy. The size of the clusters grew over time, resulting in spherical shapes with densely packed cells at day 10. Also, the outgrowth of cells from the periphery of most clusters was observed and cells formed tissue-like structures, indicating the initiating of hESCs differentiation. The viability of cells in 3D collagen/Matrigel culture was determined by calcein-AM/PI live/dead cell staining. Almost all the cells in 3D culture were viable, and the viability remained high (approximate 98% viable cells) even after 10 days of differentiation (Figure 17F). These results suggested that the 3D collagen/Matrigel culture system developed in this study provided a suitable cell housing microenvironment for hESCs proliferation and differentiation.

4.4.4. ILV treatment promoted the generation of pancreatic progenitor cells

In order to promote the commitment of hESCs differentiation into PDX1-expression progenitor cells, a small molecular (-)-indolactam V (ILV) was combined with growth factors reported to be involved in pancreatic development, including retinoic acid (RA), FGF7 and noggin. ILV was found to be able to specifically induce pancreatic progenitors from definitive endoderm. We found that the addition of ILV at stage II resulted in increase of gene expression of pancreatic progenitor markers including PDX1, SOX9, and HNF6 by 20-fold, 16-fold, and 63 fold respectively, on day 8 of pancreatic differentiation (Figure 18B). Consistent with the gene expression analysis, immunostaining revealed that larger population of cells were stained both PDX1 and HNF6 positive in the culture that treated with ILV compared to non-ILV treatment control, which indicated the importance role of ILV signaling in pancreatic progenitor generation. Specifically, the 3D structure of pancreatic progenitors was observed in 3D collagen/Matrigel culture system after 4 days of ILV treatment along with other growth factors for pancreatic progenitor differentiation.

4.4.5. Immunohistochemical characterization of hESCs-driven insulin-producing cells in collagen/Matrigel scaffold

To obtain insulin-producing cells in vitro, the stage 3 EP cells were incubated with exendin-4, nicotinamide, BMP4 and bFGF for 7 days. As shown in Figure 19, at the end of differentiation in this experiment, insulin-producing cells were observed, and these cells tend to be organized into a 3D islet-like structure. Also, the insulin-producing cells co-produced C-peptide, a by-product from proinsulin process, indicating the de novo endogenous insulin production, as opposed to uptake from the culture medium. As an essential regulation of pancreatic development, the expression of PDX1 was also observed, with co-expression of

NKX6.1 and NGN3, which confirmed their pancreatic β cell characteristics. Within the 3D cellular architect, the endocrine hormones that secreted from pancreatic α , δ and PP cells- glucagon, somatostatin and pancreatic polypeptide were detected in a small number of cells, which is consistent with the hormone expression pattern of mature islets. These results indicate that hESCs can be differentiated into insulin-producing cells through a four-stage protocol and organized into islet-like 3D structure in the developed collagen/Matrigel scaffold.

4.4.6. Gene expression profile of hESCs-derived insulin-producing cells in 2D and 3D

The expression pattern of pancreatic markers in 2D and 3D culture throughout differentiation was monitored by quantitative real-time PCR. As illustrated in Figure 20, the expression peak of Sox17 was observed at the end of stage I and the expression level in cells cultured in collagen/Matrigel 3D culture was enhanced by 14 folds compared to cells in 2D, indicating the enhancement of definitive endoderm differentiation in 3D culture. The expression of *PDX1* and *NGN3* emerged at stage II and reached the peak at the end of stage III, suggesting pancreatic specialization. The data showed that the enhancement of *PDX1* and *NGN3* expression in collagen/Matrigel scaffold compared to 2D culture persisted throughout the differentiation process. In addition, we observed enhanced *Insulin* gene expression in Collagen/Matrigel scaffold at each time point and reached the peak at the end of stage IV differentiation, which resulted in 5 fold increase as compared to cells cultured in 2D. *Glut2* is a glucose transporter found in the cell membrane of mature β -cells and is not only an important indicator of β -cell maturity but also is required for glucose-induced insulin release. *Glut2* gene expression level was enhanced in 3D culture at each time point or compared to 2D culture values. Additionally, *MafA* gene expression is a hallmark of fully differentiated pancreatic endocrine cells. Our data showed

that *MafA* gene was upregulated along with the process of pancreatic differentiation process increased 5 folds compared to 2D culture at the end of differentiation.

4.4.7. Insulin secretion in 2D and 3D culture

The biological function of hESCs-derived insulin-producing cells β cells in 2D and 3D culture were determined by insulin secretion upon glucose challenges (Figure 21A). A nearly 4.5-fold and 7 fold increase in insulin secretion from 3D induced cells were observed when cells were incubated in 15 mM and 25 mM high glucose-containing medium, in comparison with buffer containing lower glucose concentration (5.5 mM). Conversely, only 2.8-fold and 3.7 fold increase in insulin secretion was detected in 2D induced cells when they were incubated in 15 mM and 25 mM high glucose-containing medium. Approximately, 44 ± 4.9 μ IU insulin/mg cellular proteins were secreted from 3D-induced cells in high glucose (25 mM)-containing medium, whereas only 10.8 ± 3.2 μ IU insulin/mg cellular proteins from 2D-induced cells. This represents an approximate four-fold increase in 3D-induced cells compared to 2D-induced cells when cells challenged with high glucose concentration. These results indicate that 3D induced-insulin producing cells are more sensitive to a glucose challenge due to their improved maturity. Furthermore, we analyzed the percentage of insulin+ cells by using flow cytometry. After approximate 21 days of pancreatic induction, the insulin-positive cells were reached approximately 20% in 3D collagen/Matrigel culture, compared to 5% in 2D. It suggested 3D culture not only promote the maturity of hESCs-induced β cells, but also enhanced the production of insulin-secreting cells in a higher population.

4.4.8. Ultrastructural characteristics of hESC-derived pancreatic cells

We used transmission electron microscopy to determine whether the hESCs-derived cells formed mature secretory granules. The typical mature insulin granules were observed in 2D and 3D induced cells (Figure 22), which is characterized by round electron-dense crystalline core surrounded with the distinctive large, clear halo. The inner crystalline core of insulin granule is less electron opaque in mature β cells than those found in glucagon-containing and somatostatin-containing α - and δ - cells, which confirmed the generation of insulin-producing β cells. The granule number was approximately 12 times fewer in 2D-induced cells than in 3D-induced cells as counted from 5 individual cells from each sample.

4.5. Discussion

Current protocols for stem cell differentiation mainly rely on mimicking the sequence of signaling events that underlies the differentiation of tissues in embryological development. Apart from specific soluble growth factors for lineage specific differentiation, the importance role of ECM on stem cell differentiation is greatly ignored. In this study, we established a new model for hESCs differentiation and we demonstrated that more mature insulin-producing cells can be generated from hESCs with higher efficiency in the designed three-dimensional culture system.

Collagen I hydrogel is mechanical robust and easy to handle, which is of practical importance when translate their use as engineered tissues in the clinic. In addition, the main ECM of mature human islets has most often been reported to be composed of laminin and collagen IV [185]. Therefore, it is possible that the addition of Matrigel allows hESCs to preferentially attach to the properties of their native environment and perform the differentiation

close to *in vivo* development in the composite matrices that developed in this study. Recent studies in stem cell biology revealed that when exposed to the intrinsic properties of the extracellular matrix, such as matrix structure, elasticity, and composition, stem cells can differentiate into various lineage of mature tissue cells [149]. Incorporation of Matrigel in collagen gel can cause distinct changes in the constructs morphologies and mechanical properties. Thus, in this study; we incorporated Matrigel at different ratio (10% v/v, 35% v/v or 50% v/v) in collagen gel and tried to figure out the preferred condition for pancreatic differentiation. The changes in fibrillar structure were confirmed by SEM. At low Matrigel concentration (10% v/v), the matrix structure was uniform with a fine fiber structure, whereas at higher percentages of Matrigel, larger fibrils appeared with uniform pore size. Also, the mechanical properties differed in various collagen/Matrigel scaffolds has been reported [211]. The higher concentration of Matrigel incorporated in collagen gel resulted in increased Young's moduli of the various collagen-Matrigel compositions[211]. The differences in architectural and mechanical properties of collagen/Matrigel scaffolds were related to stem cell differentiation efficiency. Our data showed that 35% Matrigel gave rise to the highest expression of definitive endoderm gene, such as Sox17, Foxa2 and CXCR4. The efficient generation of DE cells would facilitate the following differentiation step. Thus, the collagen gel incorporated with 35% Matrigel was used in other experiments.

Another factor that may contribute to expansion and maturation of insulin-producing cells in 3D culture is the use of growth factors and small molecules. Activin A has been used to induce DE cells in most reports. However, recently study by Mclean *et al.* showed that Activin A efficiently specified DE differentiation from hESCs only when phosphatidylinositol 3-kinase (PI3K) signaling is suppressed [107]. In this study, wortmannin, a PI3K inhibitor, was used for

DE induction and it showed 95% of cells in collagen/Matrigel (35% v/v) scaffolds were Sox17 positive. For differentiation of DE cells into pancreatic progenitors, the combinational use of Noggin, an inhibitor of bone morphogenetic protein (BMP) signaling, retinoic acid, and fibroblast growth factor 7 (FGF7 or KGF), which were reported to induce pancreatic progenitor cells generation in our studies [106, 212-214], was applied in our protocol. In addition, by using high-content screen in a chemical library of 5,000 compounds, (-)-indolactam (ILV) was identified to induce PDX1-positive pancreatic progenitor cells at high efficiency [215]. Here, we included small molecule ILV in the growth factor regimen and found out that with the addition of ILV, the pancreatic progenitor markers *PDX1*, *HNF6* and *Sox17* were increased dramatically compared to cells treated without ILV. The induction of insulin-producing cells was characterized at the final stage. As revealed by immunohistochemical staining, the cluster formed in 3D culture consist as lease three types of cells, including insulin-producing β cells, glucagon-secreting α cells and somatostatin-secreting δ cells, suggesting the expression pattern of mature islets. Moreover, the co-expression of Insulin, C-peptide, PDX1 and NKX6-1 was observed in the induced insulin-producing cells in 3D culture, which is considered to be a specific functional characteristic of mature β cells [216]. The quantitative PCR-based gene expression profiling demonstrated that β -cell specific transcription factors including *PDX1*, *NKX6-1*, *Insulin* and *Glut2* were significantly increased in the 3D culture and presented a closer gene expression pattern to human pancreas development. Furthermore, the maturation phenotype of insulin-producing was confirmed. For example, the 3D-induced cells can secrete insulin in response to glucose stimulation in a more sensitive manner, and the insulin-positive cells comprised about 20% of population at the final stage. Furthermore, the insulin-containing granules were detected as a symbol of mature β cells.

To summarize, in this work we established a novel 3D model to induce hESCs differentiate into mature insulin-producing cells that demonstrated more close phenotype and gene expression profile to adult human islets. We believe this presented strategy would not only provide an efficient method to use hESCs for clinical-relevant application, but also facilitate the future study of the mechanism of human pancreatic specialization and maturation *in vitro*.

Chapter 5

Conclusion and Future Directions

In this work, we have established a novel 3D culture system by using nature ECM proteins for pancreatic lineage differentiation from hESCs. We believe the data presented in this study offered direct evidence supporting the hypothesis that 3D pancreatic differentiation of hESCs may represent a valuable technique for generating clinically relevant β cells *in vitro*. These work provided a proof-of-concept study and this method can be transformed to generate other lineage specific tissue from ESCs such as hepatocyte and neural cells.

The main goal of directing the differentiation of hESCs to β cells is to provide a new source of β cells for transplantation therapy. Due to the interesting findings, in order to further characterize the maturity of hESCs-induced insulin-producing cells, our future research may lead to perform an animal study to further test their ability to maintain blood glucose levels following transplantation. hESCs-derived β cells can be transplanted into mouse kidney capsule, and function of β cells can be determined by the insulin and glucose concentrations in serum after challenging with high glucose. A rapid glucose-responsive insulin release following transplantation is highly desired. Creating functional, adult-like β cells *in vitro* may require further understanding of β cell metabolism, the role of islet structure, the pathways or molecules involved in 3D niches for pancreatic specification.

The development of microscale technologies offers powerful tools for stem cell study and tissue engineering [217]. Scaffold can be fabricated at microscale and nanoscale by the use of 3D printing, microsyringe deposition, and electrospinning of nanofibers. These techniques allow control of cellular microenvironment *in vitro* and provide templates for cell aggregate formation or perform high-throughput assays. We anticipate that the use high-throughput

screening methodologies will contribute to the design of new 3D scaffolds for the expansion and lineage-specific differentiation of hESCs. In addition, understanding other limitations of 3D stem cell culture may provide guidance for more efficient generation of lineage specific cells. For example, vascularization is the capstone in large-scale tissue-engineering application [218]. Recent findings suggested that co-culture β cells with microvascular endothelial cells help maturation of hESCs differentiation into β cells [219]. Therefore, development of a 3D patterned co-culture system in regulating various aspects of cellular microenvironment would be an imperative direction for complete maturation of pancreatic β cells generated from human pluripotent stem cells.

Reproducibility of results across hESCs line is of critical importance for stem cell research. Recently, much attention have been given to the description and explanation of differences between various hESCs lines [220]. These differences result in large variations in propensity of differentiation between cell lines. The data obtained in this study on based on H9 cell line acquired from Wicell. Although H9 cell line have been widely used in hESCs differentiation, the adaptation of this technique in other pluripotent stem cell lines may be necessary.

Table 1. List of PCR primers

Gene	Sequence	Product (bp)	Annealing temperature (°C)
SOX17	5'-GGCGCAGCAGAATCCAGA-3' 5'-CCACGACTTGCCCAGCAT-3'	102	61
FOXA2	5'-GGGAGCGGTGAAGATGGA-3' 5'-TCATGTTGCTCACGGAGGAGTA-3'	82 bp	60
CXCR4	5'-CACCGCATCTGGAGAACCA-3' 5'-GCCCATTTCTCGGTGTAGTT-3'	86 bp	62
OCT4	5'-TGGGCTCGAGAAGGATGTG-3' 5'-GCATAGTCGCTGCTTGATCG-3'	92 bp	62
PAX6	5'-TCTCCTCCATCAACCGAGTC-3' 5'-GAGCCACTATGGGGAGTGAG-3'	151 bp	60
N-CAD	5'-CCCACACCCTGGAGACATTG-3' 5'-GCCGCTTTAAGGCCCTCA-3'	96 bp	60
BRACH	5'-TGCTTCCCTGAGACCCAGTT-3' 5'-GATCACTTCTTTCCTTTGCAGTT-3'	112 bp	61
SOX3	5'-CCCAGCCTACAAAGGTGAA-3' 5'-CCCAGCCTACAAAGGTGAAA-3'	102 bp	60
FN1	5'-CCCATCAGCAGGAACACCTT-3' 5'-GGCTCACTGCAAAGACTTTGAA-3'	82 bp	60
LAMC1	5'-TGGGCATTCTTCTGTCTGTACAA-3' 5'-GCCACCCATCCTCATCAATC-3'	86 bp	60
Col4A1	5'-ACTCTTTTGTGATGCACACCA-3' 5'-AAGCTGTAAGCGTTTGCCTA-3'	151 bp	60
COL3A1	5'-AACACGCAAGGCTGTGAGACT-3' 5'-GCCAACGTCCACACCAAATT-3'	88 bp	60
COL1A1	5'-GAACGCGTGTCATCCCTTGT-3' 5'-GAACGAGGTAGTCTTTCAGCAACA-3'	91 bp	62
COL1A2	5'-AAGGTCATGCTGGTCTTGCT-3' 5'-GACCCTGTTCACCTTTTCCA-3'	115 bp	60
SOX9	5'-AGACCTTTGGGCTGCCTTAT-3' 5'-ACTTGTAATCCGGGTGGTCCTT-3'	121 bp	60
HNF6	5'-TGTGGAAGTGGCTGCAGGA-3' 5'-TGTGAAGACCAACCTGGGCT-3'	131 bp	60
PDX1	5'-AAGTCTACCAAAGCTCACGCG-3' 5'-GTAGGCGCCGCCTGC-3'	199 bp	60
NGN3	5'-CCCTCTACTCCCCAGTCTCC-3' 5'-CCTTACCCTTAGCACCCACA-3'	114 bp	62
INSULIN	5'-GCAGCCTTTGTGAACCAACAC-3' 5'-CCCCGCACACTAGGTAGAGA-3'	147 bp	62
MAFA	5'-CTTCAGCAAGGAGGAGGTCATC-3' 5'-CTCGTATTTCTCCTTGTACAGGTCC-3'	208 bp	62
GLUT2	5'-GCTACCGACAGCCTATTCTA-3' 5'-CAAGTCCCCTGACATGAAG-3'	267 bp	62

Table 2. List of Antibodies used in immunocytochemistry and immunohistochemistry

Antibodies	Host	Dilution or Concentration	Producer
Anti-Sox17	Mouse	1:50	R&D Systems
Anti-Foxa2	Rabbit	1:1000	Abcam
Anti-Pdx1	Rabbit	1:2000	Abcam
Anti-Collagen IV	Rabbit	1:200	Abcam
Anti-HNF-6	Mouse	1:200	Santa Cruz Biotechnology, Inc.
Anti-Nkx2.2	Mouse	2 µg/ml	Developmental Studies Hybridoma Bank
Anti-Ngn3	Mouse	2.5 µg/ml	Developmental Studies Hybridoma Bank
Anti-Nkx6.1	Mouse	3 µg/ml	Developmental Studies Hybridoma Bank
Anti-Insulin	Rabbit	1:400	Cell Signaling Technology, Inc.
Anti-Glucagon	Mouse	1:4000	Millipore
Anti-C-Peptide	Mouse	1:100	Millipore
Anti-Somatosatatin	Rat	1:100	Millipore
Anti-Pancreatic polypeptide	Mouse	1:50	R&D Systems
TRITC-conjugated anti-rabbit IgG	Donkey	1:100	Jackson ImmunoResearch
Alexa Fluor [®] -conjugated anti-rat IgG	Donkey	1:500	Jackson ImmunoResearch
DyLight [™] 488-conjugated anti-mouse IgG	Goat	1:500	Thermo Scientific
PE anti-human Sox17	Mouse	1 µg/ml	BD Biosciences
PE IgG1 κ isotype control	Mouse	1 µg/ml	BD Biosciences

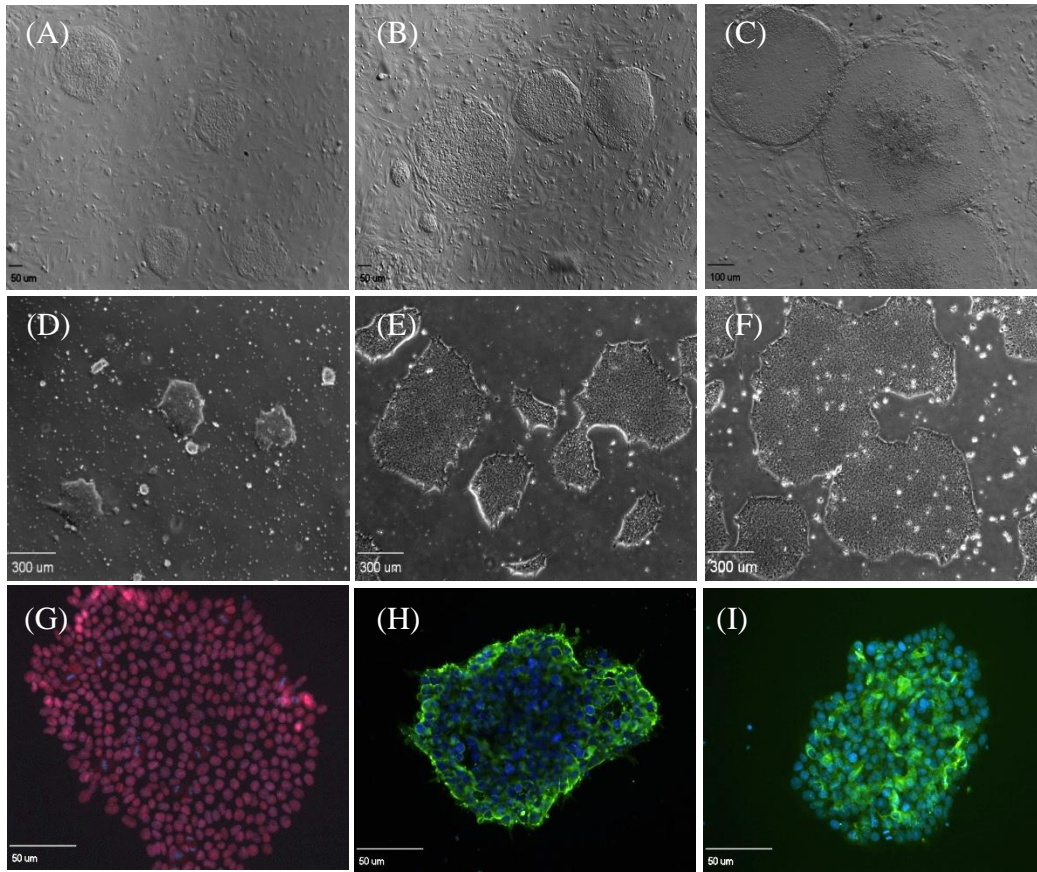


Figure 1. Morphological changes and expression of pluripotent markers of hESCs before differentiation. (A-F) Phase-contrast microscopy images of hESCs cultured on MEF feeder layers (A-C) or Matrigel™ (D-F). hESCs proliferated from day 2 (A, D), day 3 (B, E) to day 4 (C, F). (G-I) Immunocytochemical analysis of pluripotency in H9 hESCs. Cells were stained with antibodies against pluripotency marker proteins SOX2 (G), SSEA4 (H), and TRA-1-60 (I) after five passages. Cells were also labeled with diaminophenylindole (DAPI) in order to localize the nucleus. Stained cells were observed under a fluorescence microscope (Olympus IX 71) equipped with a CCD camera. Scar bar (A-C, G-I) 50 μm, (D-F) 300 μm.

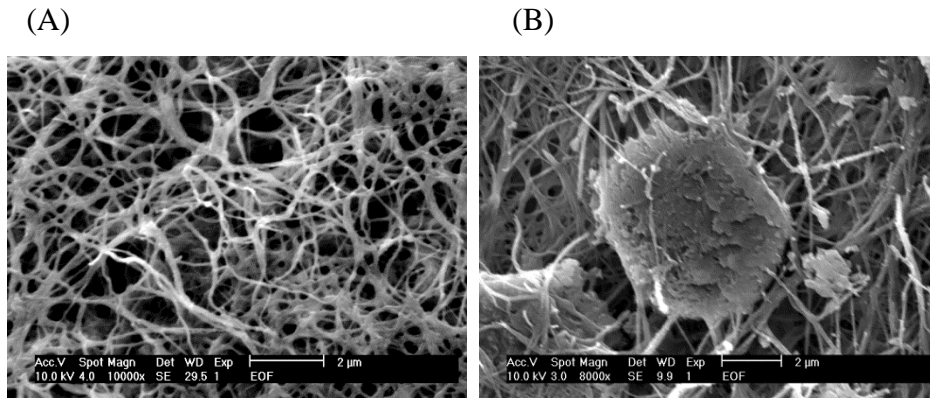


Figure. 2. Scanning electron microscopy (SEM) images of the collagen I scaffold. (A) Micrographic structure of 1.5 mg/ml collagen I scaffold. (B) hESCs integrated in collagen scaffold. Scale bar: 2 μ m.

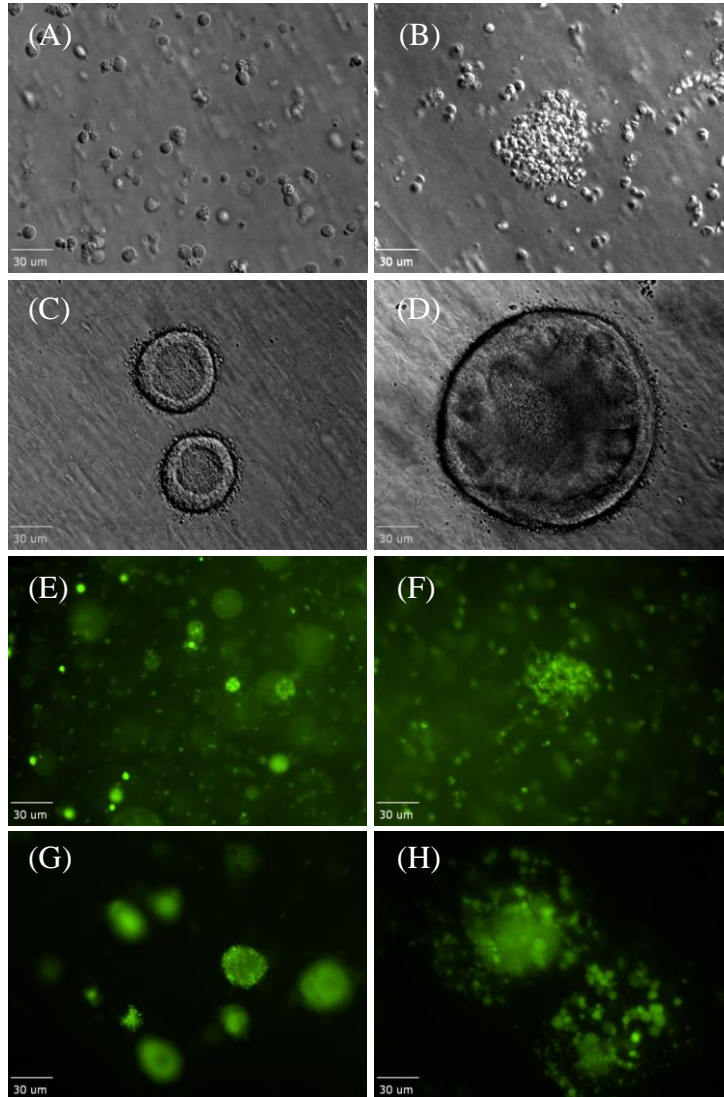


Figure 3. Morphological and viability analysis of hESCs-derived definitive endoderm in 3D collagen cultures. hESCs were seeded into a 3D collagen scaffold (1.5mg/ml) as single cells (A, B, E, F) or cell clusters (C, D, G, H) in a 24-well plate (2.5×10^6 cells/ml). A-D: Bright field images of hESCs on day 2 (A, C) and day 4 (B, D) of DE differentiation in 3D cultures. E-H: hESCs proliferated and maintained a high viability on day 2 (E, G) and day 4 (F, H) as determined by live/dead cell staining. Scale bar: 30 μ m.

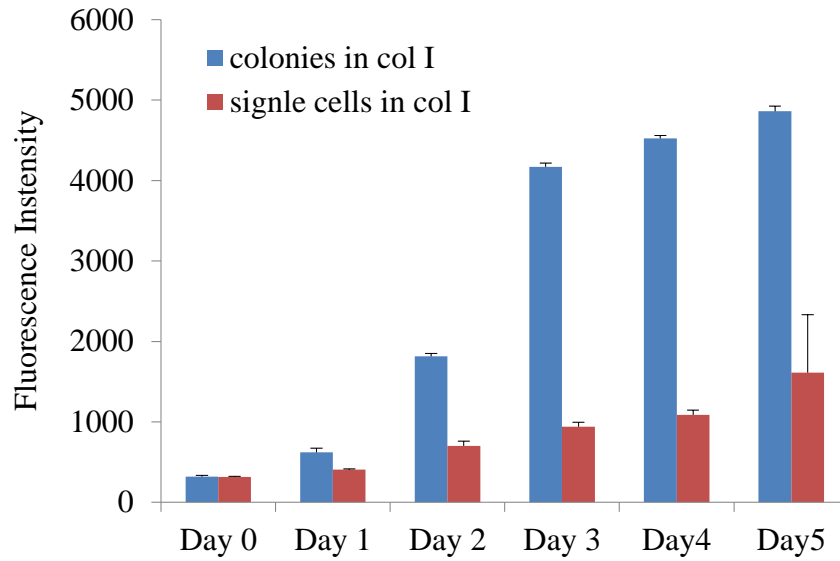


Figure. 4. hESCs proliferation in 3D collagen scaffold. hESCs were seeded in collagen scaffold as single cells or cell clusters and time course of cell proliferation was performed by Alamarblue assay from day 0 to day 5. Fluorescence intensity was detected at excitation wavelength of 570 nm and fluorescence emission at 590 nm. Data were the measurements in triplicate experiments at indicated time intervals.

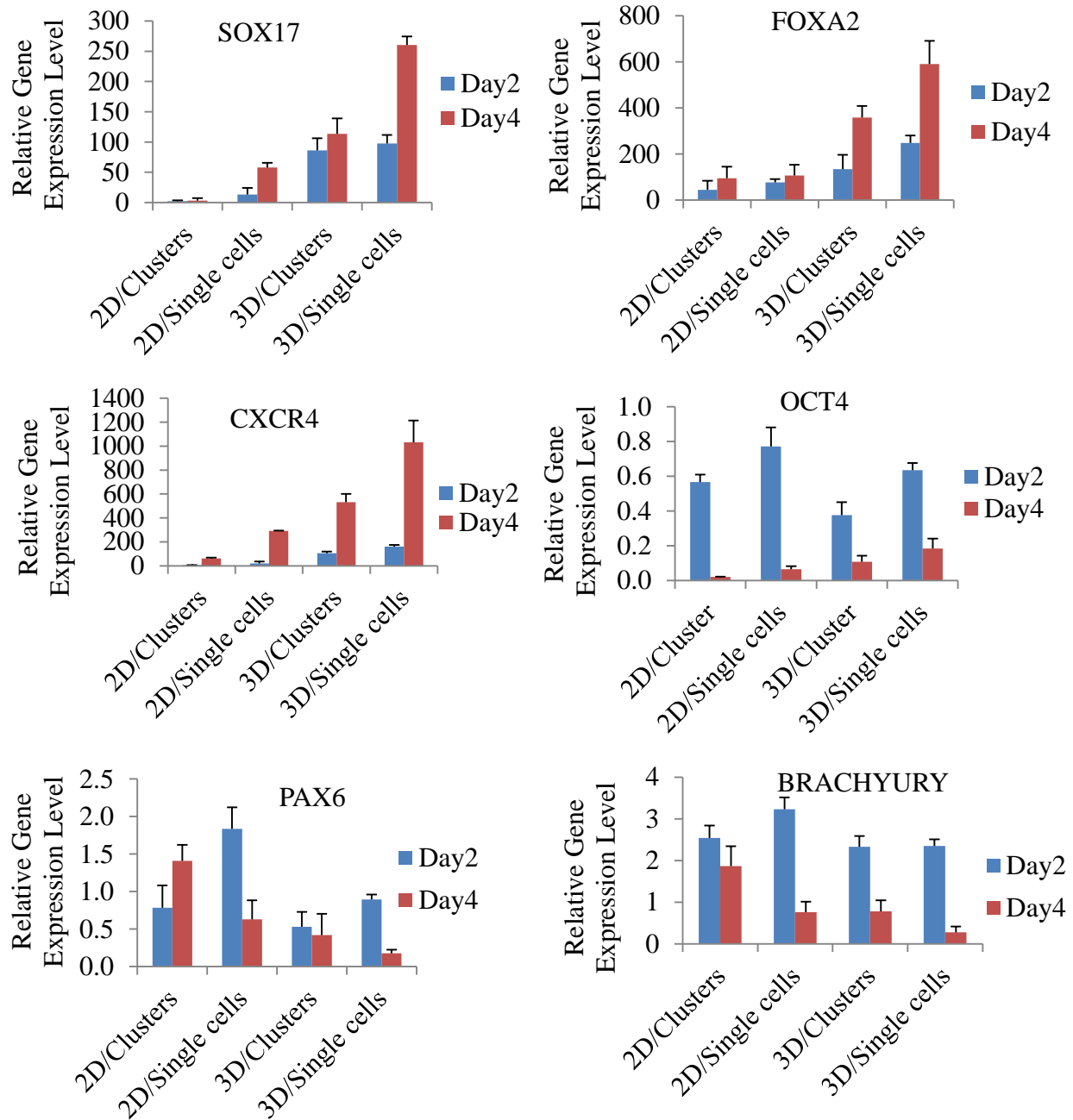


Figure 5. Quantitative PCR analysis of DE marker genes and other germ layer marker genes of hESCs-induced DE cells after 4 day of differentiation by using single cells inoculation method or cell clusters inoculation method. Undifferentiated hESCs were served as control and the mRNA levels were normalized to β -actin

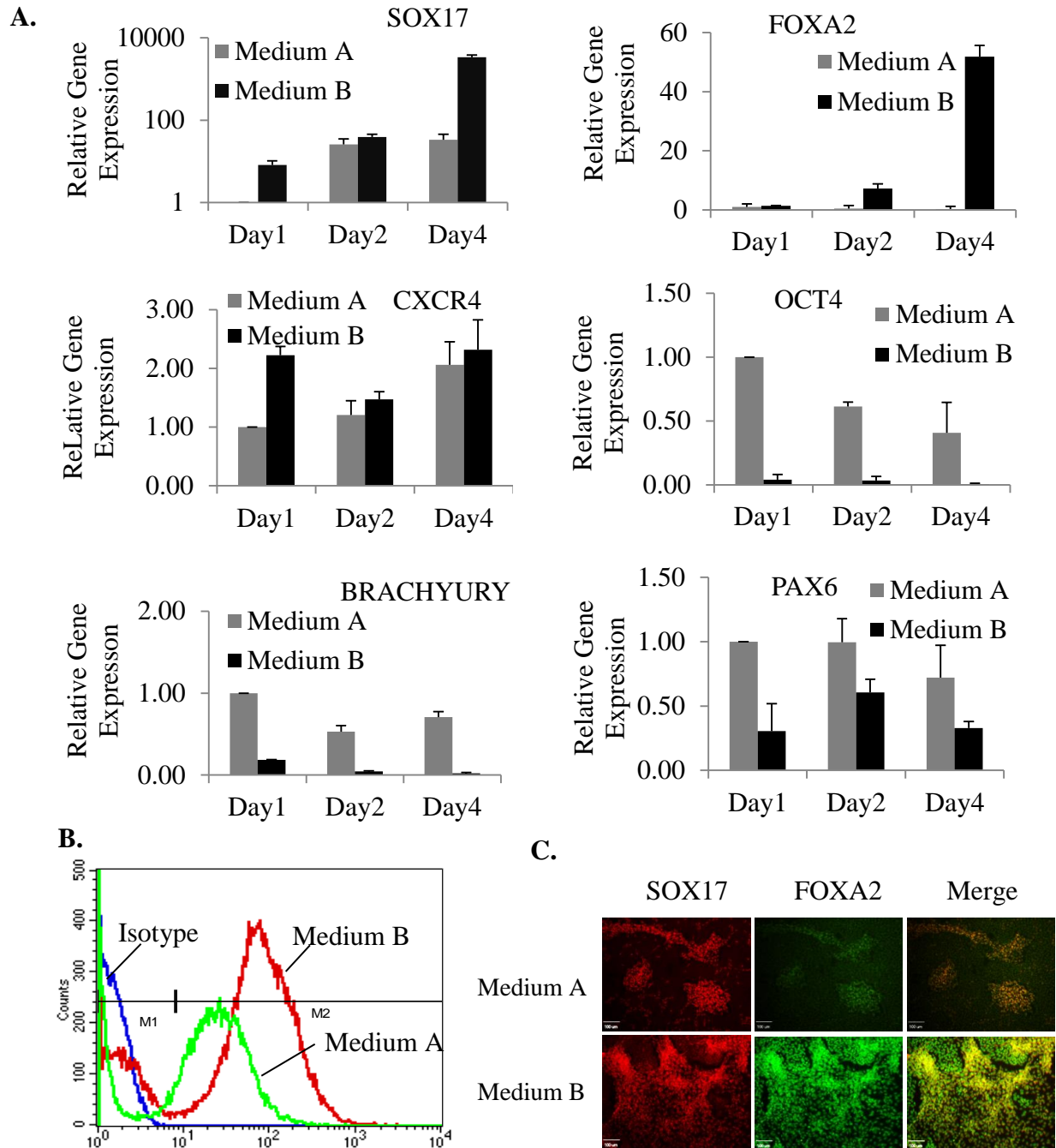


Figure 6. Comparison of DE differentiation efficiency by culture hESCs in DE differentiation medium A (Activin A and Wnt3a) or medium B (Activin A and wortmannin). (A) Quantitative PCR analysis of DE and three germ layers marker genes expression of hESCs-induced cells on day 1, day2 and day4 of DE differentiation. Expression levels were normalized to β actin. (B) Flow cytometric analysis of SOX17 positive cells in hESCs-induced cells on day 4. (C) Immunofluorescence staining of SOX17 (red), FOXA2 (green) in hESCs-induced cells on day 4.

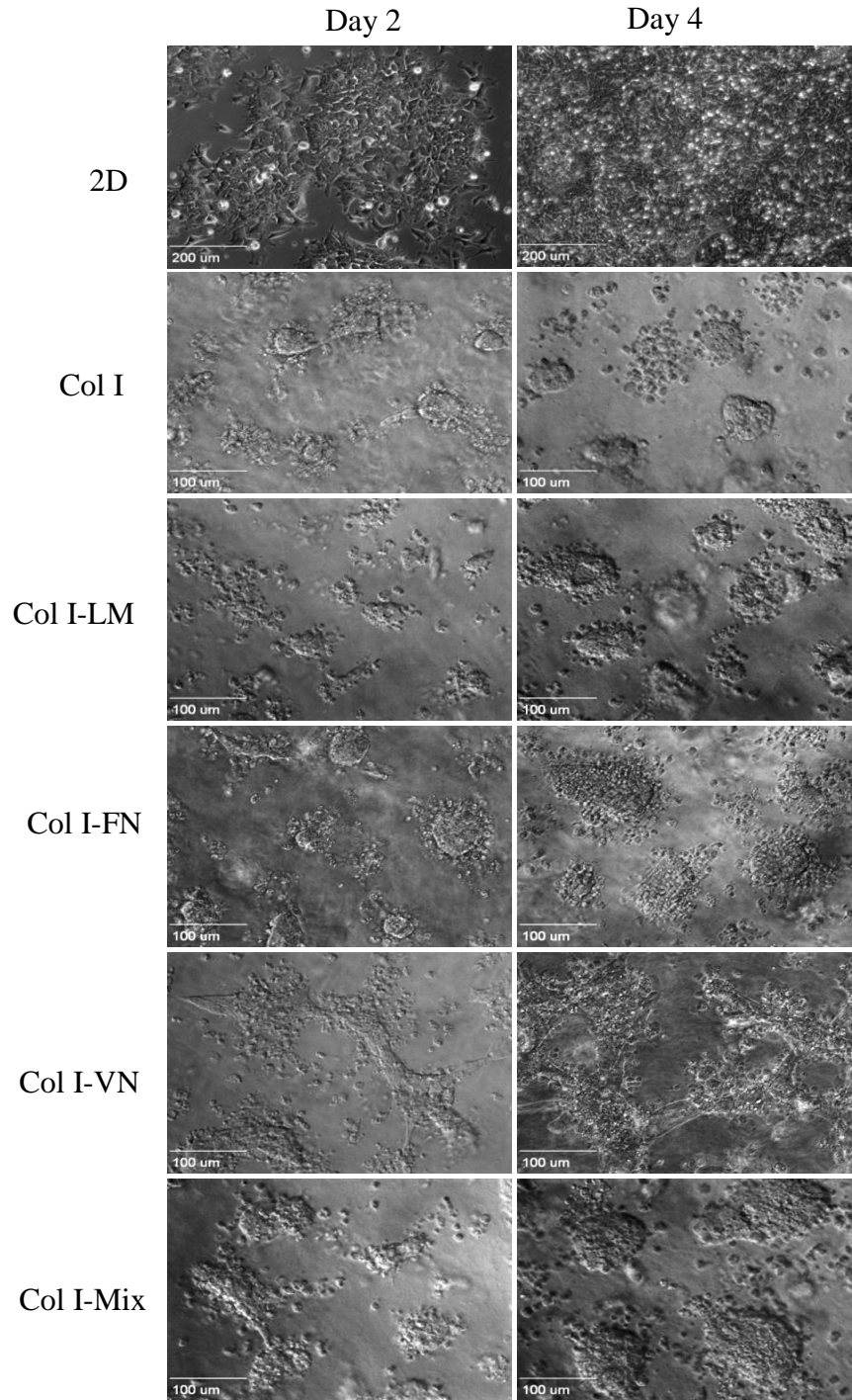


Figure. 7. Bright field microscopy images of hESCs-induced cells in 2D and 3D ECM scaffolds. hESCs were induced into DE in 2D (A and B), type I collagen scaffolds (Col I, C and D), and collagen along with laminin (LM, E and F), fibronectin (FN, G and H), vitronectin (VN, I and J) or mixture of ECM proteins (Mix, K and L). Morphologies were observed on day 2 (left panel) and day 4 (right panel) of DE differentiation. Scale bar (A-B) 200 μm , (C-L) 100 μm .

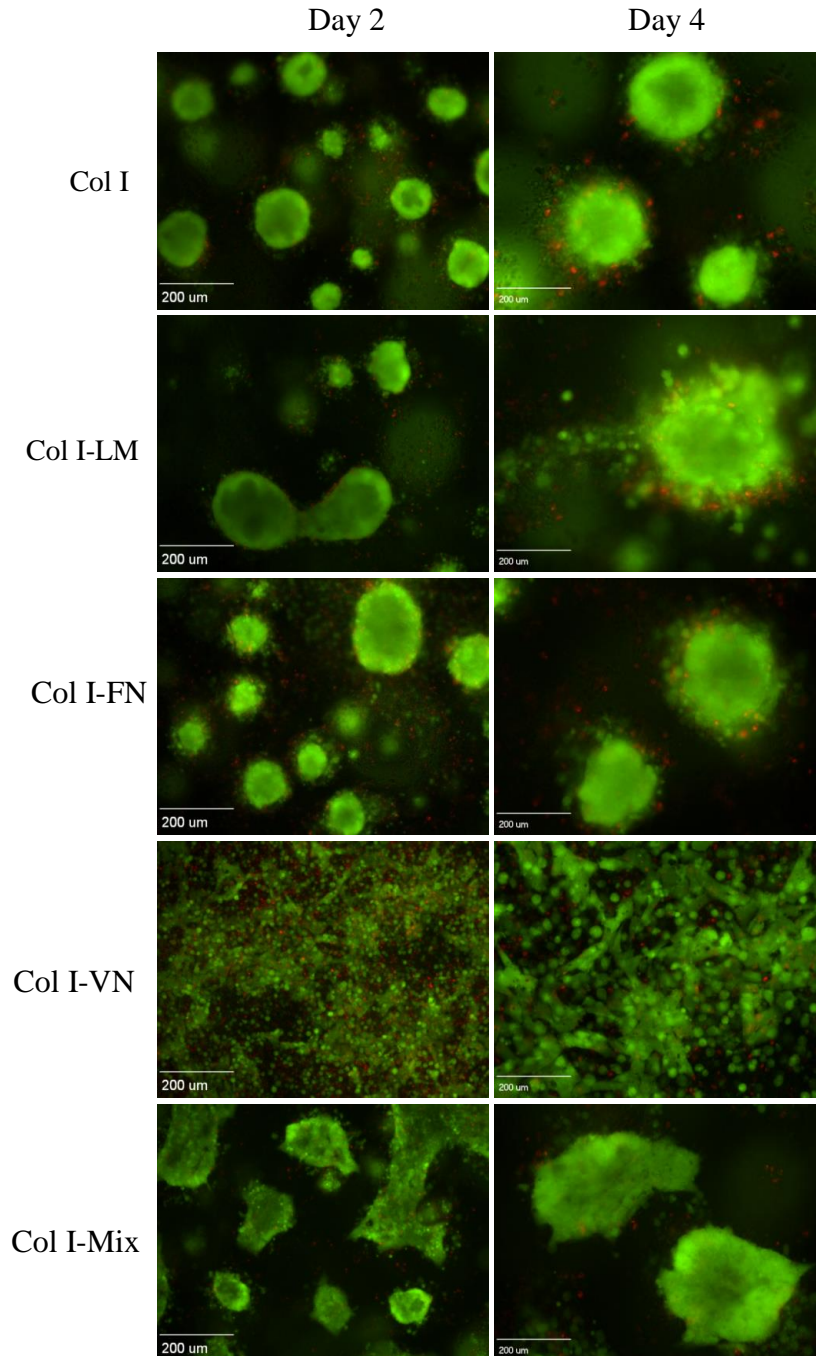


Figure 8. The viability of hESCs-induced DE cells in 3D ECM scaffolds. hESCs were cultured into type I collagen scaffolds (Col I, A and B), and collagen I along with laminin (LM, C and D), fibronectin (FN, E and F), vitronectin (VN, G and H) or mixture of ECM proteins (Mix, I and J) in DE differentiation medium for 4 days. Live/dead staining were performed on day 2 (left panel) and day 4 (right panel) of DE differentiation. Images were taken using an inverted fluorescence microscopy Olympus IX-71. Scale bar = 200 μm .

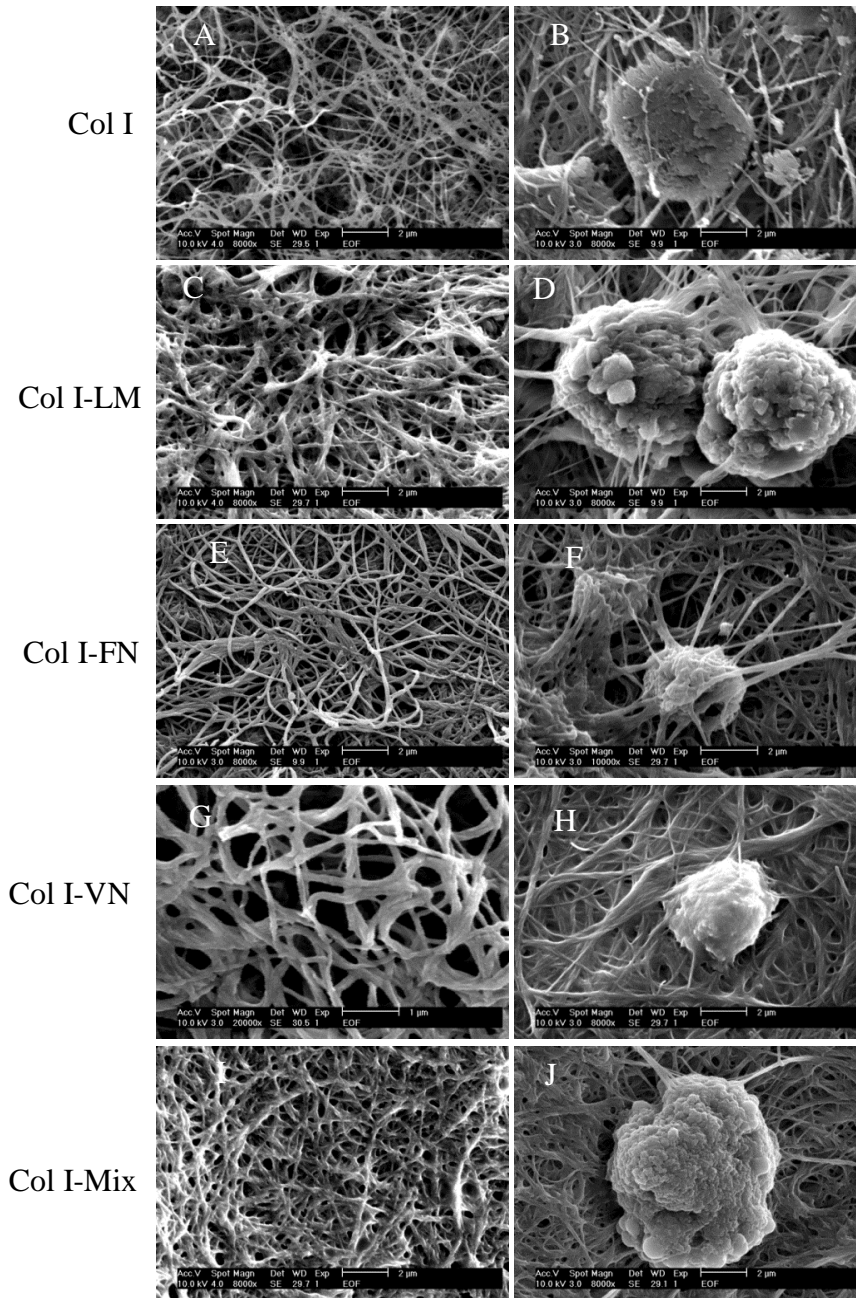
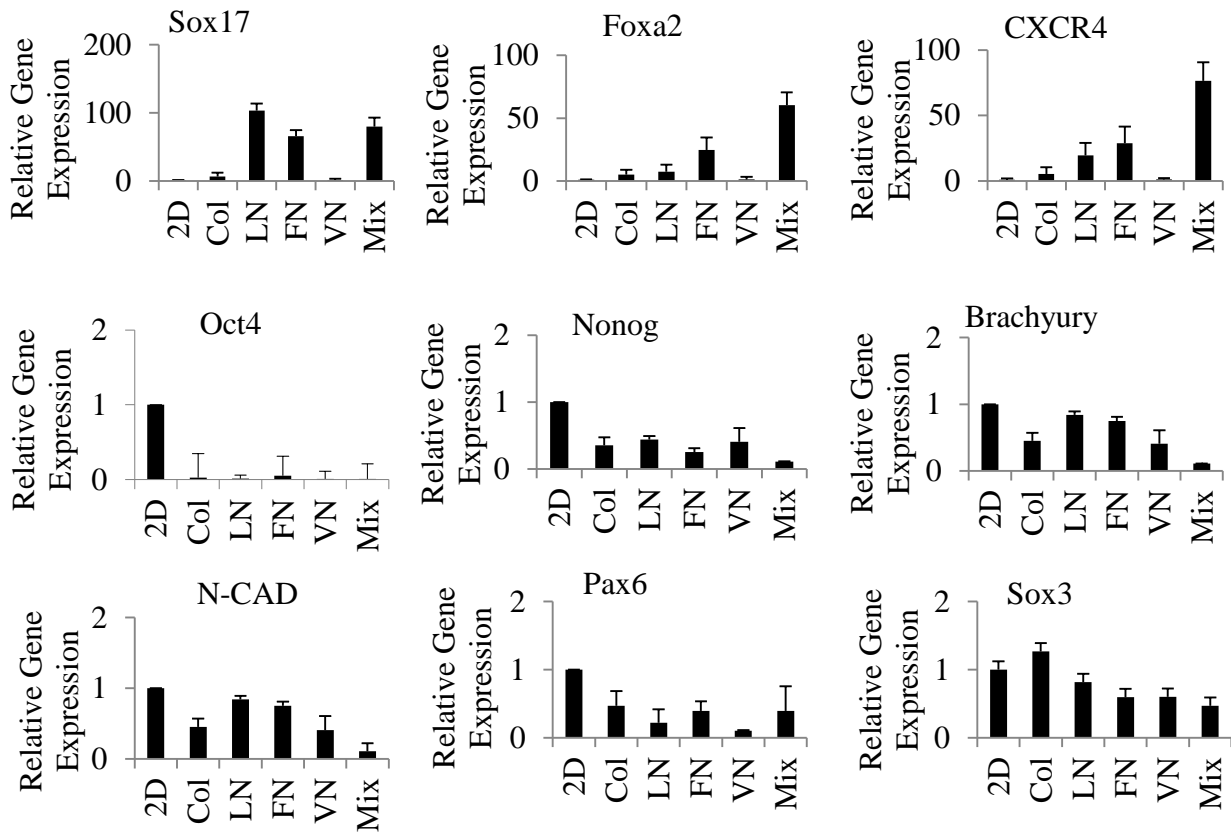


Figure. 9. Scanning electron microscopy of collagen scaffolds along with various ECM proteins without (left panel) or with hESCs (right panel). The following scaffolds were presented: Col I (A, B), Col I + LM (C, D), Col I + FN (E, F), Col I + VN (G, H), Col I + Mix (I, J). Scale bar = 2 μm.

A.



B.

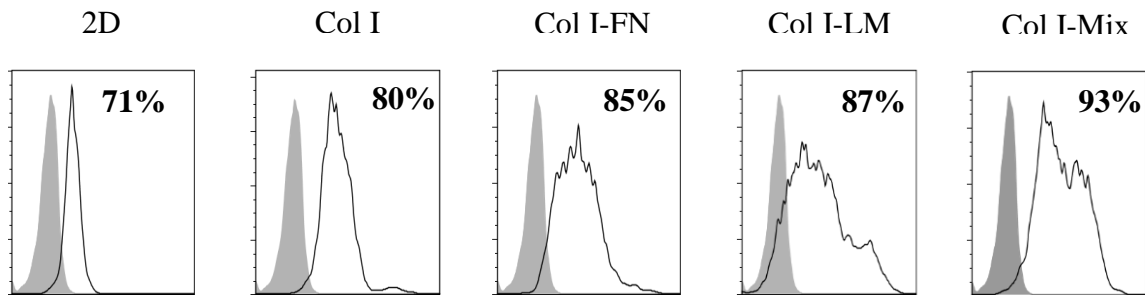


Figure 10. Enhancement of DE differentiation in 3D collagen-based ECM scaffolds. (A) Quantitative PCR analysis of hESCs-induced DE cells after 4 days of culture in 2D and 3D collagen gel along with ECM proteins LM, FN, and VN. Relative gene expression levels in DE cells cultured in 3D were normalized to DE cells in 2D culture and beta-actin was used as calibration gene. (B) Flow cytometric analysis of Sox17 in definitive endoderm derived from human embryonic stem (ES) cells. DE cells were stained with either PE Mouse IgG1, κ isotype control (filled histogram) or PE Mouse Anti-human Sox17 antibody (open histogram) at matched concentrations.

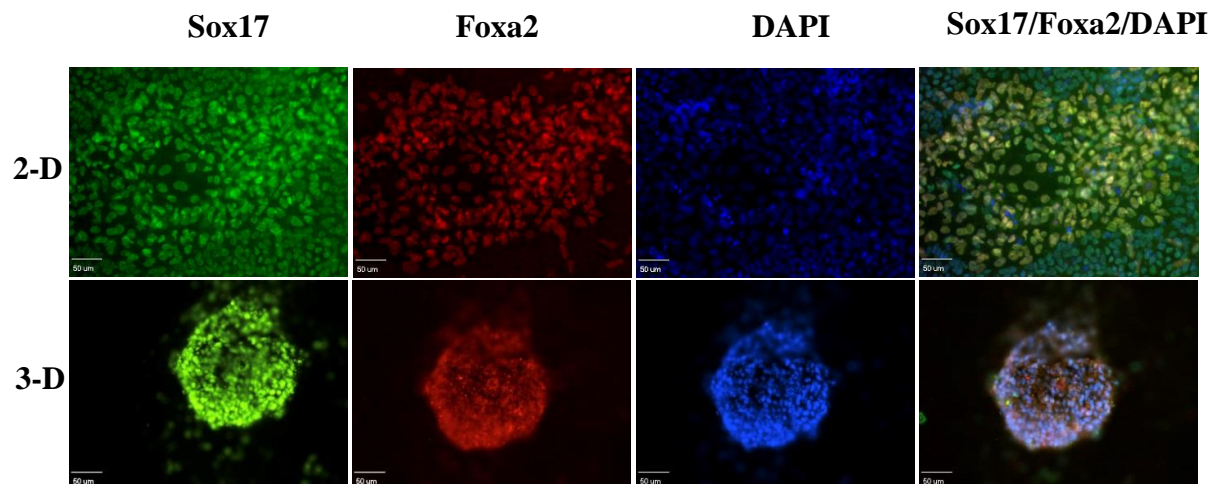


Figure. 11. Immunohistochemical staining of definitive endoderm markers, Sox17 and Foxa2 in hESCs-induced cells culture in 2D and 3D scffolds made of collagen I along with laminin, fibronectin, and vitronectin. The definitive endoderm cells were examined after 4 days of differentiation. The nuclei were conterstained with DAPI. Scale bar = 50 μ m.

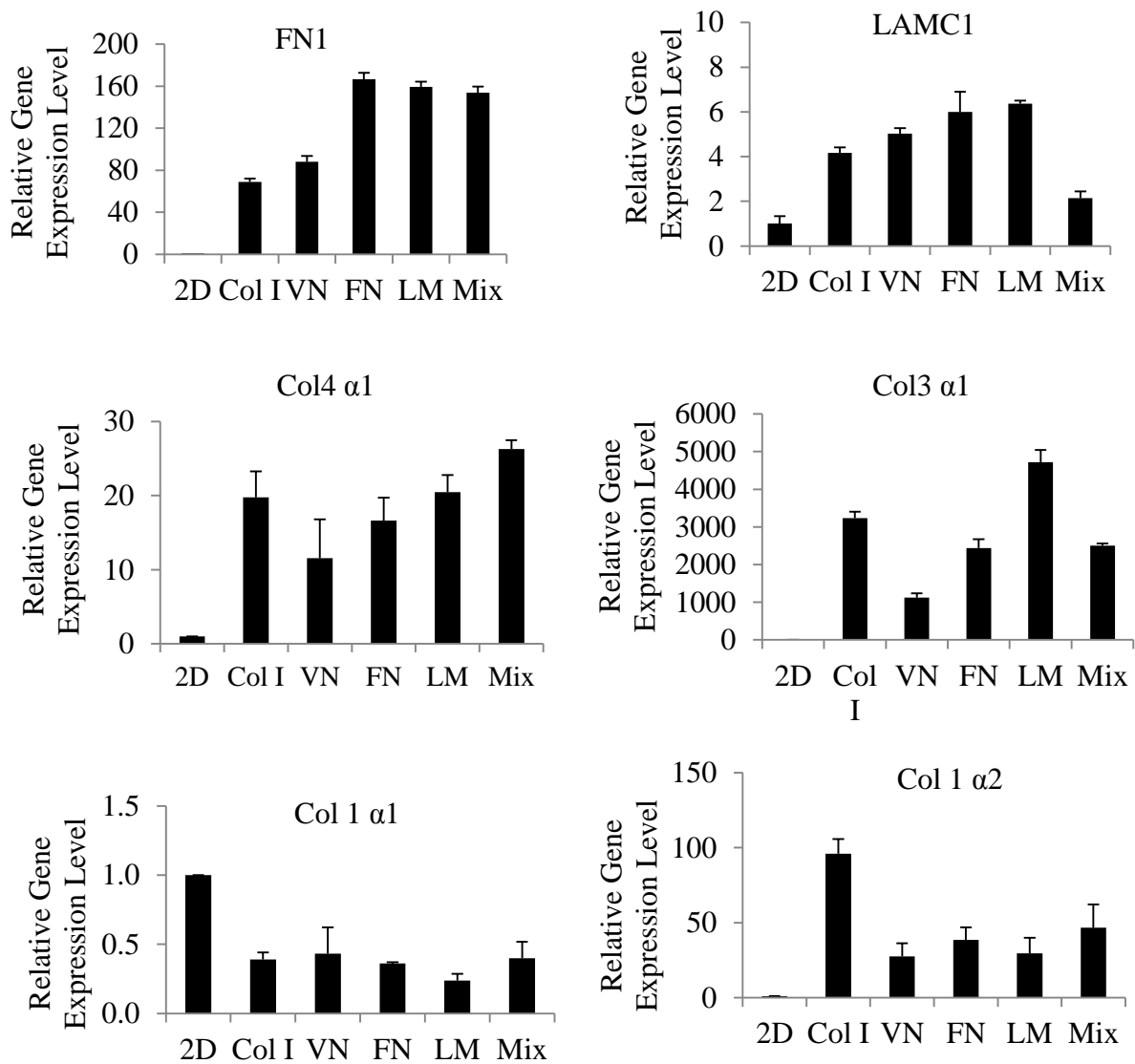


Figure. 12. Quantitative PCR analysis of ECM gene expression of hESCs-induced DE cells in 2D and 3D culture. hESCs were induced into DE cells for 4 days in 2D or 3D collagen gel along with various ECM proteins such as LM, FN, and VN. Relative gene expression levels in DE cells cultured in 3D scaffolds were normalized to DE cells in 2D and beta-actin was used as calibration gene.

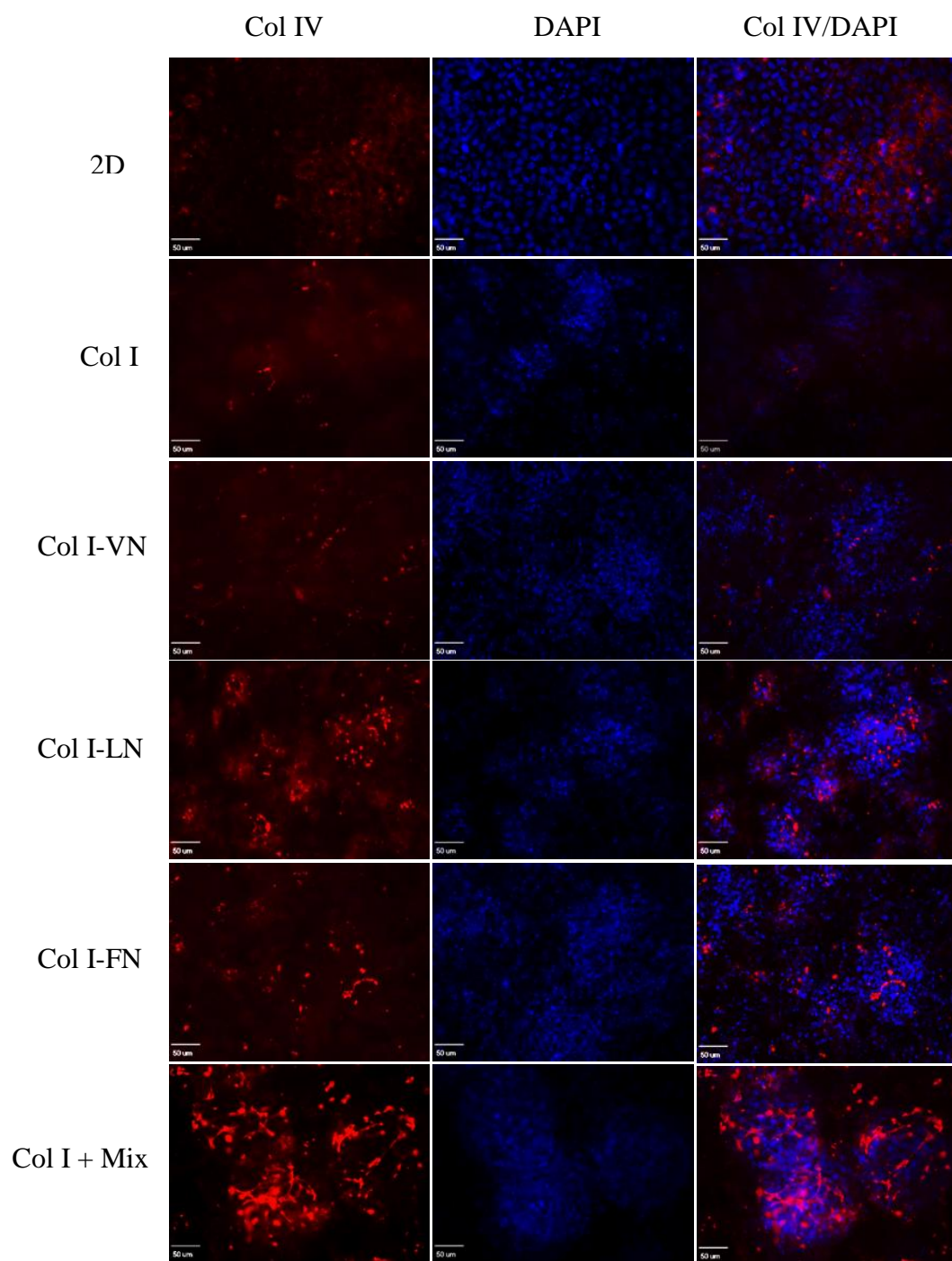


Figure. 13. Immunohistochemical staining of collagen IV secretion by DE differentiated cells in 3D scaffolds made of various ECM proteins. After 4 days of DE differentiation, cells in 2D and 3D culture were stained with rabbit anti-collagen IV primary antibody and TRITC conjugated donkey anti rabbit secondary antibody. Nucleus was counterstained with DAPI. Scale bar=50 μm .

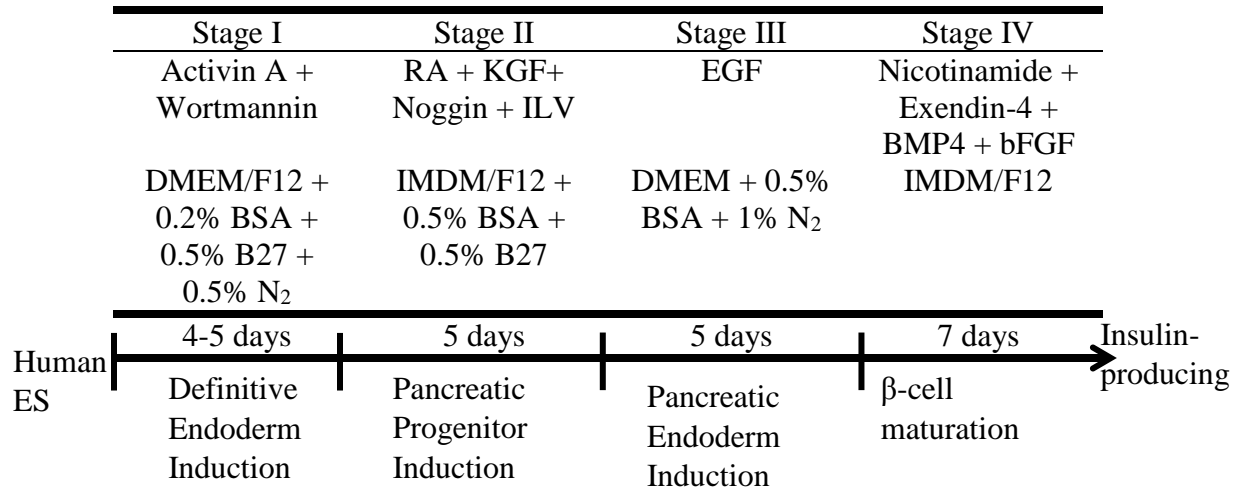


Figure. 14. A modified step-wise protocol for differentiating human ES cells into insulin-producing cells. Stage I: human ES cells were induced into definitive endoderm in the presence of activin A and wortmannin. Stage II: the differentiated endoderm cells were treated with RA, KGF, Noggin and ILV to induce pancreatic progenitor formation. Stage III: cells were exposed to EGF to endorse pancreatic endoderm lineage specific differentiation. Stage IV: a cocktail of factors including nicotinamide, extendin-4, BMP4 and bFGF as utilized to promote the maturation of pancreatic β cells (this protocol is similar to Zhang, D. *et al.*'s approach but with some modification).

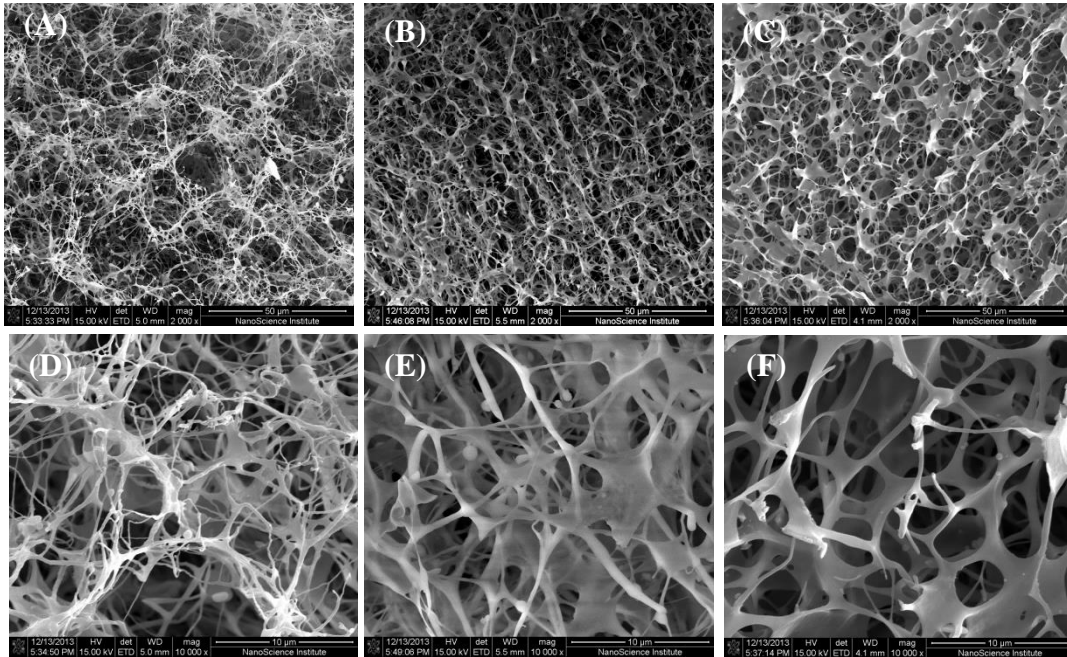


Figure. 15. Scanning electron micrographs of collagen I network incorporated with various concentration of Matrigel: (A, D) 10% Matrigel, (B, E), 35% Matrigel, (C, F) 50% Matrigel. Scale bars: A-C, 50 μm, D-F, 10 μm.

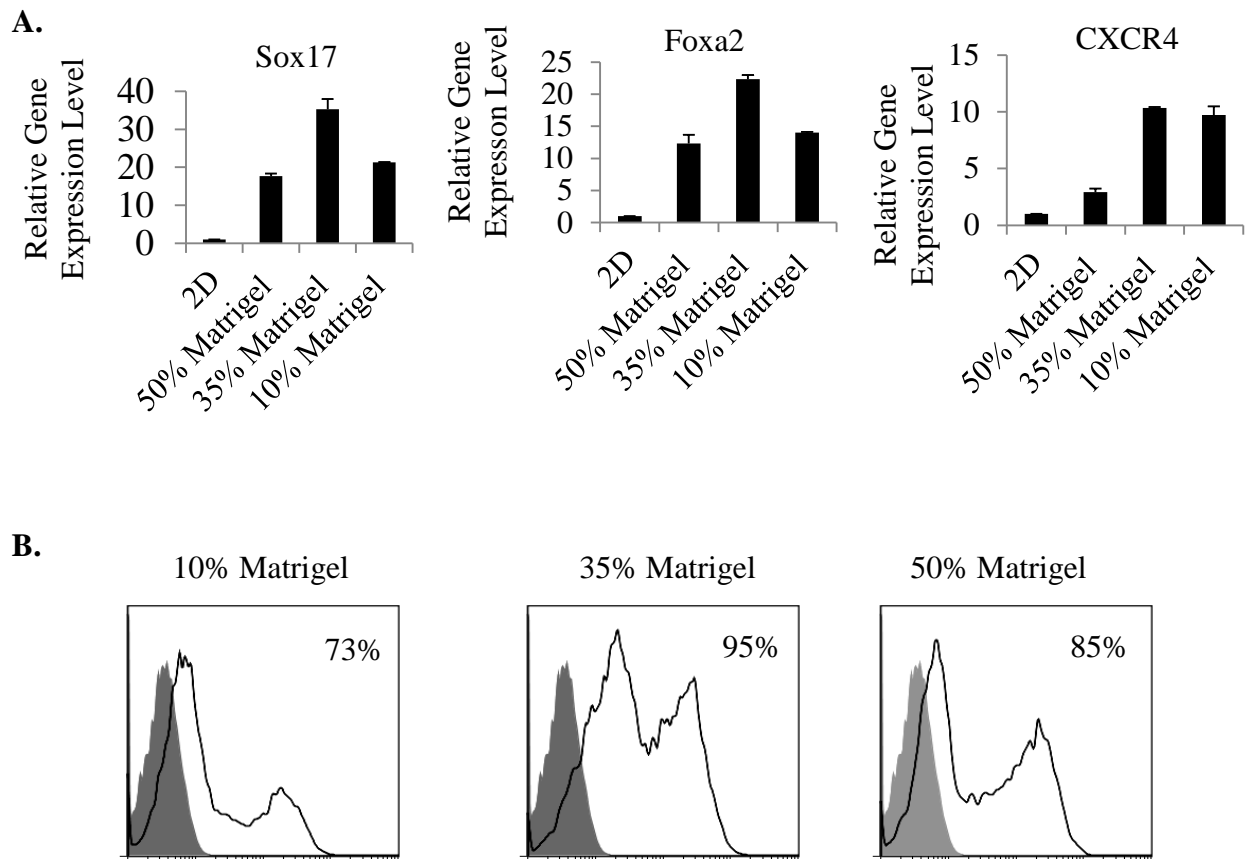


Figure. 16. Effect of Matrigel concentration in 3D collagen-I based scaffold on hESCs differentiation into definitive endoderm. (A) Quantitative PCR analysis of definitive endoderm markers of hESCs-derived DE cells after 4 days of differentiation in 2D and 3D collagen gel along with 10%, 35%, 50% Matrigel. Expression level were normalized to β -actin. For each sample, relative expression levels were normalized to corresponding levels in cells under 2D culture. (B) Intracellular flow cytometric analysis of Sox17 at day 4 of DE differentiation in 2D and 3D collagen gel along with 10%, 35%, 50% Matrigel. DE cells were stained with either PE Mouse IgG1, κ isotype control (filled histogram) or PE Mouse Anti-human Sox17 antibody (open histogram) at matched concentrations.

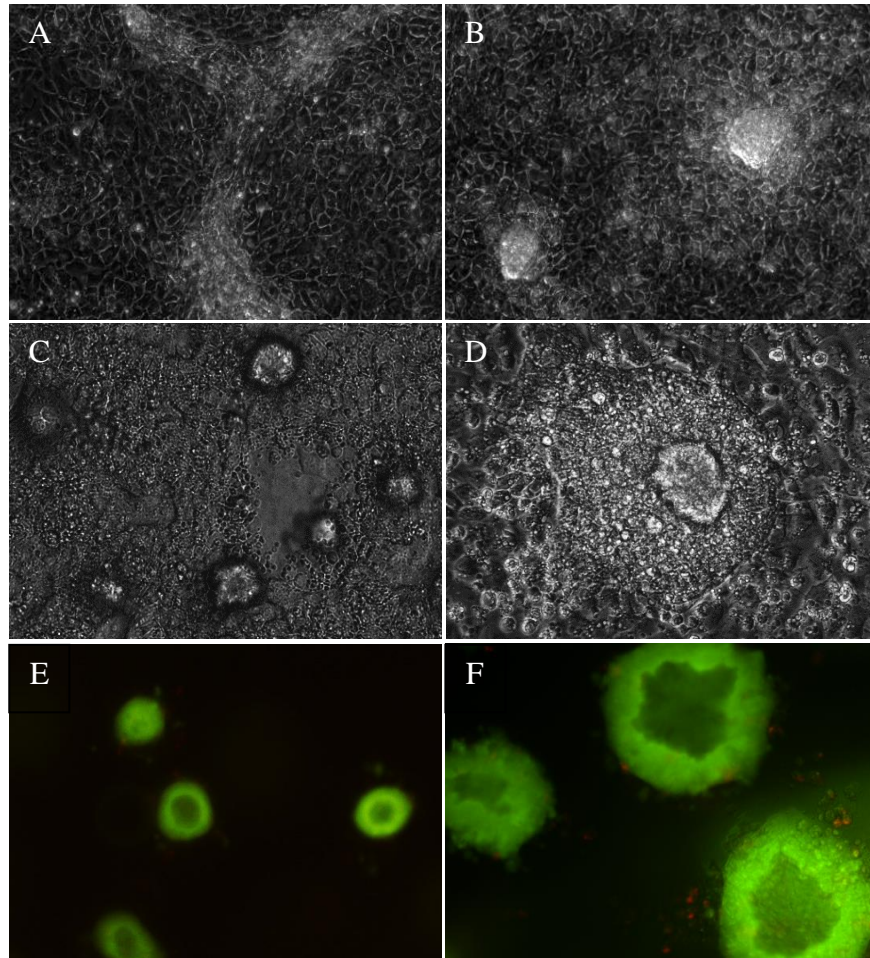


Figure. 17. The morphology and viability of hESCs during pancreatic differentiation process in 3D collagen/Matrigel scaffolds. (A-D) Phase contrast microscopy images of hESCs pancreatic differentiation at day 4 (A, C) and day 10 (B, D) in 2D (A, B) and collagen/Matrigel scaffold (C, D). (E-F) Live/dead staining of hESCs-differentiating cells in collagen/Matrigel scaffold on day 4 (E) and day 10 (F).

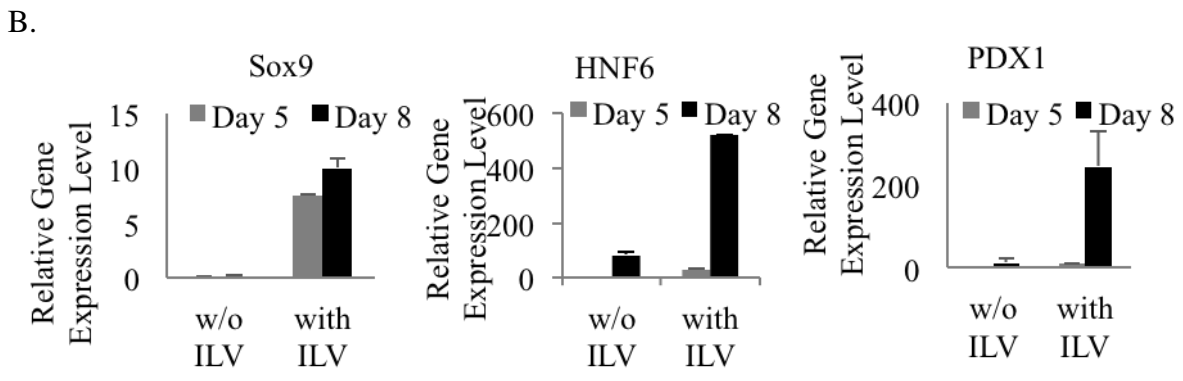
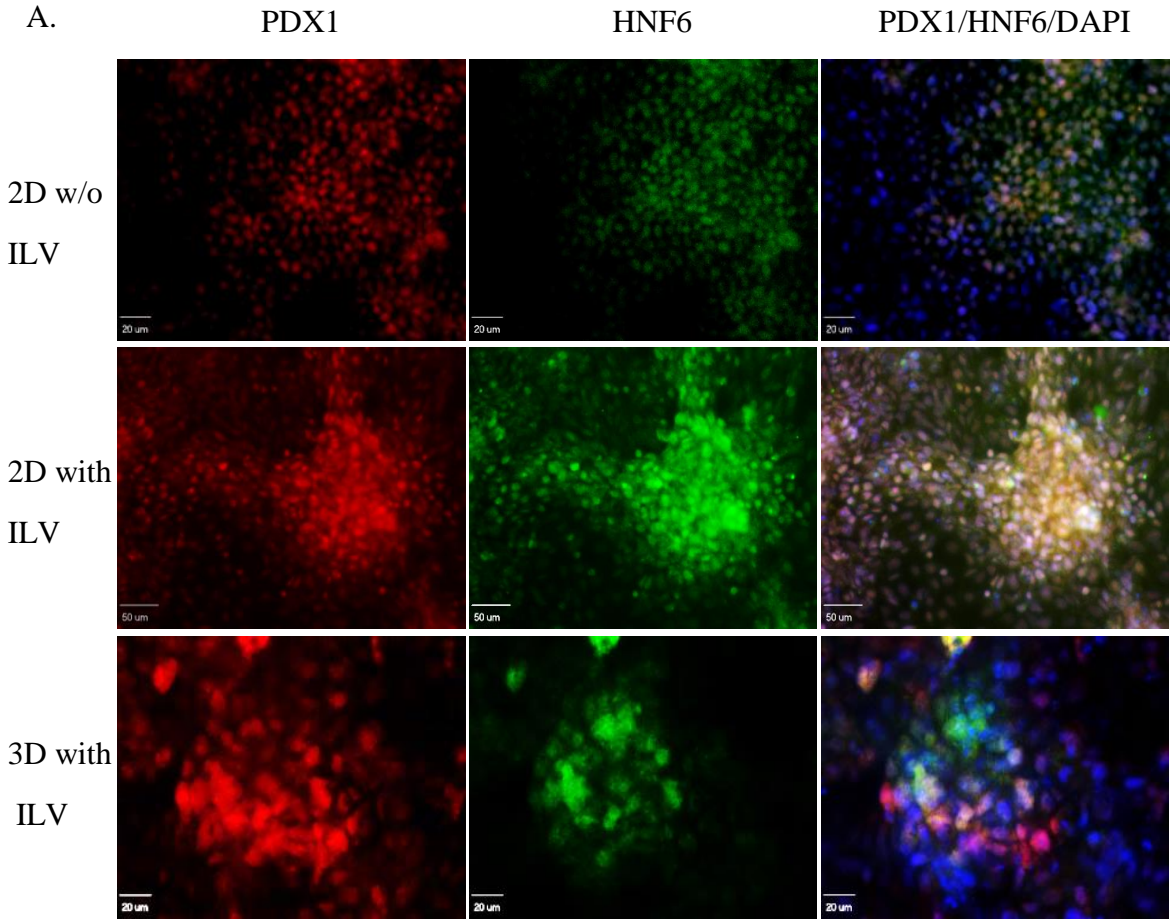


Figure. 18. The effect of (-)-indolactam V (ILV) on the differentiation of pancreatic progenitor from DE. (A) Immunofluorescence analysis of coexpression of PDX1 and HNF6 in hESCs-induced pancreatic progenitor cells treated with or without ILV in 2D and 3D collagen/Matrigel. (B) Quantitative PCR analysis of pancreatic progenitor marker genes in hESCs-induced cells treated without or with ILV on day 5 and day 8. Expression level were normalized to β -actin. All values are normalized to cells cultured on day 5 without ILV treatment.

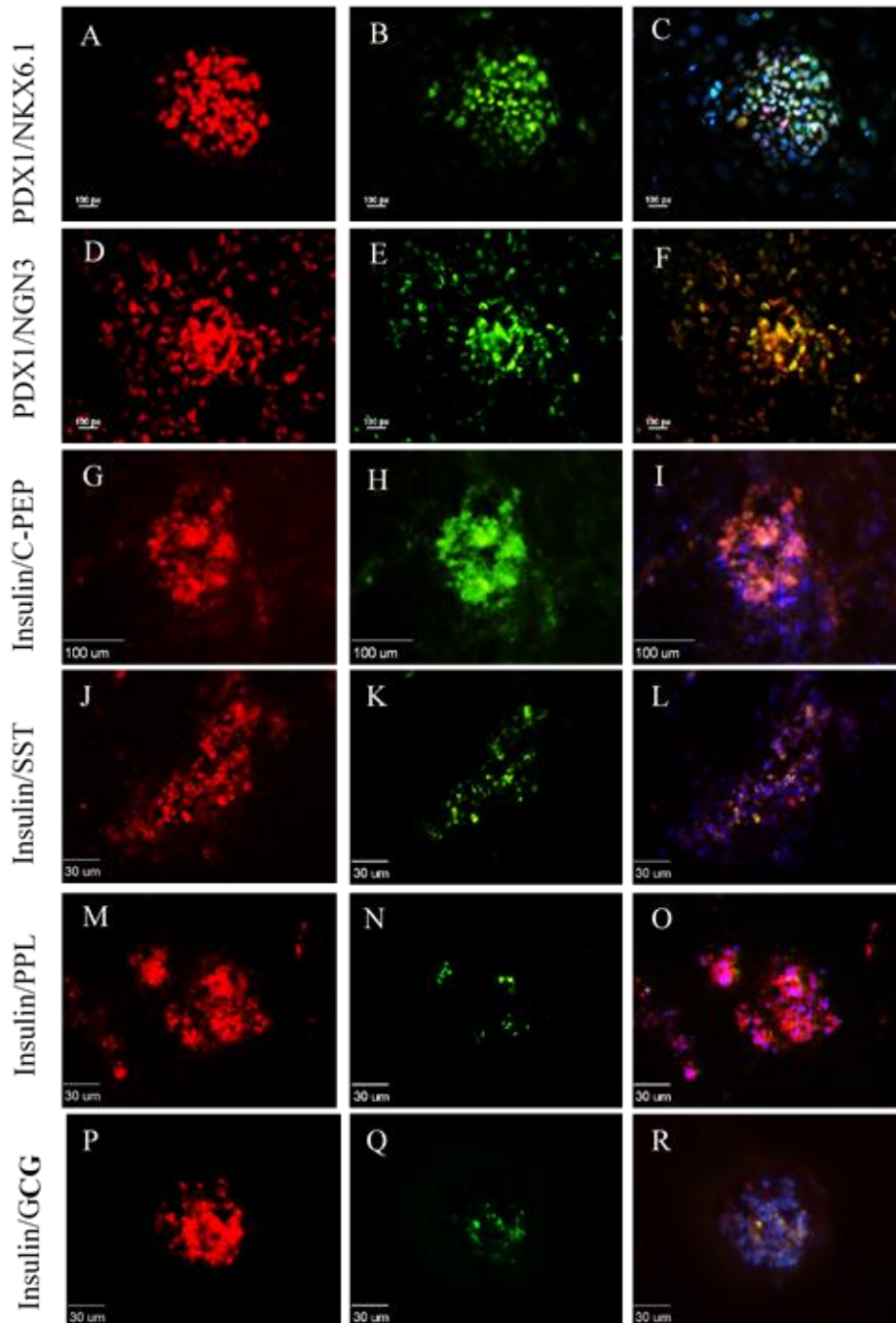


Figure. 19. Double immunofluorescence analysis of pancreatic cells differentiated from hESCs. (A-C) PDX1 (A); NKX6.1 (B); merged images of PDX1, NKX6.1 and DAPI (C). (D-F) PDX1 (D); NGN3 (E); merged images of PDX1, NGN3 and DAPI (F). (G-I) Insulin (G); C-peptide (H); merged images of insulin, C-peptide and DAPI. (J-L) Insulin (J); Somatostatin (K); merged images of insulin, somatostatin and DAPI. (M-O) Insulin (M); polypeptide (N); merged images of Insulin, polypeptide and DAPI. (P-R) Insulin (P); glucagon (Q); merged images of insulin, glucagon and DAPI (R).

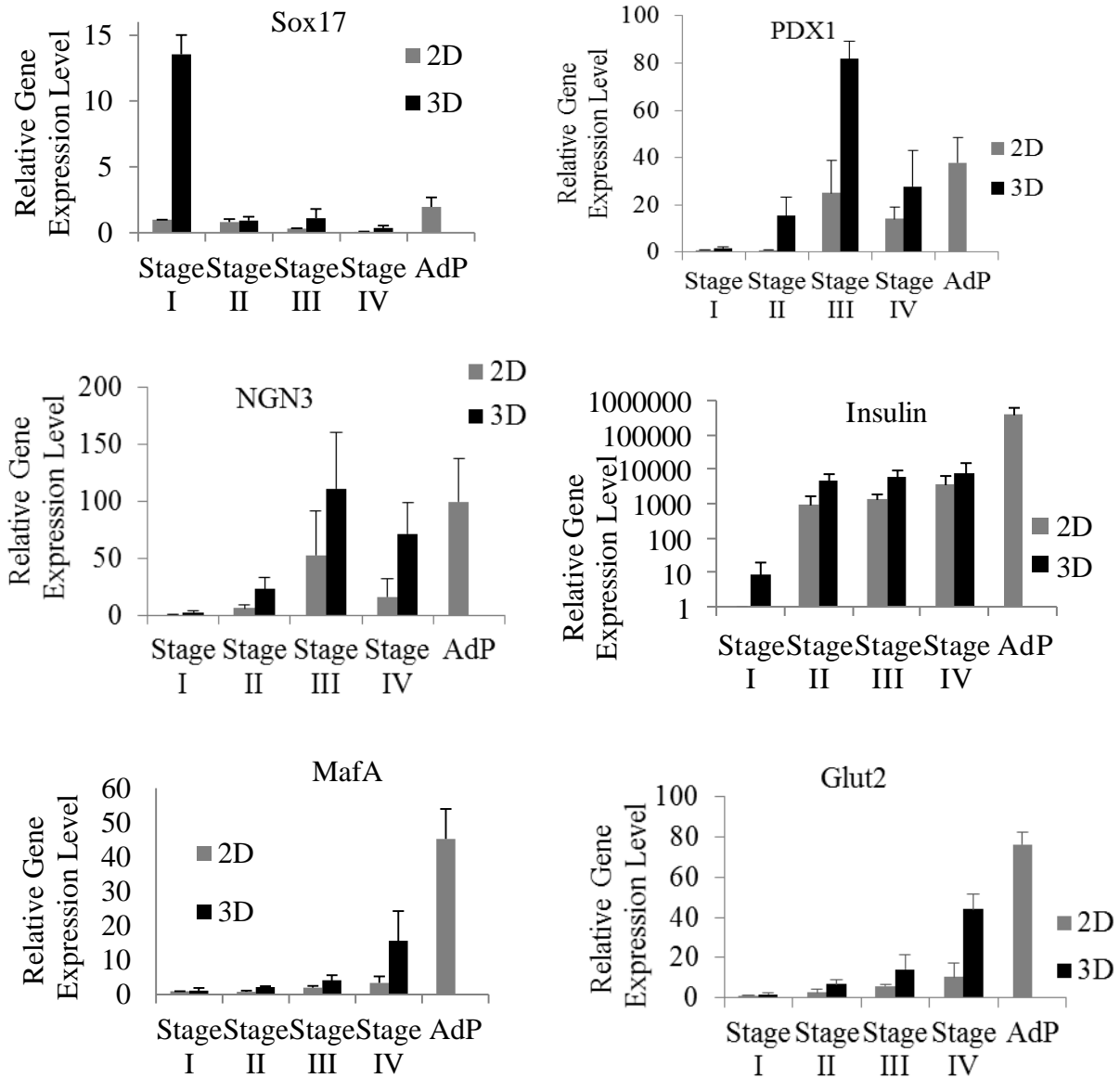


Figure. 20. Quantitative PCR analysis showed the dynamic expression of several key genes during hESCs-induced pancreatic β cell development. Cell samples were collected at the end of stage I, stage II, stage III, and stage IV. mRNA of hESCs-induced cells at stage I in 2D culture was used as control to normalize gene expression level. β -actin was used as house-keeping gene.

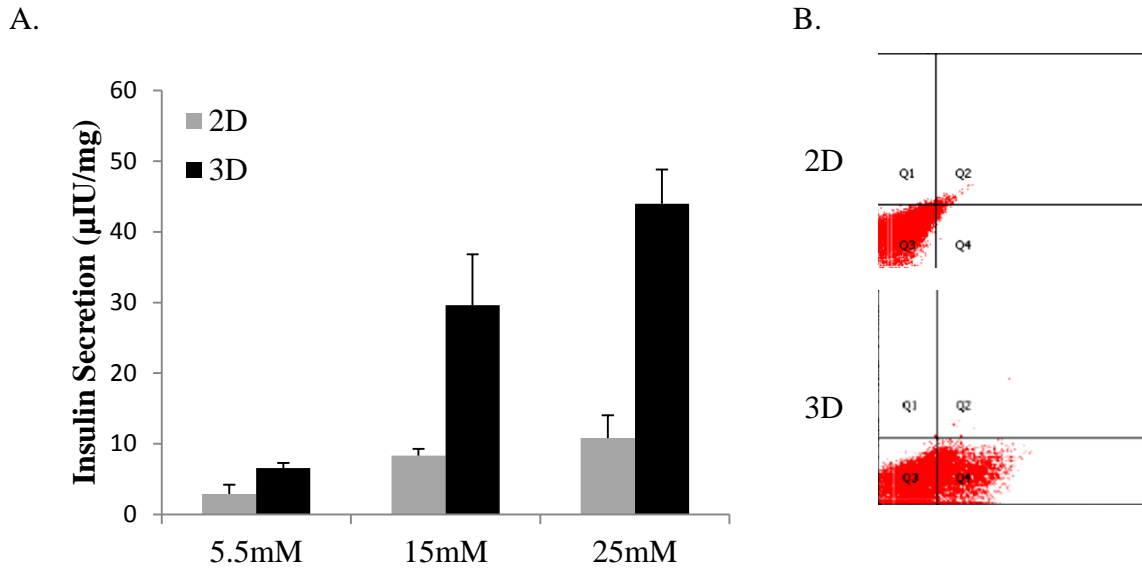
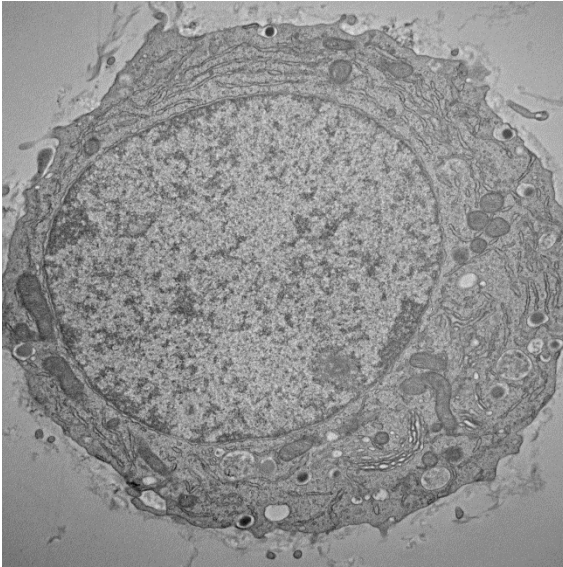


Figure. 21. Insulin secretion in 2D and 3D culture. (A) ELISA of glucose-response insulin release from 2D- and 3D- induced pancreatic cells exposed to 5.5 mM, 15 mM, and 25 mM glucose. (B) Flow cytometric analysis was performed using anti-human insulin antibodies with hESCs-induced pancreatic cells at the end of stage IV in 2D and 3D collagen/Matrigel scaffold.

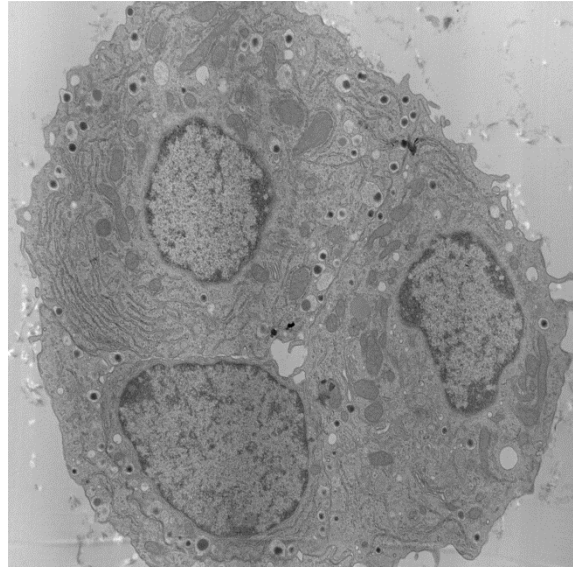
A.



pic17.tif
Print Mag: 17800x @ 7.0 in
3:35:56 PM 11/22/2013

2 µm
HV=100.0kV
Direct Mag: 15000x
University of Arkansas

B.



pic14.tif
Print Mag: 11900x @ 7.0 in
5:12:40 PM 11/22/2013

2 µm
HV=100.0kV
Direct Mag: 10000x
University of Arkansas

Figure. 22. Transmission electron microscopic examination of insulin secretory granules in hESCs-differentiated pancreatic cells seed in 2D (A) and collagen/Matrigel scaffold (B). Scale bar = 2µm.

References

1. Weissman, I.L., *Stem cells: units of development, units of regeneration, and units in evolution*. Cell, 2000. **100**(1): p. 157-68.
2. Sukoyan, M.A., et al., *Embryonic stem cells derived from morulae, inner cell mass, and blastocysts of mink: comparisons of their pluripotencies*. Mol Reprod Dev, 1993. **36**(2): p. 148-58.
3. Mitalipov, S. and D. Wolf, *Totipotency, pluripotency and nuclear reprogramming*. Adv Biochem Eng Biotechnol, 2009. **114**: p. 185-99.
4. Evans, M.J. and M.H. Kaufman, *Establishment in culture of pluripotential cells from mouse embryos*. Nature, 1981. **292**(5819): p. 154-6.
5. Martin, G.R., *Isolation of a pluripotent cell line from early mouse embryos cultured in medium conditioned by teratocarcinoma stem cells*. Proc Natl Acad Sci U S A, 1981. **78**(12): p. 7634-8.
6. Thomson, J.A., et al., *Embryonic stem cell lines derived from human blastocysts*. Science, 1998. **282**(5391): p. 1145-7.
7. Frolov, A.A. and A.S. Bryukhovetskiy, *Effects of hematopoietic autologous stem cell transplantation to the chronically injured human spinal cord evaluated by motor and somatosensory evoked potentials methods*. Cell Transplant. **21 Suppl 1**: p. S49-55.
8. Terai, S., et al., *Improved liver function in patients with liver cirrhosis after autologous bone marrow cell infusion therapy*. Stem Cells, 2006. **24**(10): p. 2292-8.
9. Subrammaniyan, R., et al., *Application of autologous bone marrow mononuclear cells in six patients with advanced chronic critical limb ischemia as a result of diabetes: our experience*. Cytotherapy. **13**(8): p. 993-9.
10. Quarto, R., et al., *Repair of large bone defects with the use of autologous bone marrow stromal cells*. N Engl J Med, 2001. **344**(5): p. 385-6.
11. Grinnemo, K.H., et al., *Xenoreactivity and engraftment of human mesenchymal stem cells transplanted into infarcted rat myocardium*. J Thorac Cardiovasc Surg, 2004. **127**(5): p. 1293-300.
12. Barry, F.P., *Mesenchymal stem cell therapy in joint disease*. Novartis Found Symp, 2003. **249**: p. 86-96; discussion 96-102, 170-4, 239-41.
13. Shihabuddin, L.S. and I. Aubert, *Stem cell transplantation for neurometabolic and neurodegenerative diseases*. Neuropharmacology. **58**(6): p. 845-54.

14. Galvin, K.A. and D.G. Jones, *Adult human neural stem cells for autologous cell replacement therapies for neurodegenerative disorders*. *NeuroRehabilitation*, 2006. **21**(3): p. 255-65.
15. Takahashi, K. and S. Yamanaka, *Induction of pluripotent stem cells from mouse embryonic and adult fibroblast cultures by defined factors*. *Cell*, 2006. **126**(4): p. 663-76.
16. Takahashi, K., et al., *Induction of pluripotent stem cells from adult human fibroblasts by defined factors*. *Cell*, 2007. **131**(5): p. 861-72.
17. Park, I.H., et al., *Reprogramming of human somatic cells to pluripotency with defined factors*. *Nature*, 2008. **451**(7175): p. 141-6.
18. Yu, J., et al., *Induced pluripotent stem cell lines derived from human somatic cells*. *Science*, 2007. **318**(5858): p. 1917-20.
19. Loh, Y.H., et al., *Generation of induced pluripotent stem cells from human blood*. *Blood*, 2009. **113**(22): p. 5476-9.
20. Eminli, S., et al., *Reprogramming of neural progenitor cells into induced pluripotent stem cells in the absence of exogenous Sox2 expression*. *Stem Cells*, 2008. **26**(10): p. 2467-74.
21. Hanna, J., et al., *Direct reprogramming of terminally differentiated mature B lymphocytes to pluripotency*. *Cell*, 2008. **133**(2): p. 250-64.
22. Woltjen, K., et al., *piggyBac transposition reprograms fibroblasts to induced pluripotent stem cells*. *Nature*, 2009. **458**(7239): p. 766-70.
23. Huangfu, D., et al., *Induction of pluripotent stem cells by defined factors is greatly improved by small-molecule compounds*. *Nat Biotechnol*, 2008. **26**(7): p. 795-7.
24. Shi, Y., et al., *Induction of pluripotent stem cells from mouse embryonic fibroblasts by Oct4 and Klf4 with small-molecule compounds*. *Cell Stem Cell*, 2008. **3**(5): p. 568-74.
25. Hou, P., et al., *Pluripotent stem cells induced from mouse somatic cells by small-molecule compounds*. *Science*. **341**(6146): p. 651-4.
26. Hockemeyer, D., et al., *A drug-inducible system for direct reprogramming of human somatic cells to pluripotency*. *Cell Stem Cell*, 2008. **3**(3): p. 346-53.
27. Lin, T., et al., *A chemical platform for improved induction of human iPSCs*. *Nat Methods*, 2009. **6**(11): p. 805-8.
28. Zhou, H., et al., *Generation of induced pluripotent stem cells using recombinant proteins*. *Cell Stem Cell*, 2009. **4**(5): p. 381-4.

29. Kim, D., et al., *Generation of human induced pluripotent stem cells by direct delivery of reprogramming proteins*. *Cell Stem Cell*, 2009. **4**(6): p. 472-6.
30. Miyoshi, N., et al., *Reprogramming of mouse and human cells to pluripotency using mature microRNAs*. *Cell Stem Cell*. **8**(6): p. 633-8.
31. Bao, X., et al., *MicroRNAs in somatic cell reprogramming*. *Curr Opin Cell Biol*. **25**(2): p. 208-14.
32. Maherali, N., et al., *Directly reprogrammed fibroblasts show global epigenetic remodeling and widespread tissue contribution*. *Cell Stem Cell*, 2007. **1**(1): p. 55-70.
33. Kang, L., et al., *iPS cells can support full-term development of tetraploid blastocyst-complemented embryos*. *Cell Stem Cell*, 2009. **5**(2): p. 135-8.
34. Zhao, X.Y., et al., *iPS cells produce viable mice through tetraploid complementation*. *Nature*, 2009. **461**(7260): p. 86-90.
35. Chin, M.H., et al., *Induced pluripotent stem cells and embryonic stem cells are distinguished by gene expression signatures*. *Cell Stem Cell*, 2009. **5**(1): p. 111-23.
36. Kim, K., et al., *Epigenetic memory in induced pluripotent stem cells*. *Nature*, 2010. **467**(7313): p. 285-90.
37. Meissen, J.K., et al., *Induced pluripotent stem cells show metabolomic differences to embryonic stem cells in polyunsaturated phosphatidylcholines and primary metabolism*. *PLoS One*, 2012. **7**(10): p. e46770.
38. Zhao, T., et al., *Immunogenicity of induced pluripotent stem cells*. *Nature*, 2011. **474**(7350): p. 212-5.
39. Gore, A., et al., *Somatic coding mutations in human induced pluripotent stem cells*. *Nature*, 2011. **471**(7336): p. 63-7.
40. Laurent, L.C., et al., *Dynamic changes in the copy number of pluripotency and cell proliferation genes in human ESCs and iPSCs during reprogramming and time in culture*. *Cell Stem Cell*, 2011. **8**(1): p. 106-18.
41. Hussein, S.M., et al., *Copy number variation and selection during reprogramming to pluripotency*. *Nature*, 2011. **471**(7336): p. 58-62.
42. Wild, S., et al., *Global prevalence of diabetes: estimates for the year 2000 and projections for 2030*. *Diabetes Care*, 2004. **27**(5): p. 1047-53.
43. Bertuzzi, F., et al., *Brittle type 1 diabetes mellitus*. *Curr Med Chem*, 2007. **14**(16): p. 1739-44.

44. Ashcroft, F.M. and P. Rorsman, *Diabetes mellitus and the beta cell: the last ten years*. Cell, 2012. **148**(6): p. 1160-71.
45. Butler, A.E., et al., *Beta-cell deficit and increased beta-cell apoptosis in humans with type 2 diabetes*. Diabetes, 2003. **52**(1): p. 102-10.
46. Tisch, R. and H. McDevitt, *Insulin-dependent diabetes mellitus*. Cell, 1996. **85**(3): p. 291-7.
47. Shapiro, A.M., et al., *Islet transplantation in seven patients with type 1 diabetes mellitus using a glucocorticoid-free immunosuppressive regimen*. N Engl J Med, 2000. **343**(4): p. 230-8.
48. Ryan, E.A., et al., *Five-year follow-up after clinical islet transplantation*. Diabetes, 2005. **54**(7): p. 2060-9.
49. Shapiro, A.M., et al., *International trial of the Edmonton protocol for islet transplantation*. N Engl J Med, 2006. **355**(13): p. 1318-30.
50. Keymeulen, B., et al., *Correlation between beta cell mass and glycemic control in type 1 diabetic recipients of islet cell graft*. Proc Natl Acad Sci U S A, 2006. **103**(46): p. 17444-9.
51. Dor, Y., et al., *Adult pancreatic beta-cells are formed by self-duplication rather than stem-cell differentiation*. Nature, 2004. **429**(6987): p. 41-6.
52. Teta, M., et al., *Growth and regeneration of adult beta cells does not involve specialized progenitors*. Dev Cell, 2007. **12**(5): p. 817-26.
53. Georgia, S. and A. Bhushan, *Beta cell replication is the primary mechanism for maintaining postnatal beta cell mass*. J Clin Invest, 2004. **114**(7): p. 963-8.
54. Stanger, B.Z., A.J. Tanaka, and D.A. Melton, *Organ size is limited by the number of embryonic progenitor cells in the pancreas but not the liver*. Nature, 2007. **445**(7130): p. 886-91.
55. Kassem, S.A., et al., *Beta-cell proliferation and apoptosis in the developing normal human pancreas and in hyperinsulinism of infancy*. Diabetes, 2000. **49**(8): p. 1325-33.
56. Perl, S., et al., *Significant human beta-cell turnover is limited to the first three decades of life as determined by in vivo thymidine analog incorporation and radiocarbon dating*. J Clin Endocrinol Metab, 2010. **95**(10): p. E234-9.
57. Cozar-Castellano, I., et al., *Molecular control of cell cycle progression in the pancreatic beta-cell*. Endocr Rev, 2006. **27**(4): p. 356-70.
58. Butler, A.E., et al., *Adaptive changes in pancreatic beta cell fractional area and beta cell turnover in human pregnancy*. Diabetologia, 2010. **53**(10): p. 2167-76.

59. Brelje, T.C. and R.L. Sorenson, *Role of prolactin versus growth hormone on islet B-cell proliferation in vitro: implications for pregnancy*. *Endocrinology*, 1991. **128**(1): p. 45-57.
60. Brelje, T.C., et al., *Effect of homologous placental lactogens, prolactins, and growth hormones on islet B-cell division and insulin secretion in rat, mouse, and human islets: implication for placental lactogen regulation of islet function during pregnancy*. *Endocrinology*, 1993. **132**(2): p. 879-87.
61. Karnik, S.K., et al., *Menin controls growth of pancreatic beta-cells in pregnant mice and promotes gestational diabetes mellitus*. *Science*, 2007. **318**(5851): p. 806-9.
62. Teta, M., et al., *Very slow turnover of beta-cells in aged adult mice*. *Diabetes*, 2005. **54**(9): p. 2557-67.
63. Rane, S.G. and E.P. Reddy, *Cell cycle control of pancreatic beta cell proliferation*. *Front Biosci*, 2000. **5**: p. D1-19.
64. Rane, S.G., et al., *Loss of Cdk4 expression causes insulin-deficient diabetes and Cdk4 activation results in beta-islet cell hyperplasia*. *Nat Genet*, 1999. **22**(1): p. 44-52.
65. Hakonen, E., et al., *Epidermal growth factor (EGF)-receptor signalling is needed for murine beta cell mass expansion in response to high-fat diet and pregnancy but not after pancreatic duct ligation*. *Diabetologia*, 2011. **54**(7): p. 1735-43.
66. Borowiak, M., *The new generation of beta-cells: replication, stem cell differentiation, and the role of small molecules*. *Rev Diabet Stud*, 2010. **7**(2): p. 93-104.
67. Yamamoto, H., Y. Uchigata, and H. Okamoto, *Streptozotocin and alloxan induce DNA strand breaks and poly(ADP-ribose) synthetase in pancreatic islets*. *Nature*, 1981. **294**(5838): p. 284-6.
68. Otonkoski, T., et al., *Nicotinamide is a potent inducer of endocrine differentiation in cultured human fetal pancreatic cells*. *J Clin Invest*, 1993. **92**(3): p. 1459-66.
69. Yamamoto, K., et al., *Recombinant human betacellulin promotes the neogenesis of beta-cells and ameliorates glucose intolerance in mice with diabetes induced by selective alloxan perfusion*. *Diabetes*, 2000. **49**(12): p. 2021-7.
70. Li, L., et al., *Promotion of beta-cell regeneration by betacellulin in ninety percent-pancreatectomized rats*. *Endocrinology*, 2001. **142**(12): p. 5379-85.
71. Xu, G., et al., *Exendin-4 stimulates both beta-cell replication and neogenesis, resulting in increased beta-cell mass and improved glucose tolerance in diabetic rats*. *Diabetes*, 1999. **48**(12): p. 2270-6.
72. Tian, L., et al., *Comparison of exendin-4 on beta-cell replication in mouse and human islet grafts*. *Transpl Int*, 2011. **24**(8): p. 856-64.

73. Caballero, F., et al., *Birth and death of human beta-cells in pancreas from cadaver donors, autopsies, surgical specimens, and islets transplanted into mice*. Cell Transplant, 2013.
74. Wang, W., et al., *Identification of small-molecule inducers of pancreatic beta-cell expansion*. Proc Natl Acad Sci U S A, 2009. **106**(5): p. 1427-32.
75. Annes, J.P., et al., *Adenosine kinase inhibition selectively promotes rodent and porcine islet beta-cell replication*. Proc Natl Acad Sci U S A, 2012. **109**(10): p. 3915-20.
76. Shen, W., et al., *Small-molecule inducer of beta cell proliferation identified by high-throughput screening*. J Am Chem Soc, 2013. **135**(5): p. 1669-72.
77. Pagliuca, F.W. and D.A. Melton, *How to make a functional beta-cell*. Development, 2013. **140**(12): p. 2472-83.
78. Noguchi, H., et al., *Fresh islets are more effective for islet transplantation than cultured islets*. Cell Transplant, 2012. **21**(2-3): p. 517-23.
79. Kondegowda, N.G., et al., *Growth Factor Mediated Regulation of Beta Cell Survival* the Open Endocrinology Journal, 2010. **4**: p. 78-93.
80. Cozar-Castellano, I., et al., *Induction of beta-cell proliferation and retinoblastoma protein phosphorylation in rat and human islets using adenovirus-mediated transfer of cyclin-dependent kinase-4 and cyclin D1*. Diabetes, 2004. **53**(1): p. 149-59.
81. Fiaschi-Taesch, N., et al., *Survey of the human pancreatic beta-cell G1/S proteome reveals a potential therapeutic role for cdk-6 and cyclin D1 in enhancing human beta-cell replication and function in vivo*. Diabetes, 2009. **58**(4): p. 882-93.
82. Guthalu Kondegowda, N., et al., *Parathyroid hormone-related protein enhances human ss-cell proliferation and function with associated induction of cyclin-dependent kinase 2 and cyclin E expression*. Diabetes, 2010. **59**(12): p. 3131-8.
83. Fiaschi-Taesch, N.M., et al., *Induction of human beta-cell proliferation and engraftment using a single G1/S regulatory molecule, cdk6*. Diabetes, 2010. **59**(8): p. 1926-36.
84. Karslioglu, E., et al., *cMyc is a principal upstream driver of beta-cell proliferation in rat insulinoma cell lines and is an effective mediator of human beta-cell replication*. Mol Endocrinol, 2011. **25**(10): p. 1760-72.
85. Rieck, S., et al., *Overexpression of hepatocyte nuclear factor-4alpha initiates cell cycle entry, but is not sufficient to promote beta-cell expansion in human islets*. Mol Endocrinol, 2012. **26**(9): p. 1590-602.
86. Rohatgi, N., et al., *Therapeutic Strategies to Increase Human beta-Cell Growth and Proliferation by Regulating mTOR and GSK-3/beta-Catenin Pathways*. Open Endocrinol J, 2010. **4**.

87. Aly, H., et al., *A novel strategy to increase the proliferative potential of adult human beta-cells while maintaining their differentiated phenotype*. PLoS One, 2013. **8**(6): p. e66131.
88. Otonkoski, T., et al., *Unique basement membrane structure of human pancreatic islets: implications for beta-cell growth and differentiation*. Diabetes Obes Metab, 2008. **10 Suppl 4**: p. 119-27.
89. Wang, R.N. and L. Rosenberg, *Maintenance of beta-cell function and survival following islet isolation requires re-establishment of the islet-matrix relationship*. J Endocrinol, 1999. **163**(2): p. 181-90.
90. Hammar, E., et al., *Extracellular matrix protects pancreatic beta-cells against apoptosis: role of short- and long-term signaling pathways*. Diabetes, 2004. **53**(8): p. 2034-41.
91. Kalluri, R. and R.A. Weinberg, *The basics of epithelial-mesenchymal transition*. J Clin Invest, 2009. **119**(6): p. 1420-8.
92. Gabbianelli, R., et al., *Fluorescence study on rat epithelial cells and liposomes exposed to aromatic nitroxides*. Comp Biochem Physiol C Toxicol Pharmacol, 2004. **137**(4): p. 355-62.
93. Morton, R.A., et al., *Endocrine precursor cells from mouse islets are not generated by epithelial-to-mesenchymal transition of mature beta cells*. Mol Cell Endocrinol, 2007. **270**(1-2): p. 87-93.
94. Wells, J.M. and D.A. Melton, *Vertebrate endoderm development*. Annu Rev Cell Dev Biol, 1999. **15**: p. 393-410.
95. Lammert, E., O. Cleaver, and D. Melton, *Induction of pancreatic differentiation by signals from blood vessels*. Science, 2001. **294**(5542): p. 564-7.
96. Jonsson, J., et al., *Insulin-promoter-factor 1 is required for pancreas development in mice*. Nature, 1994. **371**(6498): p. 606-9.
97. Burris, R.E. and M. Hebrok, *Pancreatic innervation in mouse development and beta-cell regeneration*. Neuroscience, 2007. **150**(3): p. 592-602.
98. Guo, T. and M. Hebrok, *Stem cells to pancreatic beta-cells: new sources for diabetes cell therapy*. Endocr Rev, 2009. **30**(3): p. 214-27.
99. Cabrera, O., et al., *The unique cytoarchitecture of human pancreatic islets has implications for islet cell function*. Proc Natl Acad Sci U S A, 2006. **103**(7): p. 2334-9.
100. Lumelsky, N., et al., *Differentiation of embryonic stem cells to insulin-secreting structures similar to pancreatic islets*. Science, 2001. **292**(5520): p. 1389-94.

101. Rajagopal, J., et al., *Insulin staining of ES cell progeny from insulin uptake*. Science, 2003. **299**(5605): p. 363.
102. Hansson, M., et al., *Artifactual insulin release from differentiated embryonic stem cells*. Diabetes, 2004. **53**(10): p. 2603-9.
103. Assady, S., et al., *Insulin production by human embryonic stem cells*. Diabetes, 2001. **50**(8): p. 1691-7.
104. D'Amour, K.A., et al., *Production of pancreatic hormone-expressing endocrine cells from human embryonic stem cells*. Nat Biotechnol, 2006. **24**(11): p. 1392-401.
105. D'Amour, K.A., et al., *Efficient differentiation of human embryonic stem cells to definitive endoderm*. Nat Biotechnol, 2005. **23**(12): p. 1534-41.
106. Kroon, E., et al., *Pancreatic endoderm derived from human embryonic stem cells generates glucose-responsive insulin-secreting cells in vivo*. Nat Biotechnol, 2008. **26**(4): p. 443-52.
107. McLean, A.B., et al., *Activin a efficiently specifies definitive endoderm from human embryonic stem cells only when phosphatidylinositol 3-kinase signaling is suppressed*. Stem Cells, 2007. **25**(1): p. 29-38.
108. Champeris Tsaniras, S. and P.M. Jones, *Generating pancreatic beta-cells from embryonic stem cells by manipulating signaling pathways*. J Endocrinol, 2010. **206**(1): p. 13-26.
109. Zhang, D., et al., *Highly efficient differentiation of human ES cells and iPS cells into mature pancreatic insulin-producing cells*. Cell Res, 2009. **19**(4): p. 429-38.
110. Schofield, R., *The relationship between the spleen colony-forming cell and the haemopoietic stem cell*. Blood Cells, 1978. **4**(1-2): p. 7-25.
111. Lander, A.D., et al., *What does the concept of the stem cell niche really mean today?* BMC Biol, 2012. **10**: p. 19.
112. Gattazzo, F., A. Urciuolo, and P. Bonaldo, *Extracellular matrix: A dynamic microenvironment for stem cell niche*. Biochim Biophys Acta, 2014.
113. Jones, D.L. and A.J. Wagers, *No place like home: anatomy and function of the stem cell niche*. Nat Rev Mol Cell Biol, 2008. **9**(1): p. 11-21.
114. Griffith, L.G. and M.A. Swartz, *Capturing complex 3D tissue physiology in vitro*. Nat Rev Mol Cell Biol, 2006. **7**(3): p. 211-24.
115. Discher, D.E., P. Janmey, and Y.L. Wang, *Tissue cells feel and respond to the stiffness of their substrate*. Science, 2005. **310**(5751): p. 1139-43.

116. Hynes, R.O., *The extracellular matrix: not just pretty fibrils*. Science, 2009. **326**(5957): p. 1216-9.
117. Song, J.J. and H.C. Ott, *Organ engineering based on decellularized matrix scaffolds*. Trends Mol Med, 2011. **17**(8): p. 424-32.
118. Nelson, C.M. and M.J. Bissell, *Of extracellular matrix, scaffolds, and signaling: tissue architecture regulates development, homeostasis, and cancer*. Annu Rev Cell Dev Biol, 2006. **22**: p. 287-309.
119. Liu, X., et al., *A targeted mutation at the known collagenase cleavage site in mouse type I collagen impairs tissue remodeling*. J Cell Biol, 1995. **130**(1): p. 227-37.
120. Trinh, L.A. and D.Y. Stainier, *Fibronectin regulates epithelial organization during myocardial migration in zebrafish*. Dev Cell, 2004. **6**(3): p. 371-82.
121. Ryan, M.C., et al., *Targeted disruption of the LAMA3 gene in mice reveals abnormalities in survival and late stage differentiation of epithelial cells*. J Cell Biol, 1999. **145**(6): p. 1309-23.
122. Boudreau, N.J. and P.L. Jones, *Extracellular matrix and integrin signalling: the shape of things to come*. Biochem J, 1999. **339** (Pt 3): p. 481-8.
123. Juliano, R.L. and S. Haskill, *Signal transduction from the extracellular matrix*. J Cell Biol, 1993. **120**(3): p. 577-85.
124. Legate, K.R., S.A. Wickstrom, and R. Fassler, *Genetic and cell biological analysis of integrin outside-in signaling*. Genes Dev, 2009. **23**(4): p. 397-418.
125. Suh, H.N. and H.J. Han, *Collagen I regulates the self-renewal of mouse embryonic stem cells through alpha2beta1 integrin- and DDR1-dependent Bmi-1*. J Cell Physiol, 2011. **226**(12): p. 3422-32.
126. Shen, Q., et al., *Adult SVZ stem cells lie in a vascular niche: a quantitative analysis of niche cell-cell interactions*. Cell Stem Cell, 2008. **3**(3): p. 289-300.
127. Fortunel, N.O., et al., *Comment on " 'Stemness': transcriptional profiling of embryonic and adult stem cells" and "a stem cell molecular signature"*. Science, 2003. **302**(5644): p. 393; author reply 393.
128. Veevers-Lowe, J., et al., *Mesenchymal stem cell migration is regulated by fibronectin through alpha5beta1-integrin-mediated activation of PDGFR-beta and potentiation of growth factor signals*. J Cell Sci, 2011. **124**(Pt 8): p. 1288-300.
129. Pruszek, J., et al., *CD15, CD24, and CD29 define a surface biomarker code for neural lineage differentiation of stem cells*. Stem Cells, 2009. **27**(12): p. 2928-40.

130. Campos, L.S., et al., *Notch, epidermal growth factor receptor, and beta1-integrin pathways are coordinated in neural stem cells*. J Biol Chem, 2006. **281**(8): p. 5300-9.
131. Brizzi, M.F., G. Tarone, and P. Defilippi, *Extracellular matrix, integrins, and growth factors as tailors of the stem cell niche*. Curr Opin Cell Biol, 2012. **24**(5): p. 645-51.
132. Mohammadi, M., S.K. Olsen, and R. Goetz, *A protein canyon in the FGF-FGF receptor dimer selects from an a la carte menu of heparan sulfate motifs*. Curr Opin Struct Biol, 2005. **15**(5): p. 506-16.
133. Shi, Y. and J. Massague, *Mechanisms of TGF-beta signaling from cell membrane to the nucleus*. Cell, 2003. **113**(6): p. 685-700.
134. Panayotou, G., et al., *Domains of laminin with growth-factor activity*. Cell, 1989. **56**(1): p. 93-101.
135. Iyer, A.K., et al., *Tenascin cytotactin epidermal growth factor-like repeat binds epidermal growth factor receptor with low affinity*. J Cell Physiol, 2007. **211**(3): p. 748-58.
136. Damon, D.H., et al., *Heparin potentiates the action of acidic fibroblast growth factor by prolonging its biological half-life*. J Cell Physiol, 1989. **138**(2): p. 221-6.
137. Flaumenhaft, R., D. Moscatelli, and D.B. Rifkin, *Heparin and heparan sulfate increase the radius of diffusion and action of basic fibroblast growth factor*. J Cell Biol, 1990. **111**(4): p. 1651-9.
138. Flaumenhaft, R., et al., *Role of extracellular matrix in the action of basic fibroblast growth factor: matrix as a source of growth factor for long-term stimulation of plasminogen activator production and DNA synthesis*. J Cell Physiol, 1989. **140**(1): p. 75-81.
139. Igotz, R.A., J. Heino, and J. Massague, *Regulation of cell adhesion receptors by transforming growth factor-beta. Regulation of vitronectin receptor and LFA-I*. J Biol Chem, 1989. **264**(1): p. 389-92.
140. Edwards, D.R., et al., *Transforming growth factor beta modulates the expression of collagenase and metalloproteinase inhibitor*. EMBO J, 1987. **6**(7): p. 1899-904.
141. Igotz, R.A. and J. Massague, *Transforming growth factor-beta stimulates the expression of fibronectin and collagen and their incorporation into the extracellular matrix*. J Biol Chem, 1986. **261**(9): p. 4337-45.
142. Watt, F.M. and W.T. Huck, *Role of the extracellular matrix in regulating stem cell fate*. Nat Rev Mol Cell Biol, 2013. **14**(8): p. 467-73.
143. Mammoto, T., et al., *Mechanochemical control of mesenchymal condensation and embryonic tooth organ formation*. Dev Cell, 2011. **21**(4): p. 758-69.

144. Mammoto, A., T. Mammoto, and D.E. Ingber, *Mechanosensitive mechanisms in transcriptional regulation*. J Cell Sci, 2012. **125**(Pt 13): p. 3061-73.
145. Berry, M.F., et al., *Mesenchymal stem cell injection after myocardial infarction improves myocardial compliance*. Am J Physiol Heart Circ Physiol, 2006. **290**(6): p. H2196-203.
146. Breitbach, M., et al., *Potential risks of bone marrow cell transplantation into infarcted hearts*. Blood, 2007. **110**(4): p. 1362-9.
147. Engler, A.J., et al., *Matrix elasticity directs stem cell lineage specification*. Cell, 2006. **126**(4): p. 677-89.
148. Evans, N.D., et al., *Substrate stiffness affects early differentiation events in embryonic stem cells*. Eur Cell Mater, 2009. **18**: p. 1-13; discussion 13-4.
149. Reilly, G.C. and A.J. Engler, *Intrinsic extracellular matrix properties regulate stem cell differentiation*. J Biomech, 2010. **43**(1): p. 55-62.
150. Zhang, S., *Beyond the Petri dish*. Nat Biotechnol, 2004. **22**(2): p. 151-2.
151. Cukierman, E., et al., *Taking cell-matrix adhesions to the third dimension*. Science, 2001. **294**(5547): p. 1708-12.
152. Levenberg, S., et al., *Neurotrophin-induced differentiation of human embryonic stem cells on three-dimensional polymeric scaffolds*. Tissue Eng, 2005. **11**(3-4): p. 506-12.
153. Hwang, N.S., S. Varghese, and J. Elisseeff, *Derivation of chondrogenically-committed cells from human embryonic cells for cartilage tissue regeneration*. PLoS One, 2008. **3**(6): p. e2498.
154. Marolt, D., et al., *Engineering bone tissue from human embryonic stem cells*. Proc Natl Acad Sci U S A, 2012. **109**(22): p. 8705-9.
155. Ferreira, L.S., et al., *Bioactive hydrogel scaffolds for controllable vascular differentiation of human embryonic stem cells*. Biomaterials, 2007. **28**(17): p. 2706-17.
156. Baharvand, H., et al., *Differentiation of human embryonic stem cells into hepatocytes in 2D and 3D culture systems in vitro*. Int J Dev Biol, 2006. **50**(7): p. 645-52.
157. Kraehenbuehl, T.P., R. Langer, and L.S. Ferreira, *Three-dimensional biomaterials for the study of human pluripotent stem cells*. Nat Methods, 2011. **8**(9): p. 731-6.
158. Spence, J.R., et al., *Directed differentiation of human pluripotent stem cells into intestinal tissue in vitro*. Nature, 2011. **470**(7332): p. 105-9.
159. Levenberg, S., et al., *Differentiation of human embryonic stem cells on three-dimensional polymer scaffolds*. Proc Natl Acad Sci U S A, 2003. **100**(22): p. 12741-6.

160. Willerth, S.M. and S.E. Sakiyama-Elbert, *Combining stem cells and biomaterial scaffolds for constructing tissues and cell delivery*. 2008.
161. Salasznyk, R.M., et al., *Adhesion to Vitronectin and Collagen I Promotes Osteogenic Differentiation of Human Mesenchymal Stem Cells*. *J Biomed Biotechnol*, 2004. **2004**(1): p. 24-34.
162. Goss, S.A., O'Brien, W.D., *Direct ultrasonic velocity measurements of mammalian collagen threads*. *J Acoust Soc Am*, 1979. **65**: p. 507-511.
163. Semb, H., *Definitive endoderm: a key step in coaxing human embryonic stem cells into transplantable beta-cells*. *Biochem Soc Trans*, 2008. **36**(Pt 3): p. 272-5.
164. Wang, A. and M. Sander, *Generating cells of the gastrointestinal system: current approaches and applications for the differentiation of human pluripotent stem cells*. *J Mol Med (Berl)*. **90**(7): p. 763-71.
165. Bernardo, A.S., et al., *Biphasic induction of Pdx1 in mouse and human embryonic stem cells can mimic development of pancreatic beta-cells*. *Stem Cells*, 2009. **27**(2): p. 341-51.
166. Ninomiya, H., et al., *Endoderm differentiation and inductive effect of activin-treated ectoderm in Xenopus*. *Dev Growth Differ*, 1999. **41**(4): p. 391-400.
167. Osafune, K., et al., *Marked differences in differentiation propensity among human embryonic stem cell lines*. *Nat Biotechnol*, 2008. **26**(3): p. 313-5.
168. Phillips, B.W., et al., *Directed differentiation of human embryonic stem cells into the pancreatic endocrine lineage*. *Stem Cells Dev*, 2007. **16**(4): p. 561-78.
169. Discher, D.E., D.J. Mooney, and P.W. Zandstra, *Growth factors, matrices, and forces combine and control stem cells*. *Science*, 2009. **324**(5935): p. 1673-7.
170. Levenberg, S., et al., *Engineering vascularized skeletal muscle tissue*. *Nat Biotechnol*, 2005. **23**(7): p. 879-84.
171. Chen, S.S., et al., *Multilineage differentiation of rhesus monkey embryonic stem cells in three-dimensional culture systems*. *Stem Cells*, 2003. **21**(3): p. 281-95.
172. Gomez-Lechon, M.J., et al., *Long-term expression of differentiated functions in hepatocytes cultured in three-dimensional collagen matrix*. *J Cell Physiol*, 1998. **177**(4): p. 553-62.
173. Koyama, H., et al., *Fibrillar collagen inhibits arterial smooth muscle proliferation through regulation of Cdk2 inhibitors*. *Cell*, 1996. **87**(6): p. 1069-78.
174. Watanabe, K., et al., *Establishment of three-dimensional culture of neural stem/progenitor cells in collagen Type-1 Gel*. *Restor Neurol Neurosci*, 2007. **25**(2): p. 109-17.

175. Battista, S., et al., *The effect of matrix composition of 3D constructs on embryonic stem cell differentiation*. *Biomaterials*, 2005. **26**(31): p. 6194-207.
176. Montesano, R., et al., *Collagen matrix promotes reorganization of pancreatic endocrine cell monolayers into islet-like organoids*. *J Cell Biol*, 1983. **97**(3): p. 935-9.
177. Weber, L.M., K.N. Hayda, and K.S. Anseth, *Cell-matrix interactions improve beta-cell survival and insulin secretion in three-dimensional culture*. *Tissue Eng Part A*, 2008. **14**(12): p. 1959-68.
178. Wang, X. and K. Ye, *Three-dimensional differentiation of embryonic stem cells into islet-like insulin-producing clusters*. *Tissue Eng Part A*, 2009. **15**(8): p. 1941-52.
179. O'Connor, S.M., et al., *Primary neural precursor cell expansion, differentiation and cytosolic Ca(2+) response in three-dimensional collagen gel*. *J Neurosci Methods*, 2000. **102**(2): p. 187-95.
180. Friess, W., *Collagen--biomaterial for drug delivery*. *Eur J Pharm Biopharm*, 1998. **45**(2): p. 113-36.
181. Schuldiner, M., et al., *Effects of eight growth factors on the differentiation of cells derived from human embryonic stem cells*. *Proc Natl Acad Sci U S A*, 2000. **97**(21): p. 11307-12.
182. Doyle, M.J. and L. Sussel, *Engineering islets: lessons from stem cells and embryonic development*. *Endocrinol Metab Clin North Am*, 2004. **33**(1): p. 149-62, x.
183. Watt, F.M. and B.L. Hogan, *Out of Eden: stem cells and their niches*. *Science*, 2000. **287**(5457): p. 1427-30.
184. Liu, H., J. Lin, and K. Roy, *Effect of 3D scaffold and dynamic culture condition on the global gene expression profile of mouse embryonic stem cells*. *Biomaterials*, 2006. **27**(36): p. 5978-89.
185. Stendahl, J.C., D.B. Kaufman, and S.I. Stupp, *Extracellular matrix in pancreatic islets: relevance to scaffold design and transplantation*. *Cell Transplant*, 2009. **18**(1): p. 1-12.
186. Pankov, R. and K.M. Yamada, *Fibronectin at a glance*. *J Cell Sci*, 2002. **115**(Pt 20): p. 3861-3.
187. George, E.L., et al., *Defects in mesoderm, neural tube and vascular development in mouse embryos lacking fibronectin*. *Development*, 1993. **119**(4): p. 1079-91.
188. Wartiovaara, J., et al., *Appearance of fibronectin during differentiation of mouse teratocarcinoma in vitro*. *Nature*, 1978. **272**(5651): p. 355-6.
189. Snyder, J.M., J.A. O'Brien, and H.F. Rodgers, *Localization and accumulation of fibronectin in rabbit fetal lung tissue*. *Differentiation*, 1987. **34**(1): p. 32-9.

190. Uscanga, L., et al., *Immunolocalization of collagen types, laminin and fibronectin in the normal human pancreas*. Digestion, 1984. **30**(3): p. 158-64.
191. Colognato, H. and P.D. Yurchenco, *Form and function: the laminin family of heterotrimers*. Dev Dyn, 2000. **218**(2): p. 213-34.
192. Li, S., et al., *The role of laminin in embryonic cell polarization and tissue organization*. Dev Cell, 2003. **4**(5): p. 613-24.
193. Lin, H.Y., et al., *Fibronectin and laminin promote differentiation of human mesenchymal stem cells into insulin producing cells through activating Akt and ERK*. J Biomed Sci. **17**: p. 56.
194. Lee, J.H., et al., *Collagen gel three-dimensional matrices combined with adhesive proteins stimulate neuronal differentiation of mesenchymal stem cells*. J R Soc Interface. **8**(60): p. 998-1010.
195. Cirulli, V., et al., *Expression and function of alpha(v)beta(3) and alpha(v)beta(5) integrins in the developing pancreas: roles in the adhesion and migration of putative endocrine progenitor cells*. J Cell Biol, 2000. **150**(6): p. 1445-60.
196. Yang, C.C., L. Jenkins, and K.J.L. Burg, *Adapted cryosectioning method for hydrogels used in regenerative medicine*. Journal of Histotechnology, 2007. **30**(3): p. 185-191.
197. Reilly, G.C. and A.J. Engler, *Intrinsic extracellular matrix properties regulate stem cell differentiation*. Journal of Biomechanics. **43**(1): p. 55-62.
198. Correa-Giannella, M.L. and A.S. Raposo do Amaral, *Pancreatic islet transplantation*. Diabetol Metab Syndr, 2009. **1**(1): p. 9.
199. Sipione, S., et al., *Insulin expressing cells from differentiated embryonic stem cells are not beta cells*. Diabetologia, 2004. **47**(3): p. 499-508.
200. Jiang, J., et al., *Generation of insulin-producing islet-like clusters from human embryonic stem cells*. Stem Cells, 2007. **25**(8): p. 1940-53.
201. Matveyenko, A.V., et al., *Inconsistent formation and nonfunction of insulin-positive cells from pancreatic endoderm derived from human embryonic stem cells in athymic nude rats*. Am J Physiol Endocrinol Metab, 2010. **299**(5): p. E713-20.
202. Ris, F., et al., *Impact of integrin-matrix matching and inhibition of apoptosis on the survival of purified human beta-cells in vitro*. Diabetologia, 2002. **45**(6): p. 841-50.
203. Beattie, G.M., et al., *Regulation of proliferation and differentiation of human fetal pancreatic islet cells by extracellular matrix, hepatocyte growth factor, and cell-cell contact*. Diabetes, 1996. **45**(9): p. 1223-8.

204. Schuppin, G.T., et al., *Replication of adult pancreatic-beta cells cultured on bovine corneal endothelial cell extracellular matrix*. In Vitro Cell Dev Biol Anim, 1993. **29A**(4): p. 339-44.
205. Bosco, D., et al., *Importance of cell-matrix interactions in rat islet beta-cell secretion in vitro: role of alpha6beta1 integrin*. Diabetes, 2000. **49**(2): p. 233-43.
206. Yashpal, N.K., et al., *Expression of {beta}1 integrin receptors during rat pancreas development--sites and dynamics*. Endocrinology, 2005. **146**(4): p. 1798-807.
207. Lee, J.H., et al., *Collagen gel three-dimensional matrices combined with adhesive proteins stimulate neuronal differentiation of mesenchymal stem cells*. J R Soc Interface, 2011. **8**(60): p. 998-1010.
208. Oberg-Welsh, C., *Long-term culture in matrigel enhances the insulin secretion of fetal porcine islet-like cell clusters in vitro*. Pancreas, 2001. **22**(2): p. 157-63.
209. Zimmermann, W.H., et al., *Tissue engineering of a differentiated cardiac muscle construct*. Circ Res, 2002. **90**(2): p. 223-30.
210. Lu, S.H., et al., *Reconstruction of engineered uterine tissues containing smooth muscle layer in collagen/matrigel scaffold in vitro*. Tissue Eng Part A, 2009. **15**(7): p. 1611-8.
211. Dewitt, D.D., et al., *Collagen I-matrigel scaffolds for enhanced Schwann cell survival and control of three-dimensional cell morphology*. Tissue Eng Part A, 2009. **15**(10): p. 2785-93.
212. Johannesson, M., et al., *FGF4 and retinoic acid direct differentiation of hESCs into PDX1-expressing foregut endoderm in a time- and concentration-dependent manner*. PLoS One, 2009. **4**(3): p. e4794.
213. Cai, J., et al., *Generation of homogeneous PDX1(+) pancreatic progenitors from human ES cell-derived endoderm cells*. J Mol Cell Biol, 2010. **2**(1): p. 50-60.
214. Nostro, M.C., et al., *Stage-specific signaling through TGFbeta family members and WNT regulates patterning and pancreatic specification of human pluripotent stem cells*. Development, 2011. **138**(5): p. 861-71.
215. Chen, S., et al., *A small molecule that directs differentiation of human ESCs into the pancreatic lineage*. Nat Chem Biol, 2009. **5**(4): p. 258-65.
216. Murtaugh, L.C., *Pancreas and beta-cell development: from the actual to the possible*. Development, 2007. **134**(3): p. 427-38.
217. Khademhosseini, A., et al., *Microscale technologies for tissue engineering and biology*. Proc Natl Acad Sci U S A, 2006. **103**(8): p. 2480-7.

218. Lee, J., M.J. Cuddihy, and N.A. Kotov, *Three-dimensional cell culture matrices: state of the art*. Tissue Eng Part B Rev, 2008. **14**(1): p. 61-86.
219. Jaramillo, M. and I. Banerjee, *Endothelial cell co-culture mediates maturation of human embryonic stem cell to pancreatic insulin producing cells in a directed differentiation approach*. J Vis Exp, 2012(61).
220. Bock, C., Kiskinis, E., Verstappen, G., Gu, H., Meissner, A., *Reference Maps of human ES and iPS cell variation enable high-throughput characterization of pluripotent cell lines*. CELL, 2010. **144**(3): p. 439-52.